Enclosure to
3/31/83 memo
to Browning from
Bell

NON-ISOTHERMAL FLOW MODELING OF THE HANFORD SITE

MATTHEW GORDON

MICHAEL WEBER

MARCH, 1983

DIVISION OF WASTE MANAGEMENT

U.S. NUCLEAR REGULATORY COMMISSION

Executive Summary

The finite difference code SWIFT (Sandia Waste Isolation Flow and Transport) is used to evaluate four conceptual models of the Hanford Site in terms of hydrogeologic waste isolation capability. Consideration of each model is justified with data contained in the BWIP SCR. The four models examined are:

1-U-1: Duplication of PORFLO base model presented in BWIP SCR, Section 12.4.3); a non-conservative model of the hydrogeologic system at Hanford.

2-U-1: Same as 1-U-1, except for lower porosity, higher hydraulic conductivity; a more conservative model of the Hanford flow system.

3-U-1: Homogeneous, isotropic, non-layered system to conservatively account for ubiquitous structural and stratigraphic discontinuities within the Columbia River basalts. Initial hydraulic gradients are uniform.

4-U-1: Same as 2-U-1, except for initial hydrostatic head distribution; assessment of system sensitivity to heat generated by repository.

Models are evaluated in terms of groundwater travel times from the repository location to the grid boundary for both pre- and post-emplacement conditions. The results indicate a strong sensitivity to porosity, hydraulic conductivity, and hydraulic gradient. The travel times are highly variable, ranging over three orders of magnitude. The

shortest groundwater travel times calculated for this limited set of models is less than 75 years, and the greatest calculated travel time exceeds 12,000 years. The results suggest that the range of uncertainty in hydraulic and thermal parameters must be narrowed before the suitability of the site can be properly evaluated.

These modeling efforts will aid in supporting future NRC evaluation of the DOE's Hanford Site Characterization program and other pre- and post-licensing performance assessments (e.g., the delineation of "the disturbed zone" for both generic and specific sites).

The report also highlights several NRC modeling needs, and makes recommendations for future studies.

ACKNOWLEDGEMENTS

We would like to acknowledge the technical support and discussion during the preparation of this paper provided by Mark Logsdon and Peter Ornstein, NRC; Eileen Poeter and Jerry Rowe, Golder Associates, Inc.; Mark Reeves and Charles Faust, Geotrans, Inc.; and Roy Williams, Williams and Associates.

Table of Contents

I. Introduction

1.1 Purpose

The Hanford Reservation in Southeastern Washington has been identified by the Department of Energy (DOE) as a potential site for a high-level radioactive waste repository. The Hanford site is underlain by a thick sequence of basalt flows and sedimentary interbeds which may have hydraulic properties favorable for isolation of waste from the accessible environment. The "accessible environment" is defined in 40 CFR 191 and 10 CFR 60.

After completing a series of investigations aimed at characterizing the site hydrology and other aspects relating to nuclear waste management, the DOE is expected to apply to the Nuclear Regulatory Commission (NRC) for a license to construct the repository. Upon receipt of the license application, the NRC must be in a position to address and independently evaluate licensing issues as comprehensively as possible. Among these licensing issues will be:

1. Pre-emplacement groundwater travel times to the accessible environment.

2. Integrated releases of radionuclides and post-emplacement groundwater travel times to the accessible environment.

3. Uncertainties in the above due to data limitations.

The methodology for the evaluation of these issues is strongly dependent on the application of numerical models for sensitivity analyses and predictive simulations.

Present groundwater flow and heat transport models of the Hanford site cannot be considered to provide reliable predictions of hydrologic behavior at the site due to data limitations. Also, computer models may themselves bias the results through various implicit and explicit assumptions.

The Hanford Site Characterization Program has not yet collected critical data on vertical hydraulic conductivities and porosity. The location and nature of subsurface geologic structures are largely unknown, as are the extent and characteristics of rock fractures. As new information is collected, the conceptual model of the site hydrogeology will be refined. Of course, any conceptual model of a hydrologic system is necessarily a simplification of the physical reality, which is subject to spatial and temporal heterogenities too complex to consider. However, it is hoped that sufficient information can be collected so that the uncertainties in the conceptual model can be minimized, and bounding estimates can be made of groundwater travel times and integrated radionuclide releases to the accessible environment.

Computer models of site hydrology at this stage in the site characterization of the Hanford Basalt Waste Isolation Project (BWIP) may be used to aid in identifying areas of major concern for which further information is necessary prior to licensing. The application of computer models in this mode is generally termed "sensitivity analysis," as opposed to "predictive simulation." In Figure 1, a logic diagram shows an approach which should generally be taken towards the use of numerical models. As shown, conceptual models are analyzed using numerical models in a sensitivity analysis. The sensitivity analysis should indicate whether more data is needed, or if the present level of site characterization is sufficient. Only after sufficient data have been

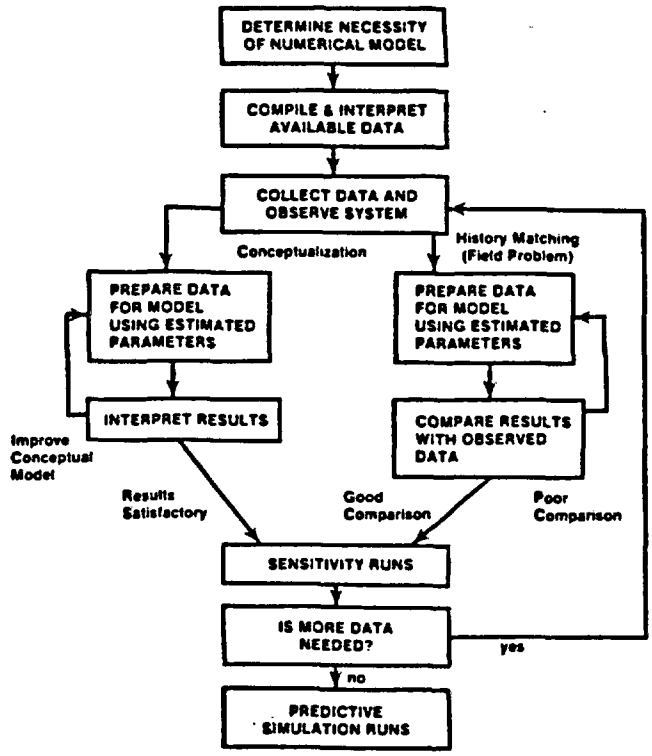

Figure 1. Flow chart showing the use of sensitivity analyses to regulate data collection and create conceptual models (Mercer and Faust, 1981).

collected to eliminate large uncertainties should a numerical model be used in a predictive mode.

This report illustrates the use of a numerical model (SWIFT) in a deterministic (i.e., non-probabilistic) sensitivity analysis. In particular, coupled groundwater flow and heat transport for a hypothetical repository site at Hanford is modeled using tools (i.e., computer codes) developed for the NRC as part of the evaluation methodology. The purpose of this analysis is four-fold:

1. to demonstrate and evaluate certain aspects of the NRC's current methodology for evaluation of licensing issues;

2. to assess future modeling needs, in terms of additional data collection, improvement of modeling tools, and resource allocations;

3. to initiate a deterministic sensitivity analysis of BWIP hydrology; and

4. to provide results of a preliminary sensitivity analysis.

1.2 Historical Background

The Hanford Site was first considered as a potential repository site by the U. S. Energy and Research Development Administration (now the DOE) in 1976. Since that time the Atlantic Richfield Hanford Company (ARHCO), and later, Rockwell Hanford Operations (RHO), have been authorized to collect and analyze data from the site. Engineers, scientists, and field technicians has been assigned to characterize the BWIP geology and hydrology in terms of chemical, hydraulic and mechanical properties.

Selected key documents which have been published since the initiation of BWIP are presented in Table 1. These reports indicate both the swift progress and the large uncertainties remaining in site characterization up to this date. Many of these reports were written to document the characteristics of projected pathlines from the BWIP repository to the biosphere. Three of the various flow paths considered in the reports are shown in Figure 2. The disparities in the directions and travel times along thepostulated flow paths indicate that much more information is required before the site can be properly evaluated in terms of flow paths and travel times.

In November, 1982, the Department of Energy released the BWIP Site Characterization Report. This three volume document describes the progress made to date and DOE's future plans for site characterization. The report also includes the results of preliminary numerical modeling studies. Although the BWIP SCR was not intended to provide any definitive judgments about the site, the DOE has expressed confidence in these preliminary modeling results in meetings with the NRC. The modeling results suggest that groundwater travel time from a nuclear waste repository for DOE's conceptual model(s) of the Hanford Site will greatly exceed 10,000 years. The validity and degree of certainty associated with this contention is important to the regulatory concerns of the NRC. If this contention were sufficiently substantiated, regulatory requirements on the waste package and engineered barriers, as described in 10 CFR 60, could be relaxed from an "overall systems performance" standpoint.

In March, 1983, the NRC released a "Draft Site Characterization Analysis" (DSCA) which challenges the validity of these modeling results. In the DSCA the NRC states that these "minimum groundwater travel time" estimates represent the use of predictive modeling, which is premature at

the present level of site characterization. Also, the NRC concludes that the hydrologic and hydraulic conditions assumed in the SCR modeling are non-conservative, and as such, cannot yield "minimum" or conservative groundwater travel time estimates.

Since the release of the DSCA, the NRC has continued to develop tools and perform analyses which are intended to support the NRC's position on these licensing issues. One analysis that is being performed is the application of two-dimensional flow and heat transport numerical models for various alternative conceptual models of Hanford. This report describes the progress of this analysis to date.

TABLE 1. SELECTED KEY DOCUMENTS IN HANFORD SITE HYDROLOGY ANALYSIS

Title	Author(s)	Date	Acc. #	Notes
"Geologic Studies within the Columbia Plateau, Washington"	Myers, et al. (RHO)	1979	RHO-BWI-ST-4	Compilation of BWIP geologic information collected up to date. Includes geophysical surveys, tectonic analysis.
"Hydrologic Studies within the Columbia Plateau, Washington"	Gephart, et al. (RHO)	1979	RHO-BWI-ST-5	Compilation of BWIP hydrologic information collected up to date. Includes regional water balance, hydraulic property measurements and preliminary modeling results.
"Preliminary Hydrologic Release Scenarios for a Candidate Repository Site in the Columbia River Basalts"	Arnett, et al. (RHO)	1980	RHO-BWI-ST-12	Considered shaft seal degradation and interconnecting fault scenarios.
"Pasco Basin Hydrologic Modeing and Far-Field Radionuclide Migration Potential"	Arnett, et al. (RHO)	1981	RHO-BWI-LD-44	Predictive numerical model application to determine groundwater flow paths from a repository at Hanford. Determined southeast to discharge at Wallula Gap.
"AEGIS Technology Demonstration for a Nuclear Waste Repository in Basalt"	Dove, et al. (RHO)	1981	PNL-3632	Compilation of regional studies, including development of an alternative conceptual model and alternative flow path.
"Comparison of Model Studies"	Lehman & Quinn (NRC)	1982	N/A	Analysis of LD-44, PNL-3632, and USGS models.
"Analysis of Boundary Conditions and Conductivity Ratios used in Pasco Basin Modeling"	Quinn (NRC)	1982	N/A	Study of basin-scale sensitivity to boundary condition uncertainties and boundary conductivities.

Title	Author(s)	Date	Acc. #	Notes
"BWIP Site Characterization Report"	DOE	1982	DOE-RL-82-3	Revie of site characterization progress and plans. Includes estimates of "minimum" groundwater travel times to the accessible environment - greater than 10,000 years.
"Draft Site Characterization Analysis"	NRC	1983	NUREG-0960	Review and critique of DOE progress and plans as presented in BWIP SCR.

COMPARISON OF TRAVEL PATHS

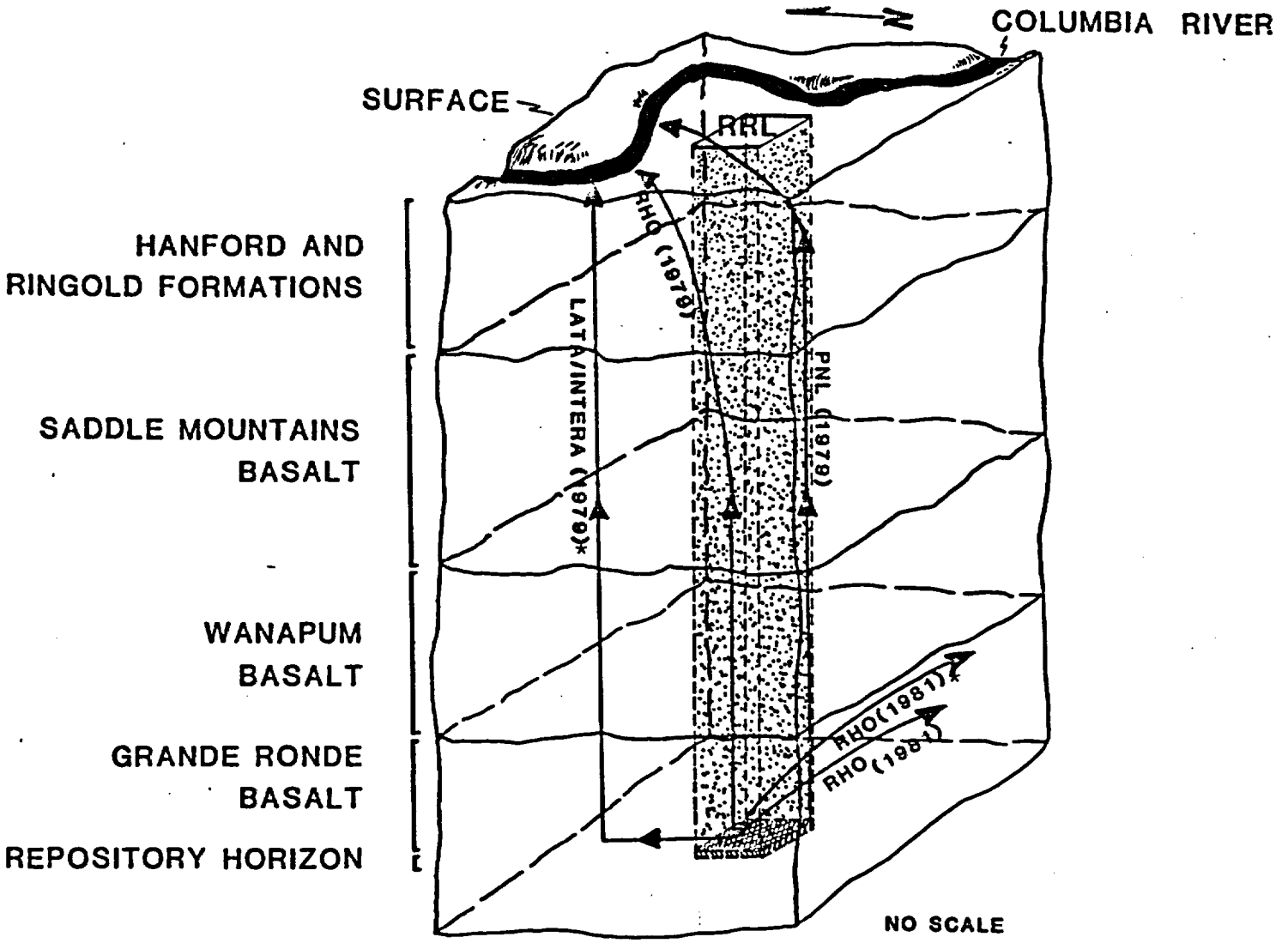

Figure 2. Comparison diagram of calculated flow paths to the accessible environment from the proposed repository at BWIP (modified from RHO slide presentation, September, 1981).

* denotes documents not discussed in text.

II. Modeling Effort

2.1 Date Base Utilized for the 1-U-1 Model

One of the most recent modeling efforts of the DOE presented in the SCR is described on pp. 12.4-28 through 12.4-50 of the SCR. The PORFLO code was used by the DOE to determine groundwater travel times and cumulative radionuclide releases from a repository placed either in the dense Umtanum flow or the dense Middle Sentinel Bluffs flow (the Cohasset). The description of the PORFLO models in the SCR includes the model grid, repository data, boundary conditions, hydraulic parameters, and results obtained. Additional model assumptions and input data were obtained by the NRC through direct communication with the DOE. The data and assumptions used in the NRC's numerical modeling are described in full in this section.

In modeling the BWIP site, information published in the SCR was used to develop several alternative conceptual models. In the DSCA, the NRC presents alternative conceptual models, or "scenarios," which are at least as reasonable as the models presented in the SCR (DSCA Chapter 3). Using these as a guide, four alternative conceptual models were developed and analyzed for this report. The basic model for our analysis was the conceptual model used by the DOE for the PORFLO simulation of the Umtanum repository base case. It was desirable that the NRC demonstrate the ability to produce results comparable to those of PORFLO using SWIFT, given equivalent (or nearly equivalent) input data and assumptions. This base case was called the "1-U-1", or "PORFLO duplication" case. A successful duplication of the PORFLO results by SWIFT demonstrates that

SWIFT introduces no code-specific biases to the solution of the flow equations.

In the PORFLO duplication efforts, the NRC received the assistance of Golder Associates of Washington. Their helpful suggestions and review of these efforts have been incorporated in this report.

Hydrostratigraphy

The hydrostratigraphy used in the SWIFT 2-D simulations of the hydrogeologic system at BWIP is identical to the one used in the PORFLO models described in Chapter 12 of the BWIP SCR. Individual basalt flows of the Grande Ronde and Wanapum Basalts are laterally extensive, of constant thickness, homogeneous, and anisotropic. Sedimentary interbeds are intercalated with the basalt flows.

Figure 3 is a simplified stratigraphic section for the Columbia River basalts. This basalt sequence consists of a series of stratiform flows. The typical basalt flow may be divided into three morphological units: the basal colonnade, entablature, and the upper colonnade. Basalt flows may also be divided into the more simple stratigraphy of dense flow interiors and flow tops. Rubble zones, commonly found at the base of individual flows, are included in the flow tops of the underlying flow units. Dense interiors are generally assumed to be poorly conductive to groundwater flow, while flow tops are characterized as having higher hydraulic conductivities. Silar (1968) describes flow tops and basal contact zones in shallow basalt flows as being "very permeable." In deep irrigation wells, contact zones and flow tops comprised an average of 30% of the saturated section (Luzier and Burt, 1974). In the SWIFT 2-D BWIP simulations, the more permeable flow tops comprise approximately 13% of the saturated, layered system.

Layer thicknesses were measured in boreholes RRL-2, DC-4, DC-5, and DC-10 as detailed in the BWIP SCR. The thickness of the Umtanum flow top, which is used in these models, was recorded in borehole RRL-2. The use of this thickness produces non-conservative estimates of travel time from the repository to the accessible environment because the Umtanum flow top is thinner in other boreholes than in RRL-2, and groundwater moves slowest through the high porosity flow tops. The actual thickness of the

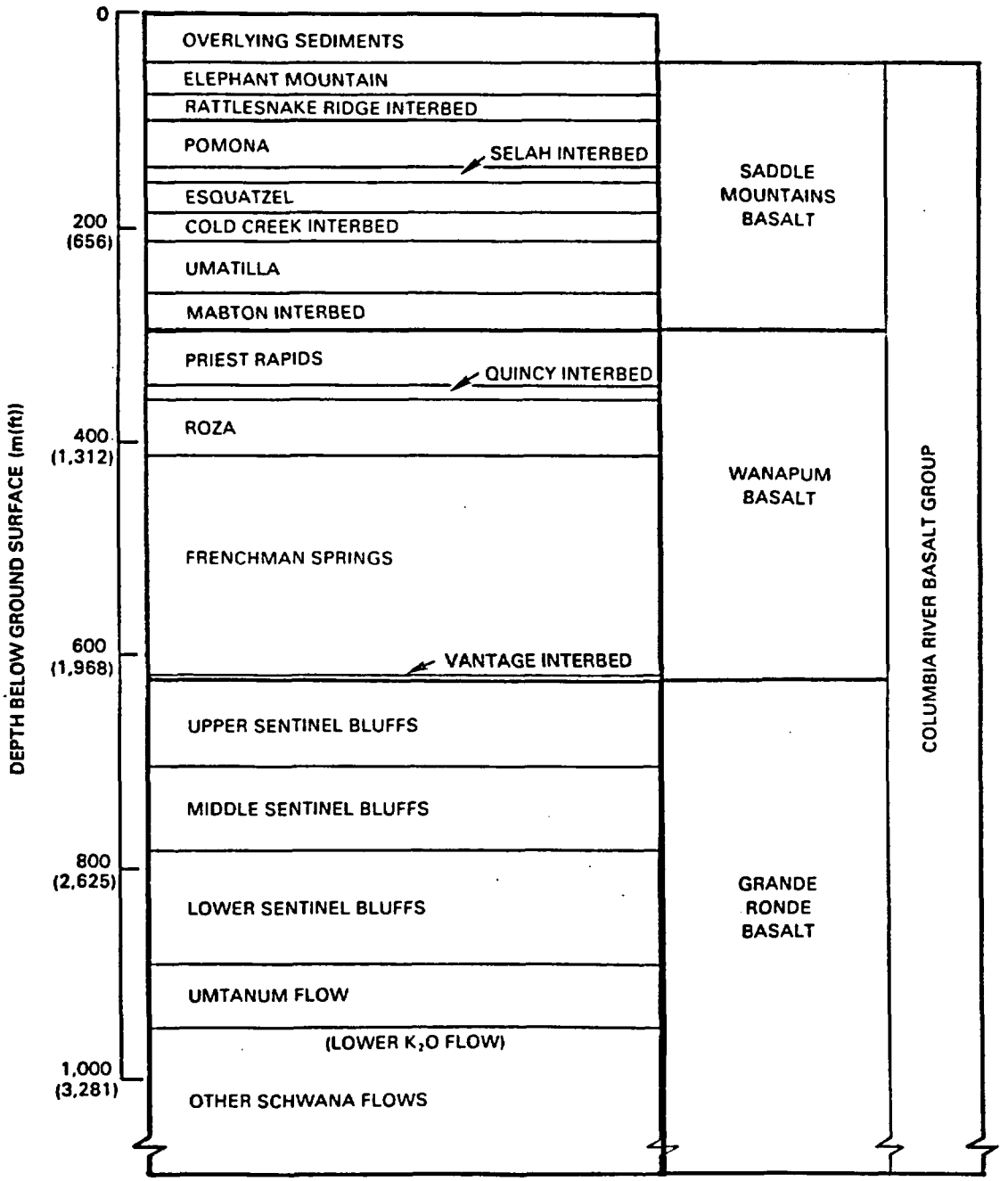

Figure 3. Simplified stratigraphic column of the Columbia River Basalts (BWIP, Fig. 12-12, SCR, 1982, p.12.4-31).

Umtanum flow top in RRL-2 is 47.6 m. In other boreholes, the Umtanum flow top approximately averages 20 m thick.

The model is composed of 32 hydrostratigraphic units, which are illustrated in Figure 4. Unit thicknesses are noted on the left margin of the diagram. The bottom hydrostratigraphic unit of the model is a composite unit below the Umtanum flow; the model is capped by the third flow of the Frenchman Springs Member of the Wanapum Basalt Formation. The units modeled in the transient and steady-state simulations of the BWIP hydrogeologic system are listed in Table 2. The hydraulic conductivities and porosities of the hydrostratigraphic units are referenced in Chapters 3, 5, and 12 of the BWIP SCR. They are also listed in this report in Tables 3, 4, and 5. These values are assumed to be "representative" of the hydraulic conductivities and porosities of groups of flows by DOE.

All flow tops in the 1-U-1 model are assumed to be isotropically conductive with conductivities of 1E-7 m/s.

Dense interiors are assumed to be anisotropically conductive with horizontal hydraulic conductivities (K_H) of 10^{-11} m/s. Vertical conductivities (K_V) of the flow interiors are an assumed order of magnitude higher to account for vertical joints in the colonnade and entablature zones in the dense portions of the flows. These hydraulic conductivity values of the dense flow interiors of the Grande Ronde Basalt are one to three orders of magnitude higher than values measured in situ. The accuracy of these very low conductivities that are determined in pump tests, which were developed for highly-permeable sediments, is subject to controversy.

The model includes only three layers that do not represent individual basalt flows. These hydrostratigraphic units include the vesicular zone of the Middle Sentinel Bluffs, the Vantage interbed at the base of the Frenchman Springs Member, and the composite basalt unit below the Umtanum

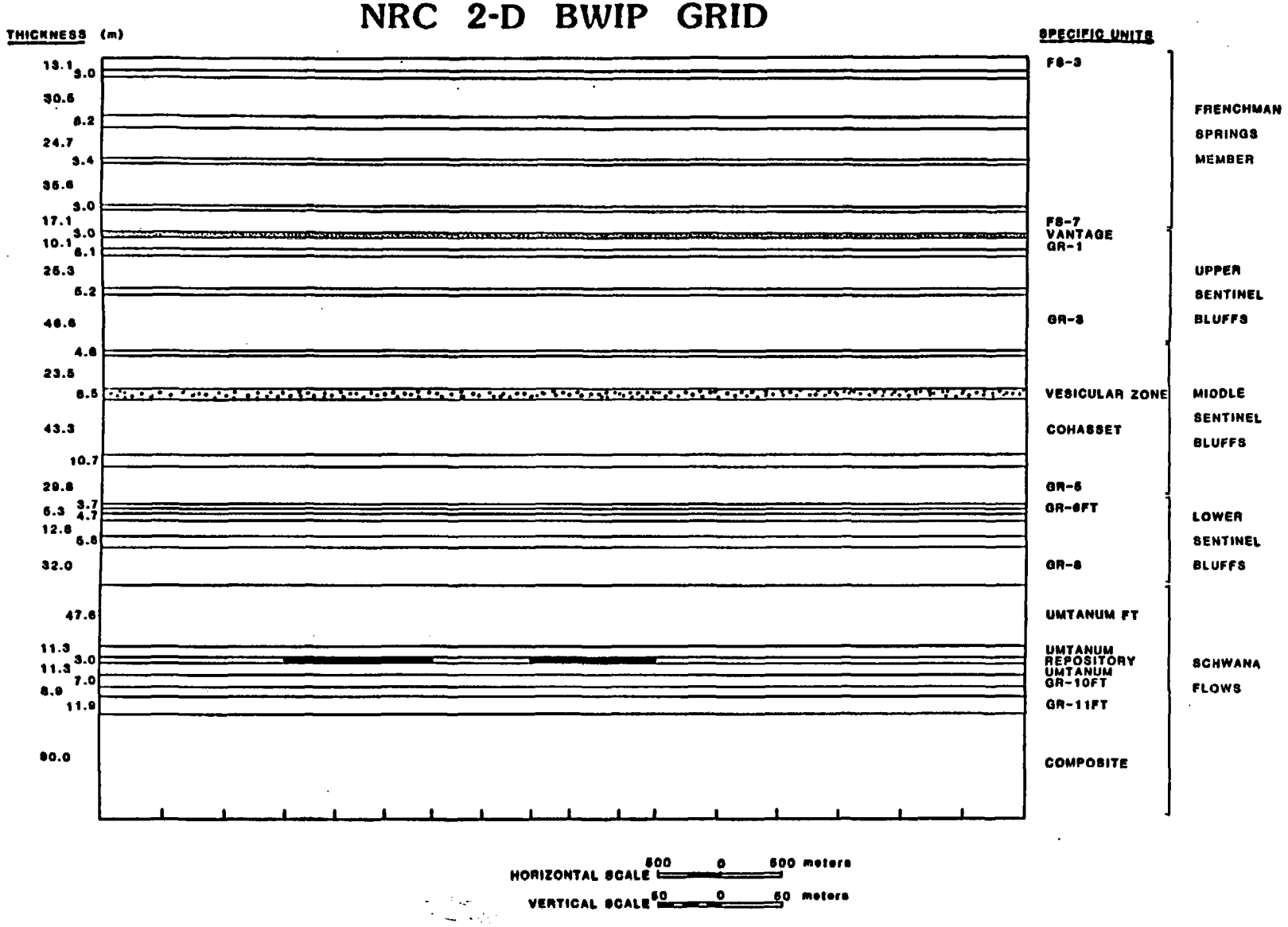

Figure 4. Simplified NRC 2-D BWIP grid showing hydrostratigraphic unit thicknesses and nomenclature. Repository blocks have been darkened. X-direction grid block spacings are marked along the bottom boundary of the grid.

flow at the base of the model. The vesicular zone is considered to be isotropically conductive with a hydraulic conductivity of 1E-8 m/s. Having an assumed isotropic hydraulic conductivity of 3E-7 m/s, the Vantage interbed is assumed to be the most conductive hydrostratigraphic unit of the BWIP system. The composite unit beneath the Umtanum flow has the vertical conductivity of the dense flow interiors and the horizontal hydraulic conductivity of the flow tops. Although the PORFLO simulations in the SCR used a composite unit below the Umtanum flow, the hydraulic properties were not determined by field measurements, so the validity of these values is subject to verification by additional site characterization.

Table 2. Hydrostratigraphic Units of the SWIFT 2-D Models

Member of Sequence	Layer	Thickness (m)[@]
Frenchman Springs	FS-3	13.1
Frenchman Springs	FS-4FT	3.0
Frenchman Springs	FS-4	30.5
Frenchman Springs	FS-5FT	8.2
Frenchman Springs	FS-5	24.7
Frenchman Springs	FS-6FT	3.4
Frenchman Springs	FS-6	35.6
Frenchman Springs	FS-7FT	3.0
Frenchman Springs	FS-7	17.1
Vantage	V-1	3.0
Upper Sentinel Bluffs	GR-1	10.1
Upper Sentinel Bluffs	GR-2FT	6.1
Upper Sentinel Bluffs	GR-2	25.3
Upper Sentinel Bluffs	GR-3FT	5.2
Upper Sentinel Bluffs	GR-3	46.6
Middle Sentinel Bluffs	GR-4FT	4.6
Middle Sentinel Bluffs	GR-4	23.5
Middle Sentinel Bluffs	Vesicular Zone	8.5
Middle Sentinel Bluffs	GR-4	43.3
Middle Sentinel Bluffs	GR-5FT	10.7
Middle Sentinel Bluffs	GR-5	29.8
Lower Sentinel Bluffs	GR-6FT	3.7
Lower Sentinel Bluffs	GR-6	5.3
Lower Sentinel Bluffs	GR-7FT	4.7
Lower Sentinel Bluffs	GR-7	12.8
Lower Sentinel Bluffs	GR-8FT	5.8
Lower Sentinel Bluffs	GR-8	32.0
Schwana	Umtanum FT	47.6
Schwana	Umtanum	25.6
Schwana	GR-10FT	7.0
Schwana	GR-10	8.9
Schwana	GR-11FT	11.9
Schwana	Composite Base	90.0

[@] 3.0 m is asssumed as a minimal thickness where hydrostratigraphic units may be less than 3.0 m in thickness.

Simplified stratigraphy, layer designations, and thicknesses are from Chapter 12 of the BWIP SCR, 1982 , especially Table 12-14.

Table 3. A Comparison of the Hydraulic Properties of Dense Flow Interiors in the 1-U-1 and 2-U-1 Models.

Units	1-U-1 Thickness (m)	2-U-1 Thickness (m)	1-U-1 K_H (m/s)	2-U-1 K_H (m/s)	1-U-1 K_V (m/s)	2-U-1 K_V (m/s)	1-U-1 Φ_E	2-U-1 Φ_E
Frenchman Springs (FS-3, 4, 5, 6, 7)	121.0	121.0	1E-11	1E-10	1E-10	1E-8	1E-3	1E-4
Upper Sentinel Bluffs (GR-1, 2, 3)	82.0	82.0	1E-11	1E-10	1E-10	1E-8	1E-3	1E-4
Middle Sentinel Bluffs (GR-4, 5)	96.6	96.6	1E-11	1E-11	1E-10	3E-9	1E-3	1E-4
Lower Sentinel Bluffs (GR-6, 7, 8)	50.1	50.1	1E-11	1E-10	1E-10	1E-8	1E-3	1E-4
Schwana Flows (Umtanum, GR-10)	34.5	34.5	1E-11	1E-11	1E-10	3E-9	1E-3	1E-4
Composite	90.0	90.0	1E-7	1E-11	1E-10	3E-9	5E-3	1E-4

Table 4. A Comparison of the Hydraulic Properties of Flow Tops in the 1-U-1 and 2-U-1 Models.

Units	1-U-1 Thickness (m)	2-U-1 Thickness (m)	1-U-1 K_H (m/s)	2-U-1 K_V (m/s)	1-U-1 K_V (m/s)	2-U-1 K_V (m/s)	1-U-1 Φ_E	2-U-1 Φ_E
Frenchman Springs (FS-4FT, 5FT, 6FT, and 7FT)	17.6	17.6	1E-7	3E-5	1E-7	3E-5	1E-2	1E-2
Upper Sentinel Bluffs (GR-2FT, 3FT)	11.3	11.3	1E-7	3E-5	1E-7	3E-5	1E-2	1E-2
Middle Sentinel Bluffs (GR-4FT, 5FT)	15.3	15.3	1E-7	3E-7	1E-7	3E-7	1E-2	3E-3
Lower Sentinel Bluffs (GR-6FT, 7FT, 8FT)	14.2	14.2	1E-7	3E-7	1E-7	3E-7	1E-2	3E-3
Schwana Flows (Um FT, GR-10FT, 11FT)	66.5	66.5	1E-7	3E-7	1E-7	3E-7	1E-2	3E-3

Table 5. Comparison of the Hydraulic Properties of the Vantage and Vesicular Zone Layers of the 1-U-1 and 2-U-1 Models.

Units	1-U-1 Thickness (m)	2-U-1 Thickness (m)	1-U-1 K_H (m/s)	2-U-1 K_H (m/s)	1-U-1 K_V (m/s)	2-U-1 K_V (m/s)	1-U-1 Φ_E	2-U-1 Φ_E
Vantage	3.0	3.0	3E-7	1E-7	3E-7	1E-7	1E-1	1E-1
Vesicular Zone	8.5	8.5	1E-8	1E-11	1E-8	3E-9	5E-2	1E-3

Hydraulic Heads and Gradients

Constant boundary pressures and temperatures are enforced in both the transient and steady-state BWIP 2-D models using SWIFT. All peripheral nodes of the model grid may be considered as flow nodes. The constant boundary temperatures initially enforce the geothermal gradient throughout the model. Constant pressure boundary conditions are enforced to establish hydraulic gradients across the Wanapum and Grande Ronde Group Basalts. A horizontal hydraulic gradient of 1E-3 m/m is enforced across the entire grid. The vertical hydraulic gradient approximates the head profile that was recorded in well RRL-2 near the proposed repository location.

The vertical profile of hydraulic head versus depth, which corresponds to the vertical hydraulic gradient in RRL-2 as seen in Figure 5, indicates that the vertical hydraulic gradient changes in magnitude and direction with increasing depth. Near the top of the NRC BWIP model within the lower units of the Frenchman Springs Member, the vertical gradient is approximately 1E-4 m/m downward. Within the Middle and Upper Sentinel Bluffs flows, the vertical gradient is nearly hydrostatic. As depth increases, the gradient increases to 1E-3 m/m upward within the Lower Sentinel Bluffs and Umtanum Flows. Below the Umtanum flow, a vertical gradient of 1E-3 m/m is enforced by lateral and basal boundary conditions.

The RRL-2 Profile may not be the most representative profile of head distribution within the layered basalt system at BWIP. Profiles from nearby wells (e.g. DC-4, DC-12, etc.) differ from the RRL-2 profile, and since models are often greatly influenced by their boundary conditions, enforcement of these profiles may result in different pathlines and travel times from the repository to the accessible environment. The 1-U-1 model does not represent a unique spatial configuration. Although the validity of a 2-D model is contingent upon the absence of flow in the third dimension, head data at BWIP cannot be interpreted presently to

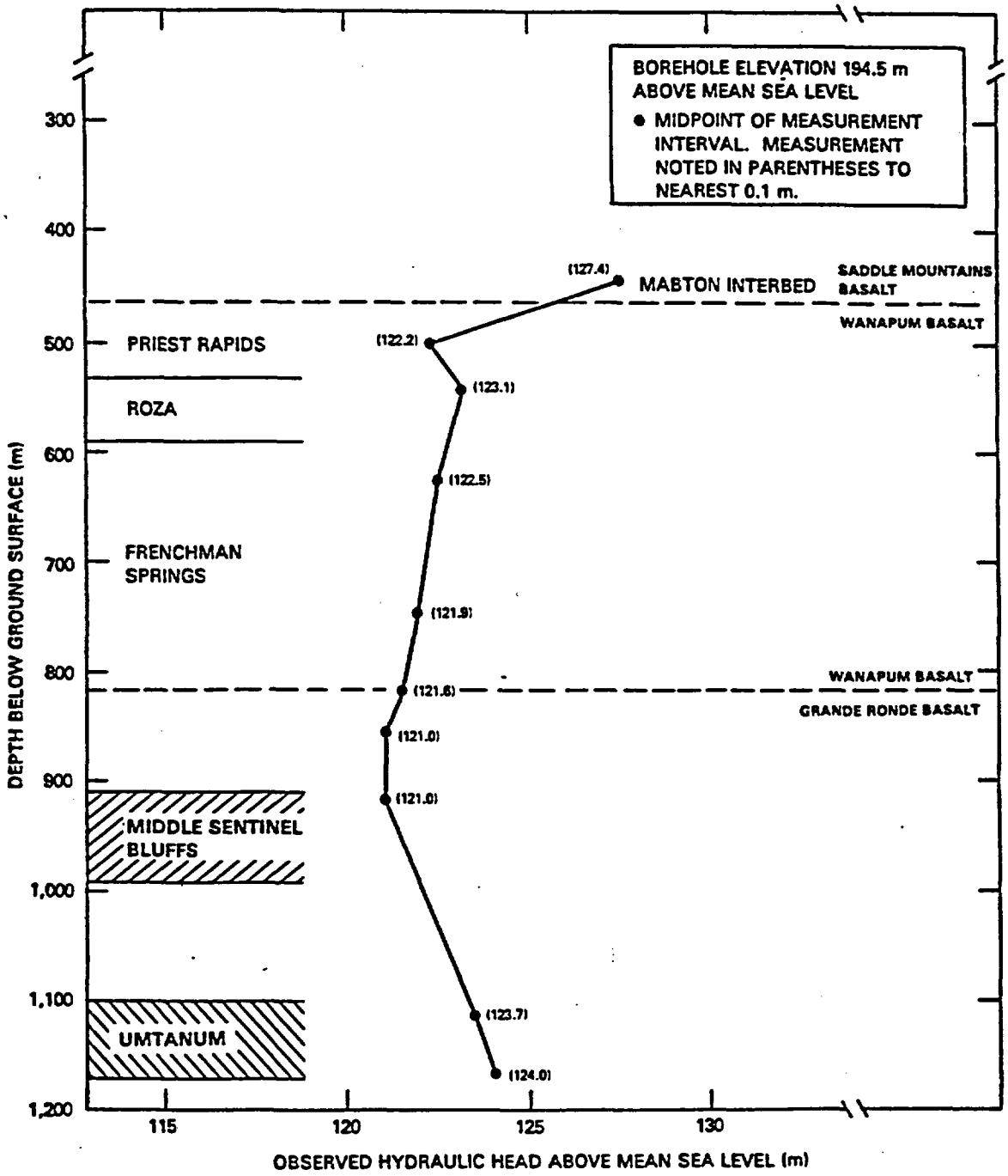

Figure 5. Hydraulic head measurements in Borehole RRL-2 (BWIP, Figure 5-41, SCR, 1982, p. 5.1-72)

yield a unique head distribution, so this assumption remains unsupported. If the model were given a prescribed orientation in space, then a spatial head configuration would be presumed, which presently cannot be confirmed.

The RRL-2 profile is imposed on the 1-U-1 model by supposing its existence at the repository midpoint and extrapolating the measured heads to the lateral boundaries of the model by assuming a horizontal gradient of 1E-3 m/m. The RRL-2 profile is not enforced within the model grid; the profile exists only along the lateral boundaries. This same approach was taken by DOE in the PORFLO simulations in the SCR. To clarify the technique used to calculate the hydraulic heads along the lateral boundaries, the side boundary heads may be calculated as

$$H_b = H_{RRL} + (I_H)(\Delta X_{RRL-b})$$

where H_b = hydraulic head at the side boundary at depth z
H_{RRL} hydraulic head as recorded for RRL-2 at depth z
I_H = constant horizontal gradient = 1E-3
ΔX_{RRL-b} = separation distance between the boundary and the repository midpoint where the RRL-2 profile is assumed (/+/ = upgradient).

To calculate constant boundary pressures, the elevation head is added to the hydraulic head. This sum is then converted to a pressure by accounting for the compressibility and thermal expansion of the water with depth as the temperature and pressure increase.

Along the top and bottom grid boundaries, the heads at the lateral boundaries are extrapolated by subtracting the product of the separation distance between the node-lateral boundary and the hydraulic gradient, from the hydraulic head at the same elevation along the left lateral boundary, or

$$H_x = H_{x+1} - (I_H)(\Delta X_{(x,x+1)})$$

where H_x = hydraulic head at node x along the top or bottom boundary
H_{x+1} = head at node (x+1) upgradient (horizontal) from node x
I_H = constant horizontal gradient
$\Delta X_{(x,x+1)}$ = displacement between nodes x and x+1

There are no internal sources of fluid in the model. The source blocks, which represent the repository, are only internal sources of heat as described in the section on heat input.

Model Grid

The 32 hydrostratigraphic units in the model are divided into a total of 74 layers, which are divided into a total of 1248 grid blocks. The grid measures 7500 m (horizontal) x 612 m(vertical) x 1 m (horizontal). To avoid numerical instabilities and improve model resolution, layer thicknesses are chosen so that no layer is more than twice as thick as an adjacent layer. The same is true in the contrasts of x-dimensions of adjacent grid blocks. The highest aspect ratio is 167 (e.g., in the 500 m x 3 m x 1 m blocks).

The repository is located 500 m from the top of the grid in the 63rd layer, approximateley 1500 m from the left lateral boundary; this description is illustrated in the simplified grid seen in Figure 4. The repository horizon is the central layer of the dense interior of the Umtanum flow and is sandwiched between two layers of the dense zone, each of which is 11.3 m thick, as detailed in the BWIP SCR. The Umtanum flow is approximately 1000 m below mean sea level at the RRL.

Constant pressure and temperature aquifer influence functions (i.e., boundary conditions) are specified for the 178 peripheral nodes of the grid. The model grid cannot be substantially varied from its present configuration without a reduction in model resolution or scale, even

though the boundaries may not be sufficiently distant from the repository to minimize boundary effects within the area of interest.

Heat Input

A geothermal gradient of 40°C/km is initially enforced throughout the model. Given an ambient surface temperature of 17.5° C at 194.5 m above Mean Sea Level (the collar elevation of well RRL-2 near the proposed facility), the sub-surface temperature is assumed to be constant to a depth of 6.5 m. Above this depth, diurnal temperature fluctuations are assumed to attenuate any increases in temperature in response to the geothermal gradient. Figure 6 illustrates the initial temperature profile used in the 2-D BWIP models. The initial temperature within the Umtanum repository layer is 64°C. The gradual increase of temperature with depth is important since density, viscosity, and hydraulic conductivity are strongly dependent upon temperature. Temperature differentials caused by repository heating above ambient temperatures will increase local hydraulic potentials, and therefore may control groundwater flow.

Although the gradual increase of ambient groundwater temperature with depth (due to the geothermal gradient) may not control groundwater flow, the thermal effects of the repository will be superimposed on the pre-emplacement thermal and pressure fields. Decay of radioactive wastes within the repository produces heat, which decreases the density and viscosity and increases the pressure of the groundwater surrounding the wastes. Thermal expansion of the rock and water elevates the pressure gradients away from the repository so the system is driven by mixed convection: the bouyancy of lower density water and the pre-existing natural hydraulic gradient.

In SWIFT, internal sources of heat may be simulated by using several alternative options. The transient models described in this report use source blocks to simulate the repository which emits heat. These source blocks have been blackened in the simplified model grid included as

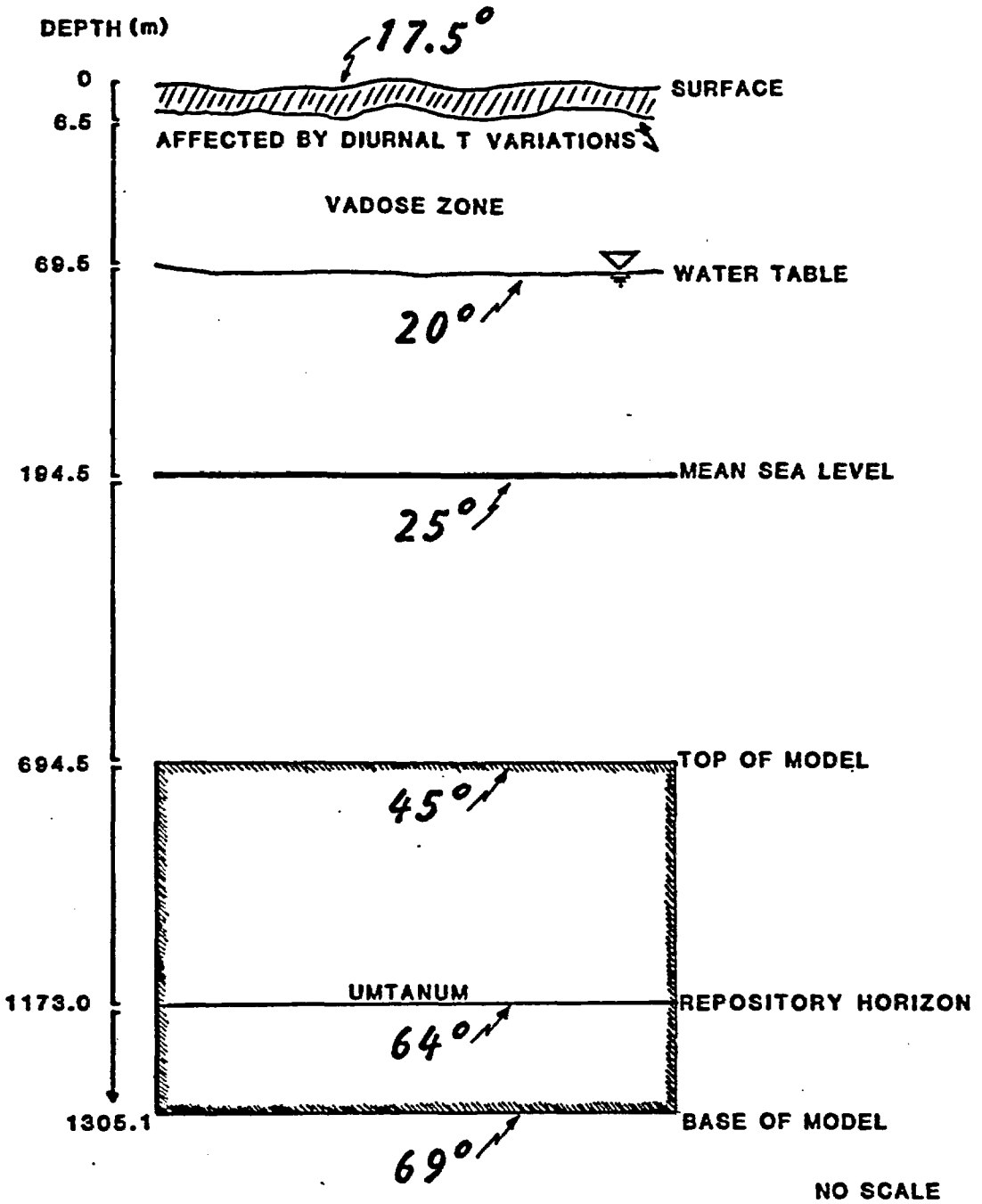

Figure 6 . Temperature profile (initial conditions) in relation to ground surface, water table, mean sea level, and top and bottom of model grid. Temperatures are in degrees Celsius.

Figure 4. By multiplying the volume of the source blocks (the repository) by the power output in terms of J/sec-m^3, an effective thermal emission of the sources may be calculated. The power output, supplied to the NRC by DOE, is a function of time. Since radioactive decay rate is constant through time for each radionuclide, but the radioisotopic inventory decreases, the total heat flux from the repository will also decrease. This decrease in heat production from a 47,000 MTHM spent fuel repository is portrayed in Figure 7. SWIFT uses discrete values for heat efflux from the source blocks, and so the power production curve must be discretized. Figure 7 shows how the first 1000 years have been discretized into four intervals (0-10, 10-100, 100-1000, and >1000 years) for the transient SWIFT models. The input of discrete power terms, which are constant during time intervals, may cause approximation errors in the transient simulations with SWIFT.

Interval values of power output are weighted in favor of the value at the mid-point within the time interval(e.g. 5 years for the 0 to 10 year interval). This technique is recognized to be non-conservative because of the exponential behavior of the curve.

The power output values used in the transient model may also be non-conservative since the normalizing volume assumed only includes the waste storage areas. These values do not account for end effects of the repository. The thermal efflux from the core of the facility will be less than the efflux from the extremities of the repository, where heat will be conducted away from the wastes parallel to the repository axis. By comparing the volumetric power terms provided to the NRC by DOE, which are listed in Table 6, with the thermal decay curves for a 47,000 MTHM repository (10 year-old spent fuel) from the General Environmental Impact Statement for Commercial Disposal of Radioactive Waste (DOE,1980), the waste volume may be calculated as 1.70E7 m^3. Given a repository thickness of three meters (in the vertical direction), the plan area of the repository would be approximately 1000 acres, which is comparable to DOE repository designs of BWIP. By multiplying the total heat flux from

the repository (using GEIS decay curves) by the fraction of the repository volume used in the NRC 2-D BWIP model, the NRC thermal flux from the repository to adjacent host rock is within 5% of the GEIS values.

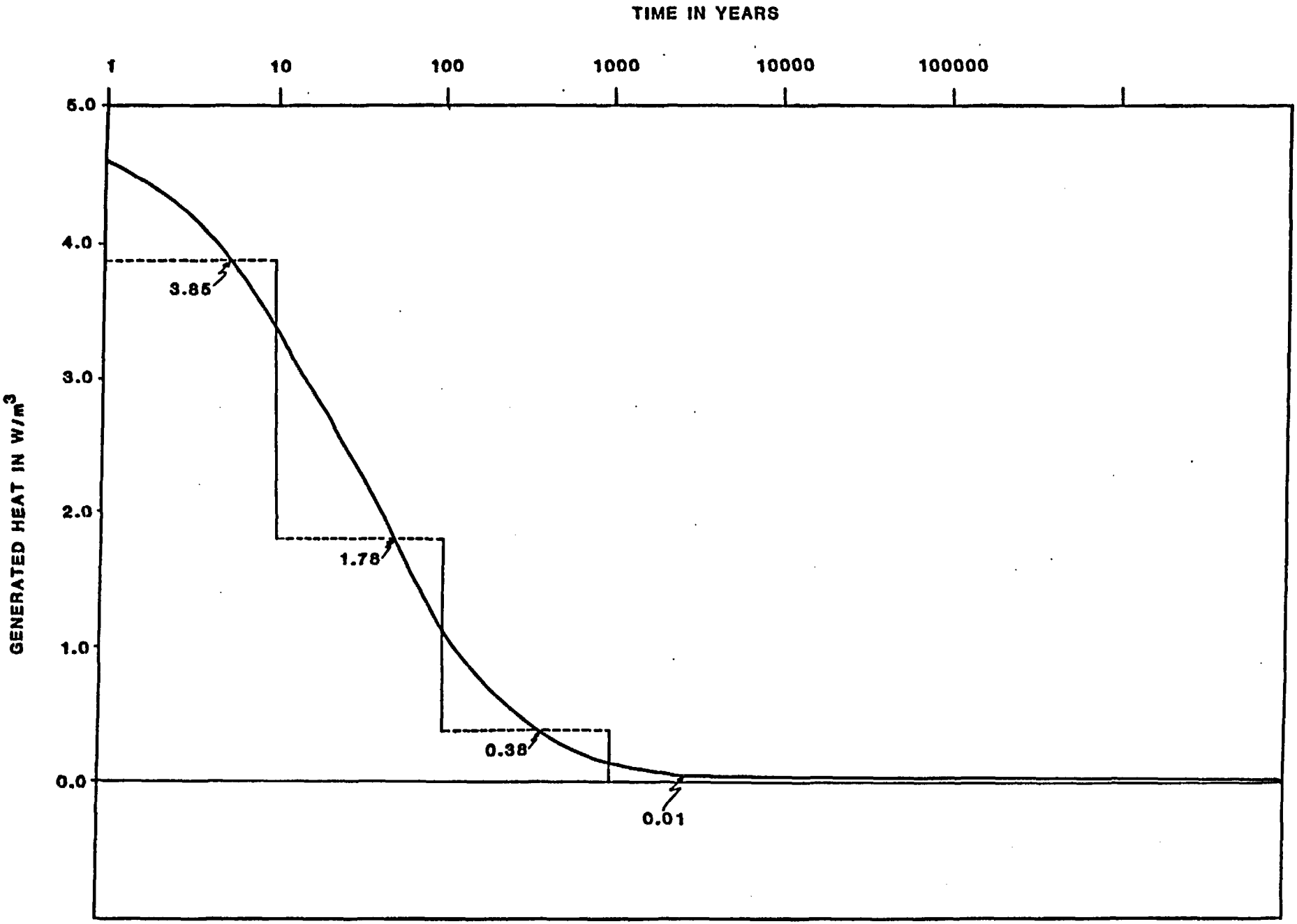

Figure 7. Heat production from 47,000 MTHM of 10-year old spent fuel for the BWIP conceptual repository design.

Table 6. Heat Source Terms from a 47,000 MTHM Repository of 10 Year-Old Spent Fuel

Time (yr.)	Q (J/m^3-yr)	Q (W/m^3)
0	1.47×10^8	4.66
5	1.214×10^8	3.85
10	1.039×10^8	3.29
15	9.393×10^7	2.98
20	8.644×10^7	2.74
30	7.31×10^7	2.318
40	6.233×10^7	1.977
50	5.66×10^7	1.79
70	4.131×10^7	1.31
100	3.146×10^7	.998
190	1.94×10^7	.62
290	1.544×10^7	.490
390	1.279×10^7	.41
490	1.32×10^7	.360
990	6.527×10^6	.21
1,990	3.44×10^6	.11
5,990	2.043×10^6	.06
9,990	1.617×10^6	.0513
50,000	6×10^5	.019
100,000	3×10^5	.010

Source: DOE Telefax Communication to NRC, December, 1983.

Physical Properties

The heat capacity of all hydrostratigraphic units in the SWIFT simulations is 2.77E6 J/m^3-°C. This value of the specific heat capacity (at constant pressure) was determined over the temperature range of 20-750°C. In comparison, the heat capacity of fine basalt (density = 2.77E3 kg/m^3) is approximately 2.3E6 J/m^3-°C (Mercer, Thomas, and Ross, 1982). The propagation of the thermally-disturbed zone away from the repository will be sensitive to changes in thermal properties since thermal conduction dominates heat transfer away from the repository.

Heat capacities and thermal conductivities of interbeds and interflow zones within the basalt sequence at BWIP are not included in the BWIP SCR. Although the sensitivity of the models to these values would be suspected to be proportional to the abundance of interbeds and interflow zones within the stratigraphic sequence, a simplified sensitivity study of their significance could be conducted as part of a systems sensitivity analysis.

Heat capacities of basalt are included in Table 7 to compare with and support the heat capacity chosen for the 2-D SWIFT models. In addition to heat capacity, the thermal conductivies of the host basalt at BWIP may significantly affect the extent of the thermally-disturbed zone around the repository.

Table 7. Heat Capacities of Basalts

Unit	Reference	T Range(°C)	Cp (J/m^3-°C)
Umtanum Pomona Columbia	RSD RSD	50-200 50-200	2.41E6 2.44E6
River Basalt	ARCO, 1976	38-316	2.32E6
Pomona	Duvall, et al, 1978	100-300	5.06E6
Pomona	Foundation Sciences, Inc. 1980	73-356	2.59E6
Umtanum	Foundation Sciences, Inc. 1981	74-347	2.68E6
Hanford Basalt	Johnston and Palmer, 1981	?	3.35E6
Panona & Umtanum Basalts	Martines-Bel & Amick, 1978	50-300	2.98E6
Literative Range	Agapito, et al., 1977	?	2.77E6@
Literative Range	Maurer, 1968	?	2.78E6
Literative Range	Ratigan, 1976	?	4.18E6
Conceptual Design in Basalt	BWIP SCR Chapter 4	?	2.63E6 *[2.63E6-2.91E6]
Umtanum	BWIP SCR	20-350°C	2.58E6 *[2.27E6-3.213E6]
Middle Sentinel Bluffs Flow	BWIP SCR	20-350°C	2.11E6 *[2.191E6-2.595E6]
Pomona Member of the Saddle Mountains Basalt	BWIP SCR	20-350°C	2.32E6 *[2.078E6-3.46E6]

* Mean (arithmetic) constant pressure heat capacity for basalt with mean density of 2.77E3 kg/m^3.

@ Heat capacity used in the SWIFT models.

Heat capacities excerpted from Repository Site Definition in Basalt: Pasco Basin, Washington, NUREG/CR-2352, by R. Guzowski, F. Nimick, and A. Muller, 1982.

All hydrostratigraphic units in the SWIFT 2-D model are assumed to be isotropic with respect to thermal conductivity. This conductivity, 2.2w/m-°C, compares well with laboratory-determined values detailed in Chapter 4 of the BWIP SCR. The estimated value of thermal conductivity for the conceptual repository design in basalt is 2.3 w/m-°C (pg. 4.4-1, BWIP SCR, 1982). The thermal conductivity used in the SWIFT 2-D models is most similar to that of the Umtanum flow. These thermal conductivities are laboratory estimates, valid for temperature ranges of 10-350°C, and they do not account for the effects that structural discontinuities may have on thermal conductivity. Because the description of the input parameters for the PORFLO simulations in the SCR is incomplete, thermal conductivity is asssumed to be isotropic and equal to 2.3 w/m-°C throughout the model. The difference between the thermal conductivities used in the NRC and DOE subregional models of BWIP, 2.2 w/m-°C and 2.3 w/m-°C, respectively, may result in differences in the extent of the thermally-disturbed zone around the repository after waste emplacement.

The mean density of the basalts and sedimentary interbeds is assumed to be 2.77E3 kg/m^3. This value corresponds to fine-grained, glassy basalt and is referenced in the Repository Site Definition for Basalt (1982). The average densities for the basalts used in the conceptual design, Umtanum entablature zone, Umtanum Colonnade zone and Umtanum interflow zone are 2.8E3, 2.77E3, 2.85E3 and 2.41E3 kg/m^3, respectively (BWIP SCR, pp. 4.1-2 to 4.1-5, 1982). The assumption that the mean density of the sedimentary units is also 2.77E3 kg/m^3 remains unsupported.

The compressibility of the basalts and interbeds is assumed to be an arbitrarily-small value of 4.4E-15 1/PA. The SWIFT models are not expected to be sensitive to this nominal value; the porous units behave as though they were incompressible.

Water compressibility is assumed to be 4.4E-10 1/PA, taken from NUREG-3066 for the initial temperature range of 20-70°C. The heat

capacity of the water (reservoir fluid), also assumed for a similar temperature range, equals 4.18E3 J/kg-°C (NUREG 3066, 1982). The water thermal expansion value for SWIFT models is equal to 5.7E-4/°C.

The hydrostratigraphic units are assumed to have an isotropic mass dispersivity (i.e., $\alpha_L = \alpha_T$) of 25 m. These values remain to be verified by tracer tests, or similar proven techniques on the same scale as the system model. Mass dispersivities are a function of the scale of mixing in a hydrogeologic system as a product of hydrodynamic dispersion (BWIP SCR, 1982, p. 12.4-25). The paucity of data to support the assumed dispersivity factors limits the ability of these values to characterize the BWIP system. In comparison with the constant dispersivity factor of 25 m used in the SWIFT 2-D BWIP models, the values used in the PORFLO models are α_L= 50 m and α_T = 2 m for flow contact zones (i.e., flow tops and interbeds), and α_L = 2 m and α_T = 0.2 m for dense interior basalts. The SWIFT 2-D models will not be sensitive to the dispersivity factors because the models are not solving for radionuclide or solute concentrations and conduction dominates heat transport. The 1-U-1 model was executed using a dispersivity factor of 250 m to determine the sensitivity of the model, and the results from this variation of the model were identical to those of the standard 1-U-1 model.

Repository Data

The conceptual repository modeled in the 2-D SWIFT models of BWIP is identical to that of the PORFLO simulations. The repository is divided into two halves: the left half has a cross-sectional area of 3600 m^2 (1200 m x 3 m) and the right half has a cross-sectional are of 3000 m^2 (1000 m x 3 m). Within the 2-D model, the repository simulates a one meter-thick vertical slab through a mined disposal area with an initial inventory of 47,000 MTHM of 10 year-old spent fuel. Because the SWIFT models are subregional, room-scale and canister-scale design parameters and phenomena are not included or accounted for. The repository is represented by six grid blocks separated into groups of 3 blocks (1

layer) by approximately 800 m of dense flow interior basalt. The repository blocks have an isotropic hydraulic conductivity of 1E-10 m/s, effective porosity of 1E-2, and a heat capacity of 2.5E6 J/m^3-°C.

2.2 Application of SWIFT

2.2.1 Basic Assumptions

The use of any practical numerical or conceptual model demands assumptions, whose validity weights the results of the system study. The following section describes the assumptions upon which the results of the 2-D SWIFT models are predicated.

The SWIFT code, as applied to the 2-D BWIP models, assumes the following:

- All porous media behave like Darcian continua.
- Mass and energy are conserved.
- Water compressibility (C_w) is constant.
- Thermal expansion factor (C_T) is constant over any given temperature range.
- Water viscosities are within the code from the reference viscosity and the data of Lewis and Squires (1934).
- The groundwater flow and heat transport equations simulate three-dimensional, transient, laminar artesian flow.
- Aquifer properties may vary with position (node to node).
- Porosity may vary in time in response to pressure changes that affect the porous media.
- Hydraulic conductivity varies in response to temperature, viscosity, and density variations of the fluid with time.

- Change in the internal energy of the system equals the difference between enthalpy input and output, excluding kinetic and electromechanical potential energies.

- Inertial effects of fluid flow are insignificant at the low velocities of groundwater flow.

- Hydrodynamic dispersion is a function of the fluid velocity distribution.

- Hydraulic gradients across grid blocks or hydrostratigraphic units are evenly distributed to be consistent with the REV concept.

- The hydraulic properties of the hydrostratigraphic units are representative averages of the properties as measured in the field and scale effects are nominal.

- The density of fractures and structural discontinuities within the dense basalt units at BWIP is sufficient to represent them as anisotropic and homogeneous porous media.

- The fractures within flow tops are oriented randomly so that the flow tops may be modeled as being isotropically conductive.

- Although discrete fracture flow may be dominant through the basalts, the empirical modification factor for fracture media, ε, is approximately equal to one, so that travel time = u/n, where u = darcy velocity and n = effective porosity.

2.2.2 Computer Processing

The SWIFT code was adapted from a code developed for use in petroleum reservoir engineering. Since petroleum engineers and geohydrologists commonly use different formulations of the governing equations of flow, SWIFT has some awkward characteristics when used for the purposes of geologic repository simulation. Foremost among these characteristics is the need to specify boundary conditions in terms of pressures rather than heads. An elevation (hydrostatic) term, which does not drive flow, is present in the pressure equation:

$$P = \rho g(h-z) \qquad \text{(constant density case)} \qquad (1)$$

where P = pressure
ρ = fluid density
g = gravitational constant
h = head
z = elevation

For the grid depth involved in this analysis, the elevation term is often much greater in absolute magnitude than the hydraulic head. Also, in the BWIP cases considered, the hydraulic head gradient in the vertical direction ($\partial h/\partial z$) is much smaller in absolute magnitude than the elevation gradient ($\partial z/\partial z$):

$$\left| \frac{\partial h}{\partial z} \right| \leq .005 \left| \frac{\partial z}{\partial z} \right|$$

For this reason it is necessary that the input pressures be very precise, so that the differential head term is not lost in computations due to round-off error.

Also, the density term in equation (1) is generally non-constant due to thermal expansion of the fluid in response to a geothermal gradient. This density variation compounds the problems with boundary pressure calculations. To facilitate SWIFT modeling, a pre-processing program was written. This program calculates pressures from known heads, considering the effects of thermal expansion and fluid compressibility. These pressures are calculated to seven significant digits.

SWIFT has also been augmented with several post-processing packages. CRSEC, a graphics plotting program, plots pressure and temperature contours and velocity vectors for the grid at selected time steps. A particle tracking program, STLINE, uses steady-state velocities and plots particle locations at specified times. When applied in transient simulations, STLINE must be run in steps, using constant Darcy velocities throughout each time step. The resultant particle tracking plots from consecutive time steps are then strung together in series, effectively simulating the flow path in the transient case.

2.3 Alternative Conceptual Models

The conceptual model, upon which 1-U-1 is based, consists of areally continuous, stratiform basalt flows that may be divided into dense flow interiors and contact zones with several relatively thin sedimentary argillaceous and arenaceous interbeds. Since the dense flow interiors behave as low conductivity confining beds, groundwater flow systems are confined in the horizontal flow tops; the flow tops and contact zones are assumed to be homogeneous, areally continuous artesian aquifers. Most of the vertical head loss through the layered groundwater systems occurs across the dense flow interiors, creating nominal vertical hydraulic gradients across the more conductive flow tops (i.e., 1E-5 m/m). In contrast to the vertical head gradients, the horizontal gradients are controlled by the flow tops because these rather conductive (1E-5 to 1E-7 m/s) units do not usually maintain large hydraulic gradients greater than 1E-2 m/m.

This model, however, does not include the effects of known structural and stratigraphic discontinuities present within the Pasco Basin hydrogeologic system. Mesoscale structural and stratigraphic discontinuities may be observed in surface exposures of the Umtanum Flow, for example, at the Emerson Nipple Section, where the Umtanum intersects the land surface on the western flank of the Cold Creek Syncline 10 km from the RRL. The importance of these discontinuities is recognized by DOE in Chapter 3 of the BWIP SCR; such features introduce heterogeneity to the geologic system and may dominate groundwater flow. Aeromagnetic anomalies within the Pasco Basin may be interpreted as significant subsurface structures that effectively control the flow system (DSCA, p. 3-4). Isopach and structural contour maps of the basalt flows at BWIP indicate that individual basalt layers may not be laterally continuous through the Pasco Basin. Outcrops show that flow thicknesses may vary substantially on the meter, decameter and kilometer scales.

The conductive rubble zone, which may be present at the base of basalt flows, is composed of rough blocks of basalt and exoliths. The basal colonnade, above the rubble zone, consists of compositionally homogeneous basalt that has been pseudo-hexagonally jointed to form vertical and subvertical columns or prisms. These columns, which average three feet across, are dissected by cross-cut joints. Cross-cut joints are generally normal or oblique to the prismatic axis. Above the basal colonnade, the hexagonal columns merge into a more complex zone of curved columns and dissected blocks of basalt. The flow sequence is capped by the upper colonnade zone which may also be pseudo-hexagonally jointed. This upper colonnade zone is commonly vesicular or scoriaceous. These structures, which may cause the basalt flows to be hydraulically anisotropic and heterogeneous, are illustrated in Figure 8.

Structural discontinuities include kilometer-scale faults, lineaments, flexures, and folds (e.g., fracture zones associated with Gable Mountain-Umtanum Ridge Anticline), decameter-scale fracture zones (e.g., the Nancy Linear), and meter to centimeter-scale tectonic breccias, columnar joints, inverted fans and cones, dimples, vesicular zones, tectonic fractures, weathering horizons, pillow layers, and cross-cut joints to name several examples.

Stratigraphic discontinuities are also present within the Pasco Basin basalts on several scales, including decameter-scale flow and interbed pinchouts and meter-scale rolls and scours.

The conceptual model, of which 1-U-1 is a numerical approximation, is an oversimplification of the hydrogeologic system at BWIP. This is one reason why the travel times included in the BWIP SCR are not supportable (DSCA, p. 3-4). Alternative models are included in this report not to examine all possibilities, but rather to begin an assessment of system sensitivities and explore the various consequences associated with these alternative defensible models.

As described in the BWIP DSCA (1982), the key hydraulic parameters of the conceptual and numerical models of the flow system at BWIP have only been constrained to ranges of several orders of magnitude. Although DOE models use "representative values" for these parameters, uncertainties in field testing methods and the hydrogeologic system extend the ranges of possible values over several orders of magnitude.

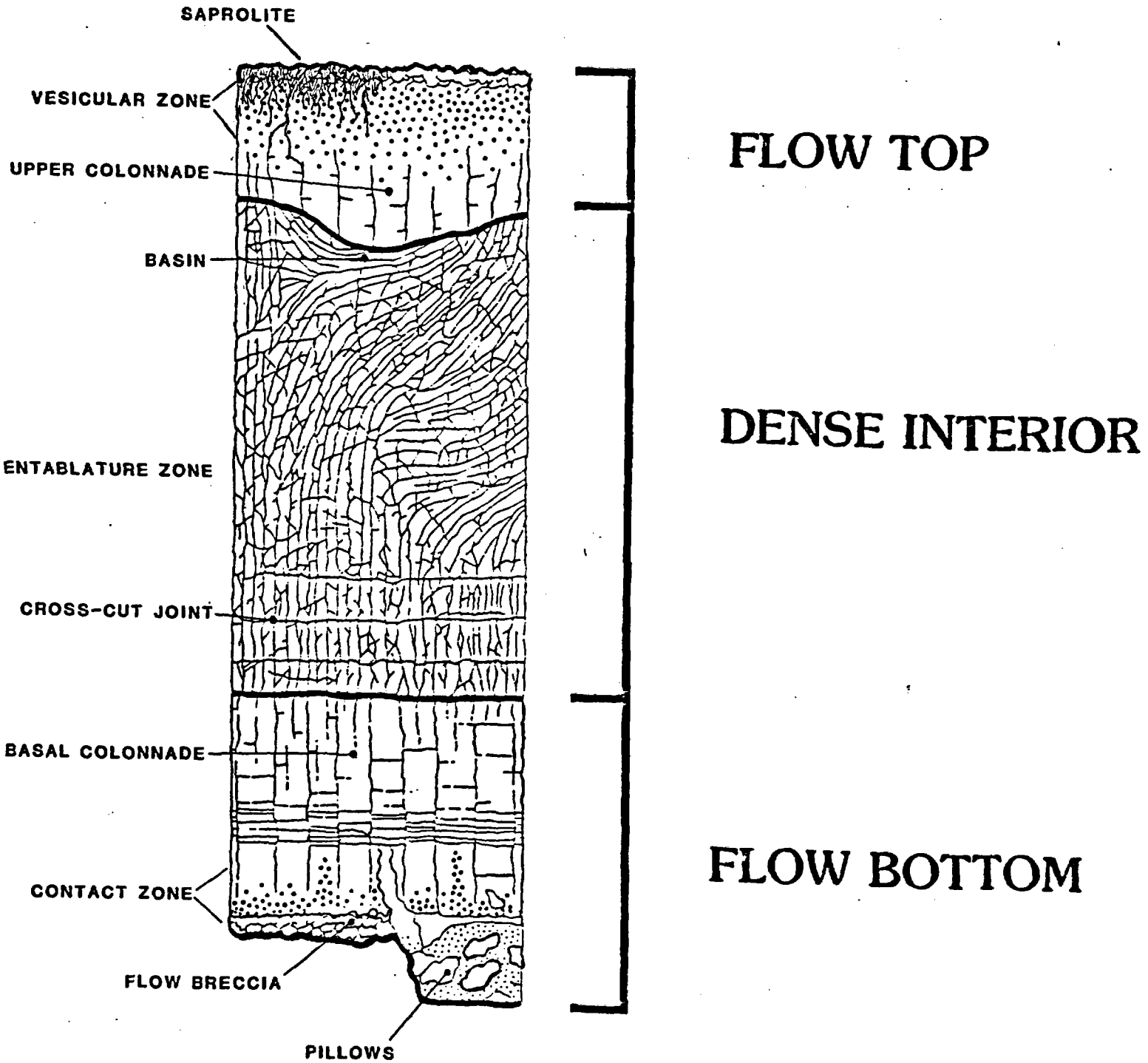

Figure 8. Intraflow structures and typical portions of basalt flows showing the predominance of structural discontinuities and inherent heterogeneities of flow basalts (modified from Jones, K., RHO-BW-ST-36 P, 1982, p.15).

Model 2-U-1: A More-Conservative Conceptual Model

Model 2-U-1 is based on a variation of the DOE conceptual model of the BWIP hydrogeologic system. Individual layers are areally continuous and homogeneous in their hydraulic properties. The boundary conditions are the same as in 1-U-1, the PORFLO duplication model. The RRL-2 profile is enforced on both lateral boundaries of the model and a constant horizontal hyrdaulic gradient of 1E-3 m/m is enforced across the grid. The difference between the 2-U-1 and 1-U-1 models is in the assigned hydraulic parameters of the hydrostratigraphic units. The values of the hydraulic parameters are compared in Tables 3, 4, and 5.

The hydraulic conductivities of the basalt units have been increased compared to the 1-U-1 model. The conductivities of all flow tops within the Frenchman Springs, and the Upper, Middle and Lower Sentinel Bluffs flows have been increased to 3E-5 m/s. Once again, the model assumes that the orientation of small-scale discontinuities within these flow tops is sufficiently random so that they are hydraulically isotropic. The hydraulic conductivity of the Umtanum flow top has also been increased to 3E-7 m/s. These values correspond to the upper limits of the 95% confidence interval for mean unit transmissivities as described in Appendix H of the BWIP DSCA (1983).

The hydraulic conductivities of the dense zones of the layered system have also been increased compared to those of the 1-U-1 model. The increased conductivities again reflect the dominant effect of structural discontinuities within the dense basalts on the flow field. The units are anisotropically conductive with the largest conductivities in the vertical direction.

Only the vesicular zone and Vantage interbed have hydraulic conductivities that are less than the values used in 1-U-1. The vesicular zone in 2-U-1 is modeled as a homogeneous anisotropic unit with

a horizontal hydraulic conductivity of 1E-11 m/s and a vertical conductivity of 3E-9 m/s. The conductivity of the sedimentary Vantage interbed between the Frenchman Springs member and the Grande Ronde Group is reduced by a factor of 3 in the 2-U-1 model compared to the value used in the 1-U-1 model. The Vantage is also the only hydrostratigraphic unit in 2-U-1 with the same porosity value, 10%, as in the 1-U-1 model.

The porosities of the other units are one to two orders of magnitude less than in the 1-U-1 model. These porosities are more representative of the effective porosity (Φ_E) value measured in a field tracer test than the porosities used in the DOE conceptual model of BWIP. The porosities are listed in Tables 3, 4, and 5.

The hydraulic properties of the repository, the individual layer thicknesses and the thermal properties of all units, as well as the grid configuration are the same in both models. These parameters were held constant so that the system could be tested to determine the sensitivity to more conservative values of the hydraulic parameters (K_H, K_V, Φ_E). Although changing the hydraulic properties of the hydrostratigraphic units while maintaining the same boundary conditions will change the head distribution throughout the modeled system, numerical problems associated with this redistribution are assumed to be negligible. This assumption will be discussed in the results section and is subject to verification.

Model 3-U-1: Conceptual Model without Layers

In this model, the basalt flows are so densely-fractured and the fractures are oriented randomly so that the entire hydrogeologic system at BWIP is vertically connected, the dense flow interiors are not low-permeability barriers to flow, and the flow tops do not behave like confined aquifers; the system is treated hydraulically as if it were not a layered system with isolated flow systems. The assumption that all the hydrostratigraphic units have the same hydraulic properties is consistent with level of site characterization which has restricted vertical

hydraulic conductivities, for example, to within 5 orders of magnitude and horizontal hydraulic conductivities to within 3 orders of magnitude (BWIP DSCA, p. 3-7). Although this system is geologically an areally discontinuous, layered system, it behaves hydraulically as a large-scale, homogeneous, anisotropic system. The ubiquitous intraflow structures, such as inverted fans, dimples, cones, basins, columnar joints and cross-cut joints are assumed to connect the flow systems of the flow tops so that the system behaves as a homogeneous, porous-flow equivalent, continuum model on the subregional scale (see BWIP DSCA Chapters 3 and 4, and Appendices L and H, 1983; and BWIP SCR, Chapter 3.5, 1982).

In this model, all hydrostratigraphic units are isotropically conductive with hydraulic conductivities of 1E-9 m/s and porosities of 1E-4. These conductivities are within 3 orders of magnitude of those used in the 1-U-1 simulation. The porosity values are within the range of uncertainty of the effective porosity measured for the Umtanum of 1E-3 magnitude uncertainty range around the measured value of 1E-3 in the SCR as detailed in the BWIP SCR (BWIP DSCA, 1983, Appendix D). While the repository details, grid configuration, layer thicknesses, and thermal properties are the same as in model 1-U-1, the boundary conditions have been altered to enforce uniform hydraulic gradients of 1E-3 m/s in the vertical and horizontal directions. Uniform and low gradients are enforced since current information on head distribution through the Pasco does not support a unique head distribution. By comparing different sets of wells, investigations have determined several alternative flow paths (Appendix H and Chapter 3, BWIP DSCA, 1983). For this reason, very general hydraulic gradients (up and to the right in model 3-U-1) are assumed without the isolated flow systems suggested by DOE.

Model 4-U-1: Initially Hydrostatic Model

The last of this suite of four models, 4-U-1, is executed solely to determine the importance of the thermal effects of the repository. To eliminate groundwater flow that may be occurring in response to natural

(pre-emplacement) hydraulic gradients, boundary conditions are chosen to enforce hydrostatic heads with depth (dh/dz = 0). Head gradients are established only after the repository begins to emit heat as the radioactive waste decays and heat is generated.

The hydraulic properties, layer thicknesses, grid configuration, repository details, and thermal properties are the same as in model 2-U-1. The only difference between 4-U-1 and 2-U-1 is the boundary conditions. In 2-U-1 the RRL-2 profile is enforced along the lateral boundaries with a horizontal gradient across the model of 1E-3 m/m. In 4-U-1, the heads along the boundary nodes are in hydrostatic equilibrium, and the nodal pressues change in response to changes in depth and density of the overlying column of water above individual nodes.

2.4 Application and Results

2.4.1 1-U-1 Modeling Results

Pre-emplacement Study - 1-U-1

The 1-U-1 conceptual model, as described in Section 2.3, was analyzed using SWIFT. A steady-state solution without any internal heat source yielded the initial steady pre-emplacement conditions. The resultant head, Darcy velocity and particle tracking plots are shown in Figures 9, 10, and 11.

As shown in Figure 9, the horizontal gradient of 10^{-3} meters/meter was maintained throughout the model grid. The vertical RRL-2 profile imposed is clearly reflected in the output heads on both vertical boundaries. In the interior of the model where the vertical profile is not enforced, the profile is less similar to the RRL-2 profile. The internal profile is a function of the hydraulic properties of the hydrostratigraphic units.

The Umtanum flow top is clearly defined in the figure. Due to the relatively more conductive properties assigned to the flow top, we would expect that little head drop will occur vertically across the flow tops, relative to the denser zones. This explains why the set of head contours are nearly vertical in the Umtanum flow top shown. The pattern suggests that horizontal flow is dominant in the isotropic Umtanum flow top. Other flow tops are less distinct in the figure because they are much thinner than the Umtanum (see Figure 4).

The steady-state, initial condition Darcy velocity vector plot is shown in Figure 10. In this plot, each of the 178 grid nodes is represented by a vector, whose orientation and length indicate the direction and

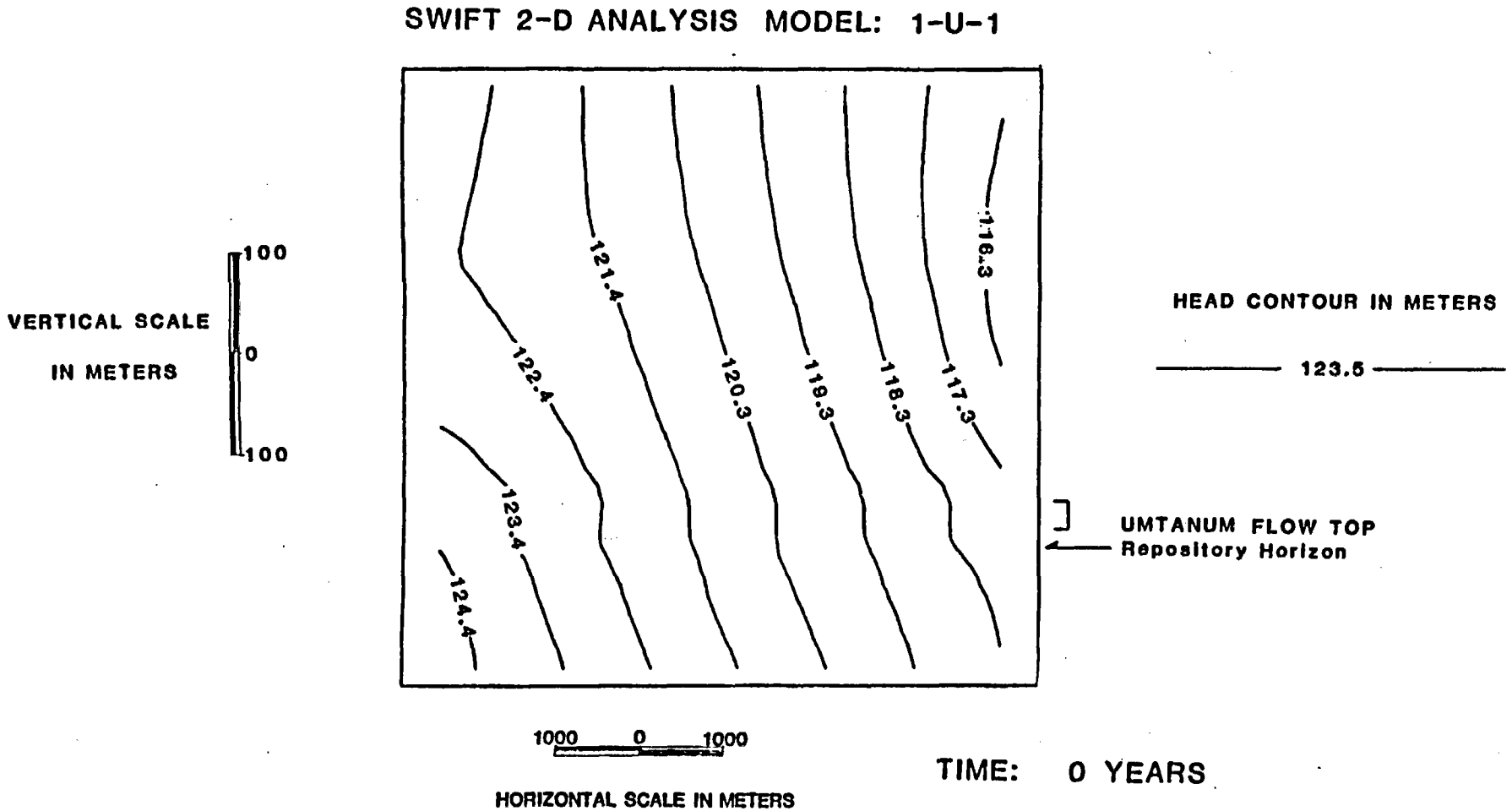

Figure 9. Initial, steady-state, pre-emplacement head distribution in the 1-U-1 model. Notice the refraction of the head contours along the contact between the Umtanum flow top and dense flow interior.

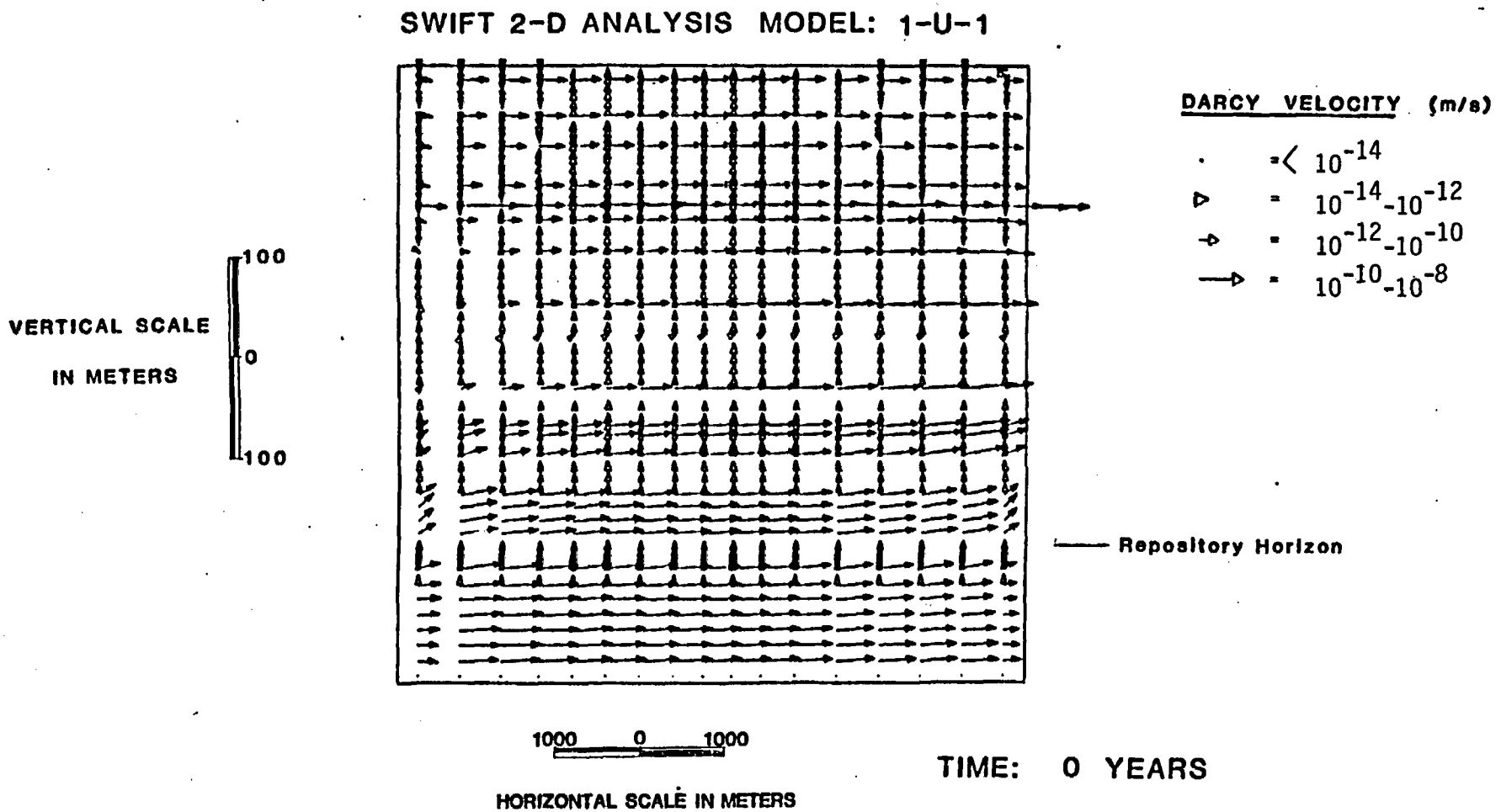

Figure 10. Darcy velocity distribution for the initial, steady-state, pre-emplacement 1-U-1 model. Notice groundwater flow is predominantly horizontal in flow tops and vertical in dense flow interiors.

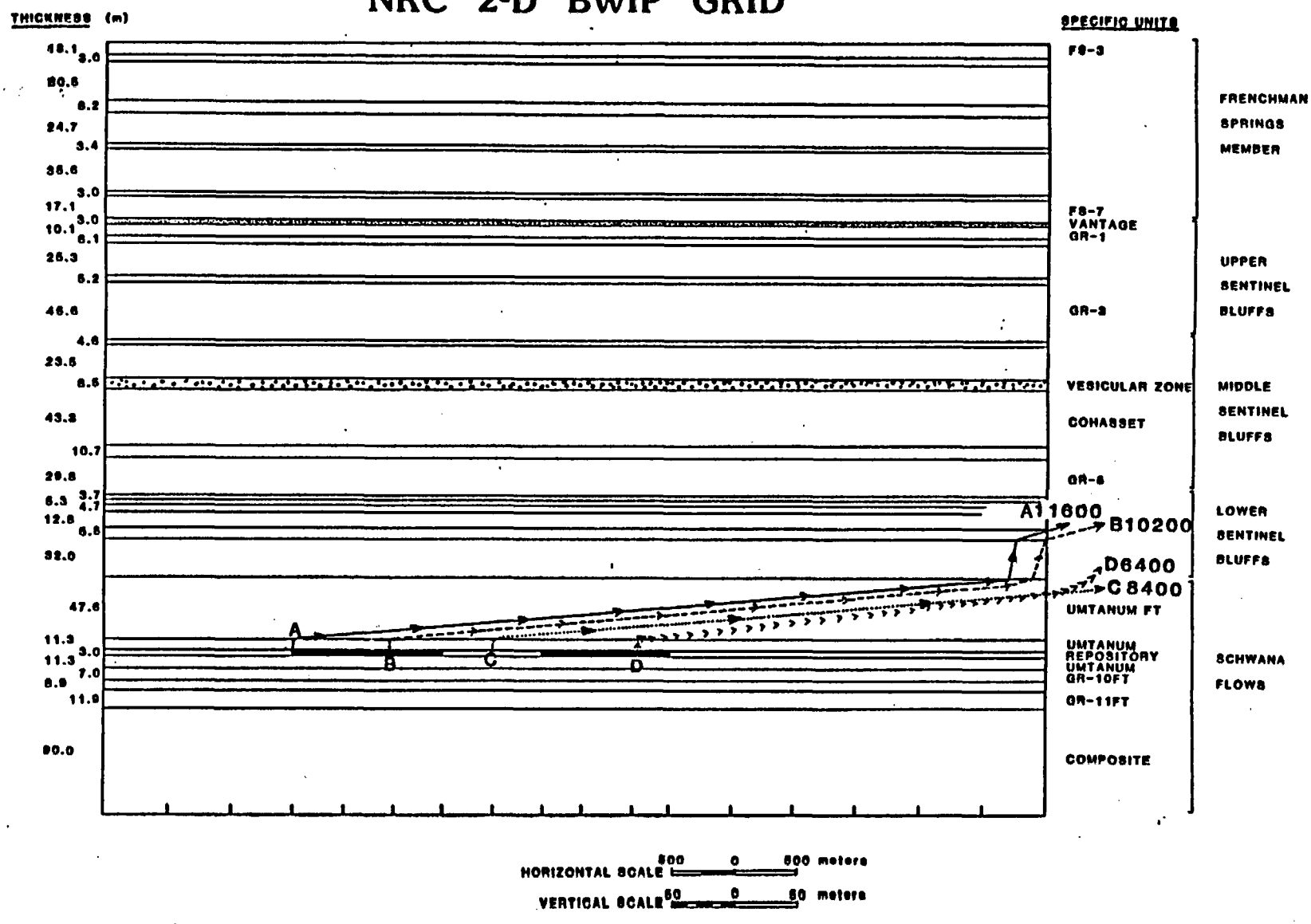

Figure 11. Pre-emplacement pathlines in the 1-U-1 model. Travel times are listed to the right of the particle label. Times listed are in years from time of release at the repository to time of exit along the right side boundary.

magnitude, repectively, of the calculated Darcy velocity for that node. The figure shows nearly vertical flow in the dense zones due to the higher vertical conductivity (relative to the horizontal conductivity) assigned to those layers and the upward boundary gradient applied. In contrast, the velocity vectors in the flow tops are principally horizontal. Given this distribution of Darcy velocities, a zig-zagging upward flow path may be inferred. This suggests that the groundwater flow could be approximated by a network of one-dimensional horizontal and vertical pipes in future pre-emplacement sensitivity studies, if desired.

The particle tracking plot (Figure 11) shows the paths of four particles (A, B, C, and D) released from various points in the Umtanum repository horizon using the SWIFT-generated Darcy velocity output. The particles are tracked from point of release to the model boundary (approximately four kilometers to the right of the center of the repository horizon). All four particles remain in the Umtanum flow top for most of the simulation period. The leftmost particle travels to the grid boundary (6 km) in 11,600 years. The rightmost particle travels 3.3 km to the boundary in 6,400 years.

Post-emplacement Study - 1-U-1

Once the heat source (repository with 47,000 metric tons of ten year old spent fuel, as described in Section 2.2) begins radiating, the heat significantly alters the flow regime at early times. In Figure 12, the head distribution at 10 years after repository closure is shown. Even at this early time, the head contours have been distorted from the initial conditions (Figure 9) due to the thermal perturbation of the system. It is apparent that water is being drawn from the area around the repository, particularly from the up-gradient side. In Figure 13, the head profile at 100 years is shown. At this time, the disturbance is

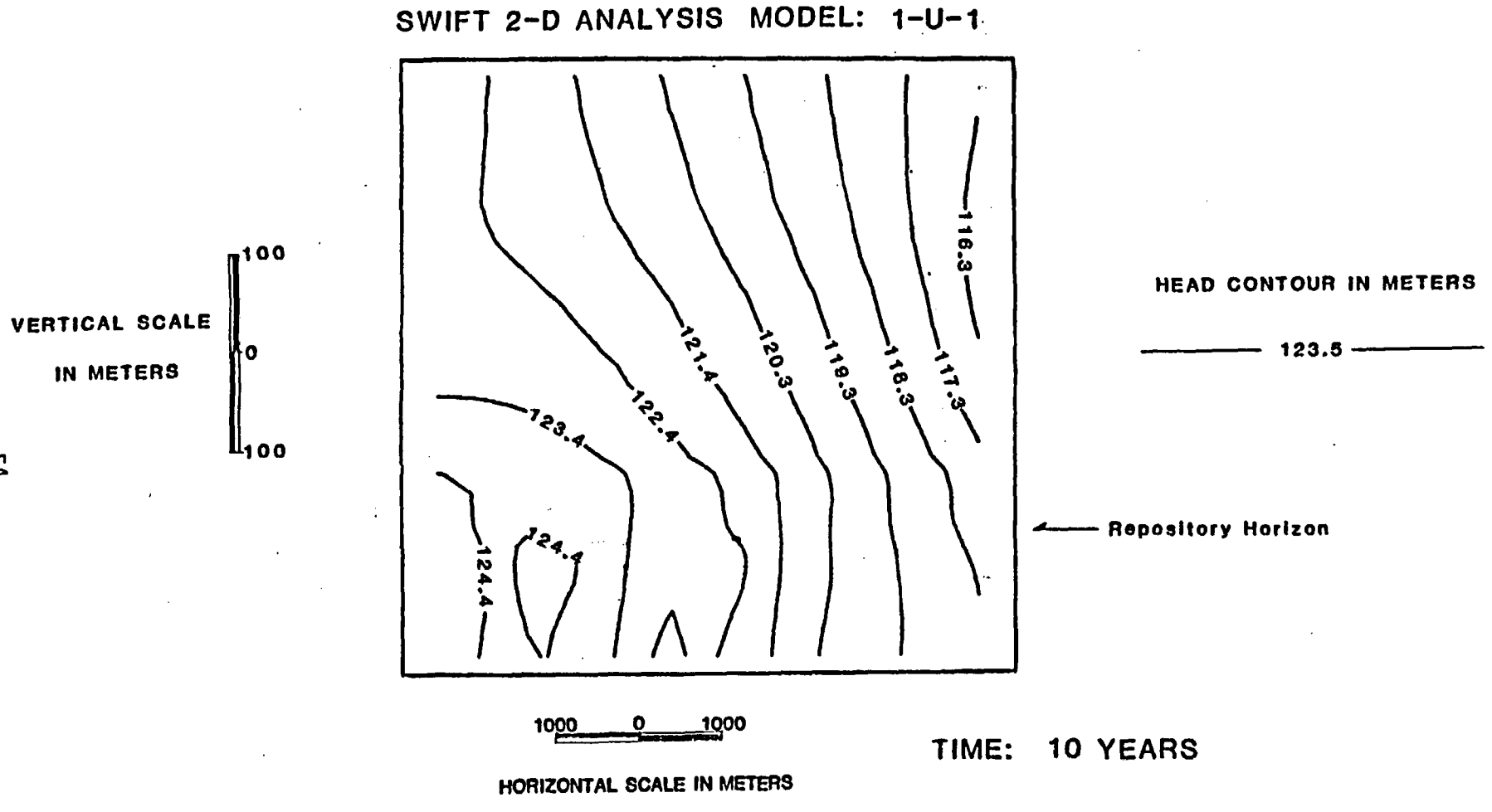

Figure 12. Head distribution in the 1-U-1 model at 10 years after waste emplacement. Compare with pre-emplacement, steady-state head distribution.

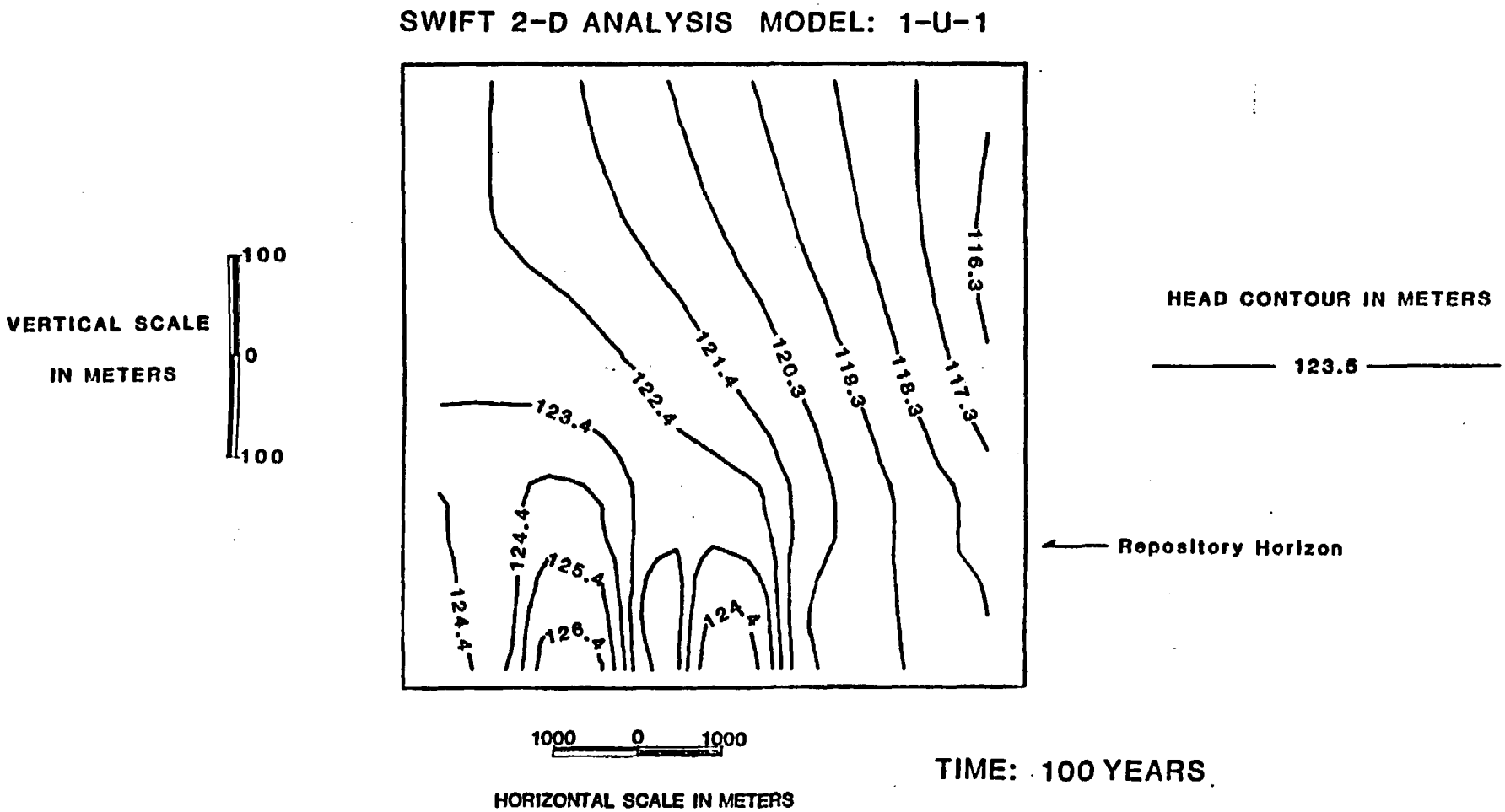

Figure 13. Head distribution in the 1-U-1 model at 100 years after waste emplacement.

much more pronounced. The hydraulic gradient in the vicinity of the repository has doubled since t=10 years. Water is being drawn upwards from below the repository and directly through the repository. A convective cell is developing between the repository halves. At the top of the grid, most distant from the repository, the heads remain at the original ambient heads. The temperature near the repository at this time is approximately 130°C (Figure 14). The symmetry of the temperature profile indicates that thermal convection is very small relative to conduction through the saturated basalt.

The head profile at 1,000 years (Figure 15) indicates a continuation of the clearly defined perturbation due to the heat source. The hydraulic gradient in the vicinity of the repository has more than doubled since t=100 years. At 2000 years, the head profile (Figure 16) indicates that the perturbation has extended vertically, but the hydraulic gradients have stopped increasing in the vicinity of the repository. The temperatures near the repository at this time have decreased to about 85°C. Between 2000 and 3000 years, the repository continues to cool down. While the heat source is still significantly affecting the groundwater flow, the extent of the perturbed zone has decreased (Figure 17). The temperature of the repository has cooled to about 76°C, about 12°C above the assumed ambient temperature at the repository horizon.

At 50,000 years, the temperature of the repository has cooled to nearly ambient (69°C) and the effects on the flow pattern have become very localized. Except for a small perturbed zone of perhaps 50 to 75 meters radius around the repository, the head distribution has returned to the pre-emplacement profile (Figure 18).

Figure 19 is a particle tracking plot through time of the transient NRC SWIFT simulation of the 1-U-1 case. The paths of four particles (A, B, C

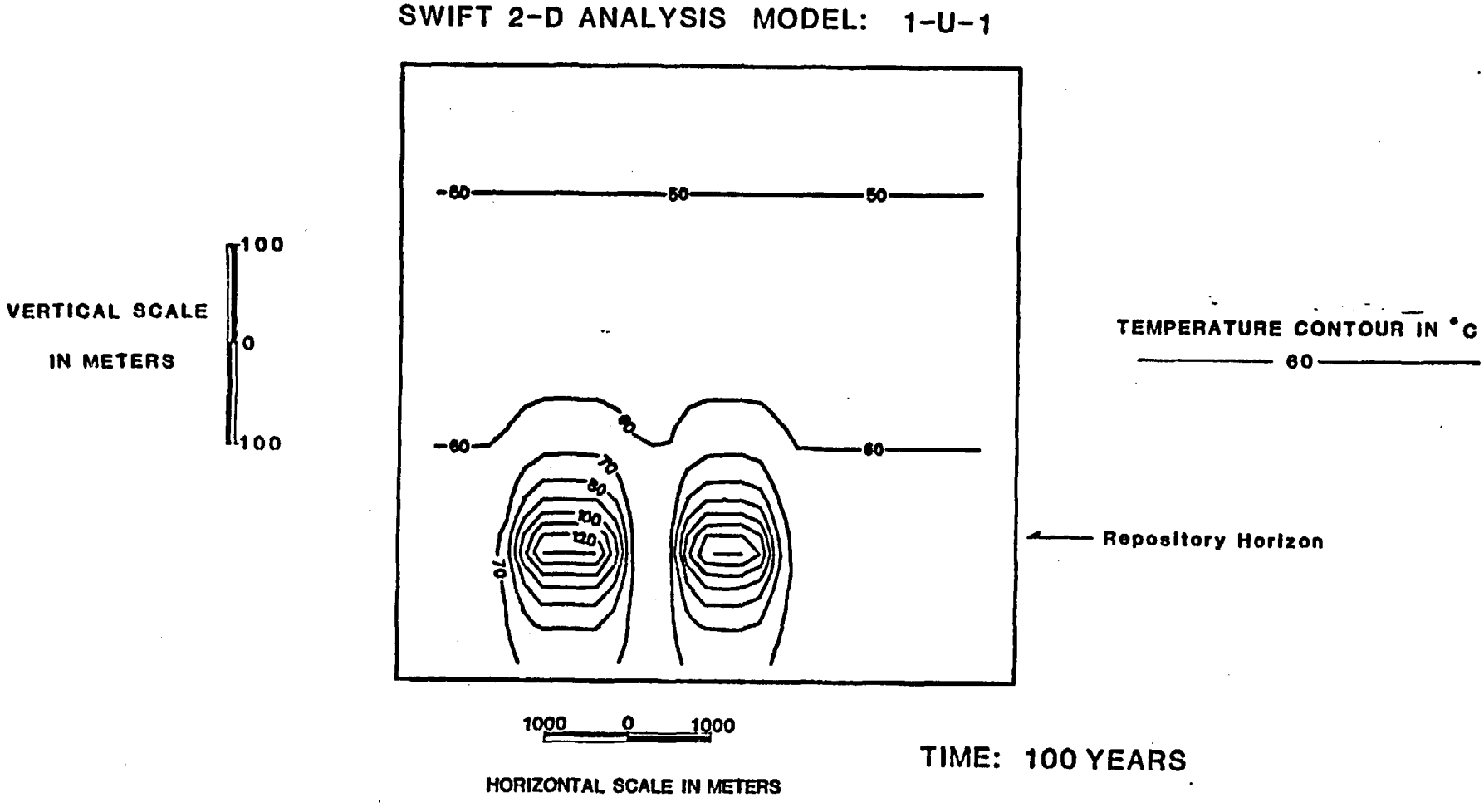

Figure 14. Temperature distribution around the repository in the 1-U-1 model at 100 years. Maximum temperature at the repository is 130° C.

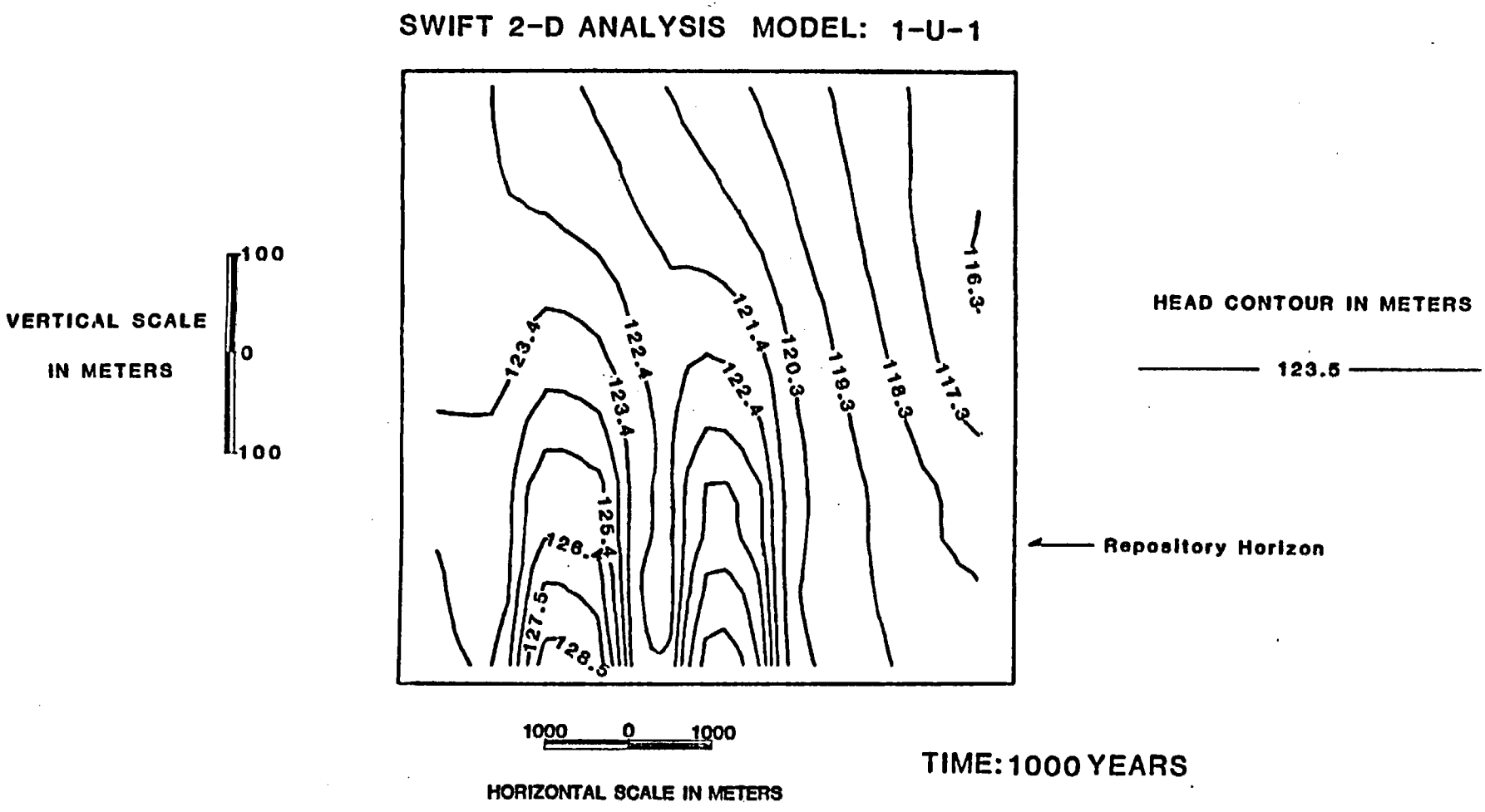

Figure 15. Head distribution in the 1-U-1 model at 1000 years after waste emplacement.

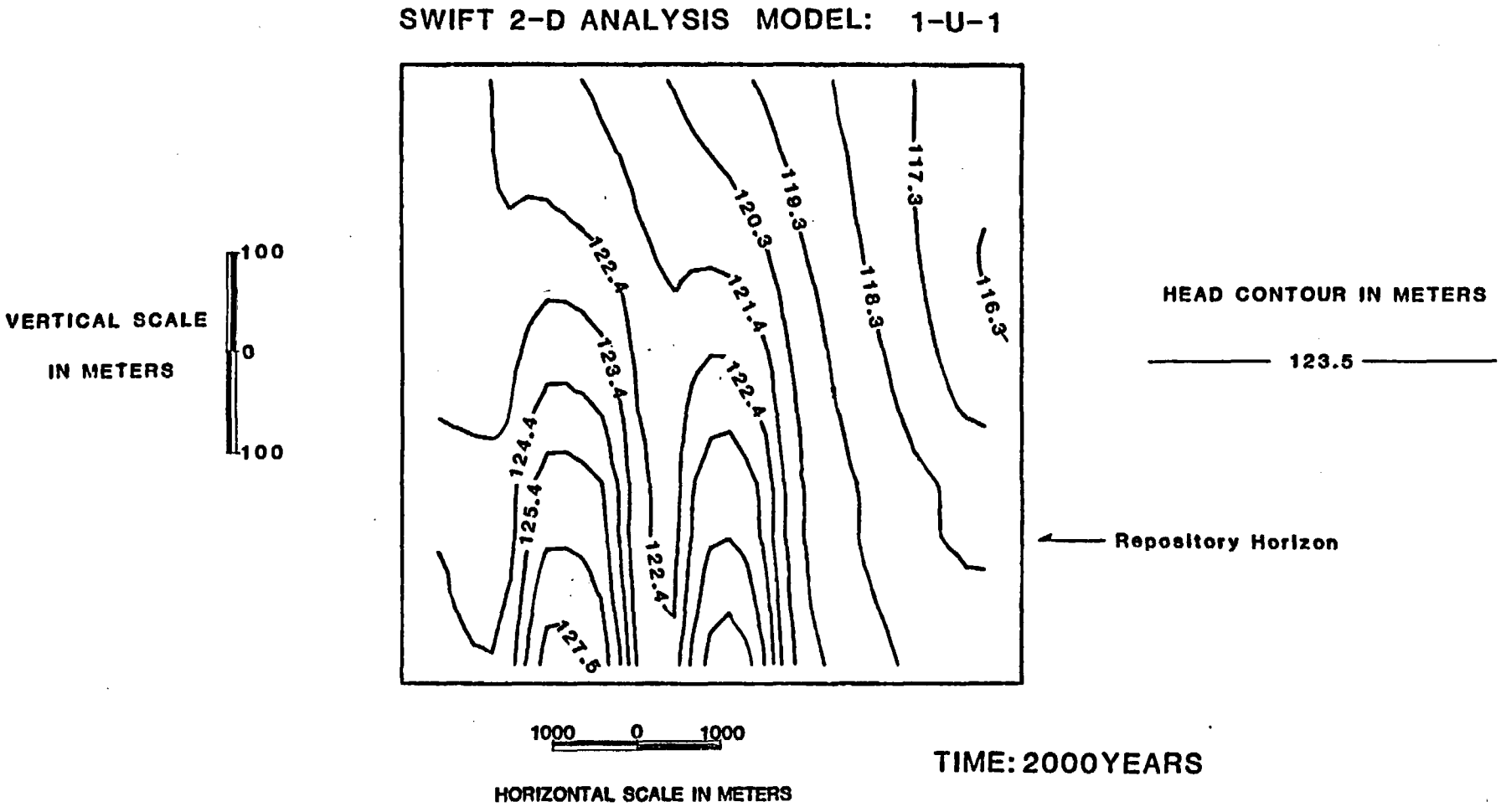

Figure 16. Head distribution in the 1-U-1 model at 2000 years after waste emplacement.

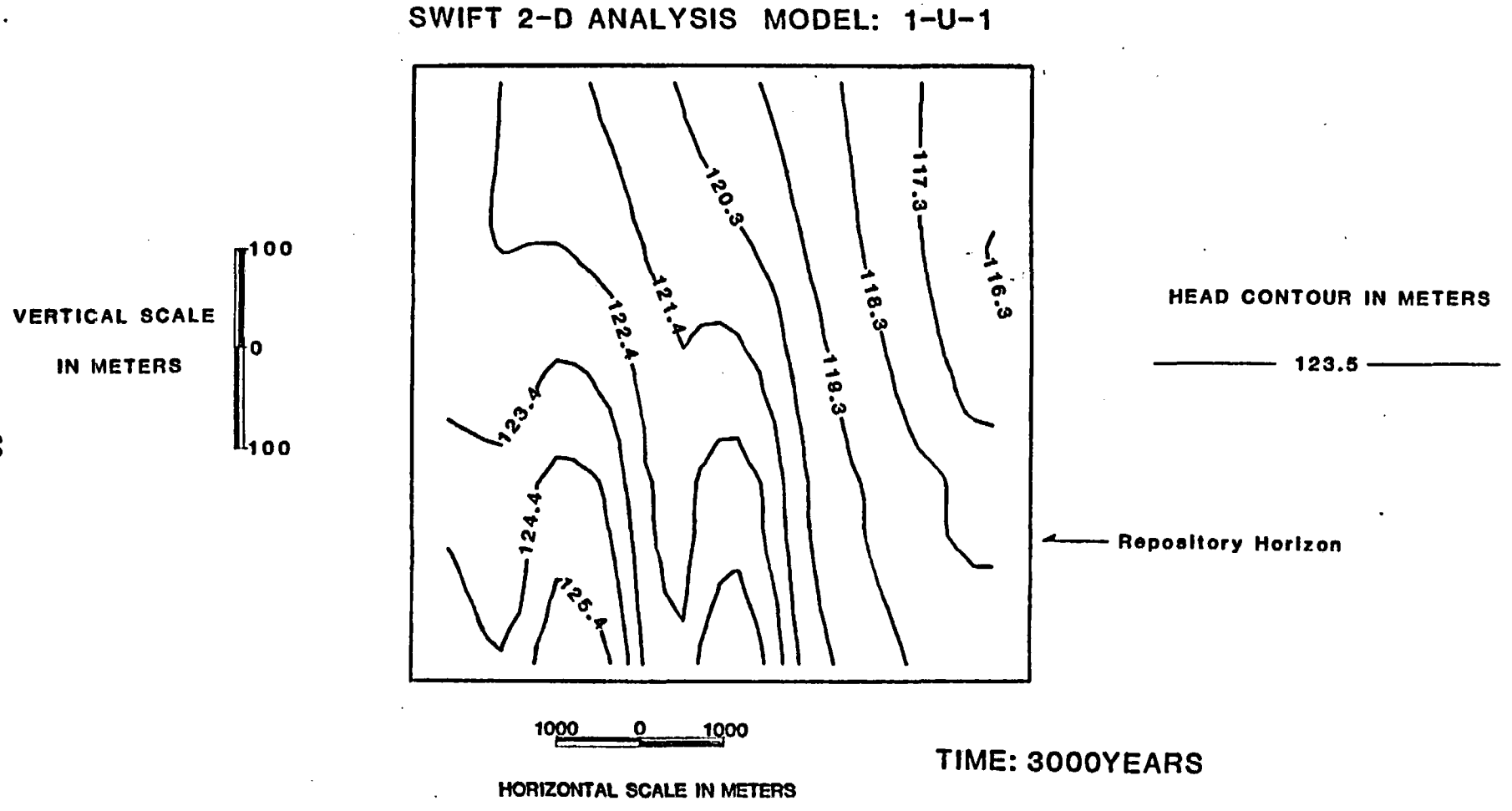

Figure 17. Head distribution in the 1-U-1 model at 3000 years after waste emplacement.

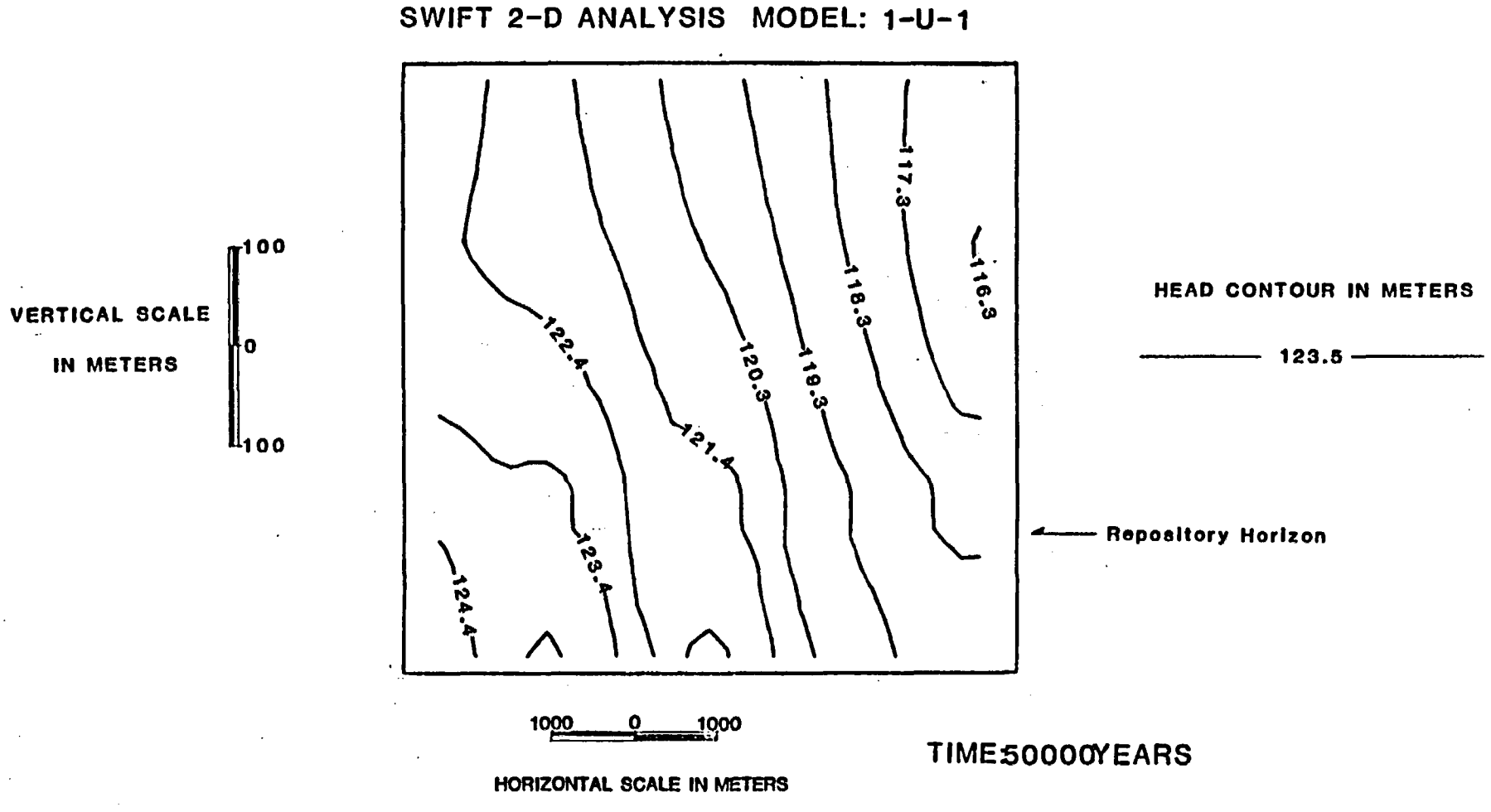

Figure 18. Head distribution in the 1-U-1 model at 50000 years after waste emplacement.

and D) have been plotted through time with the transient case variation of the STLINE program. Particle A, released from the left edge of the repository, exits the grid in the Vantage layer in approximately 9,800 years. Particle B, released from the middle of the left half of the repository, exits the grid in the Grande Ronde 3 flow top in approximately 12,700 years. Particle C, released from between the two repository halves, travels downward, horizontally, upward through the repository and then laterally in the Umtanum flow top. This particle exits the grid in approximately 7,100 years. Particle D, released from within the right half of the repository, travels laterally in the Umtanum flow top, exiting the grid in approximately 5,300 years.

Comparison of 1-U-1 With PORFLO

The DOE PORFLO simulation employs a zero upward gradient below the Umtanum, which differs from the NRC's 1-U-1 case, which employs a 10^{-3} upward vertical gradient below the Umtanum, as explained in Section 2.1. The DOE PORFLO grid extends 1.4 km less to the right than the NRC SWIFT grid.

Figure 20 shows the pathlines and travel times from DOE's PORFLO simulation, as given in the SCR (p. 12.4-39). In this figure, particles numbered 1 through 6 have been tracked through time. The precise points of release of these particles are not given in the SCR.

The DOE PORFLO model results may be compared to the NRC SWIFT model results by selecting the most nearly equivalent particles (from figures 19 and 20) in terms of release points and comparing their pathlines and travel times. The NRC simulations use lettered particles, while the DOE simulation uses numbered particles. The PORFLO particle most nearly equivalent to SWIFT particle A is PORFLO particle 1. The paths of

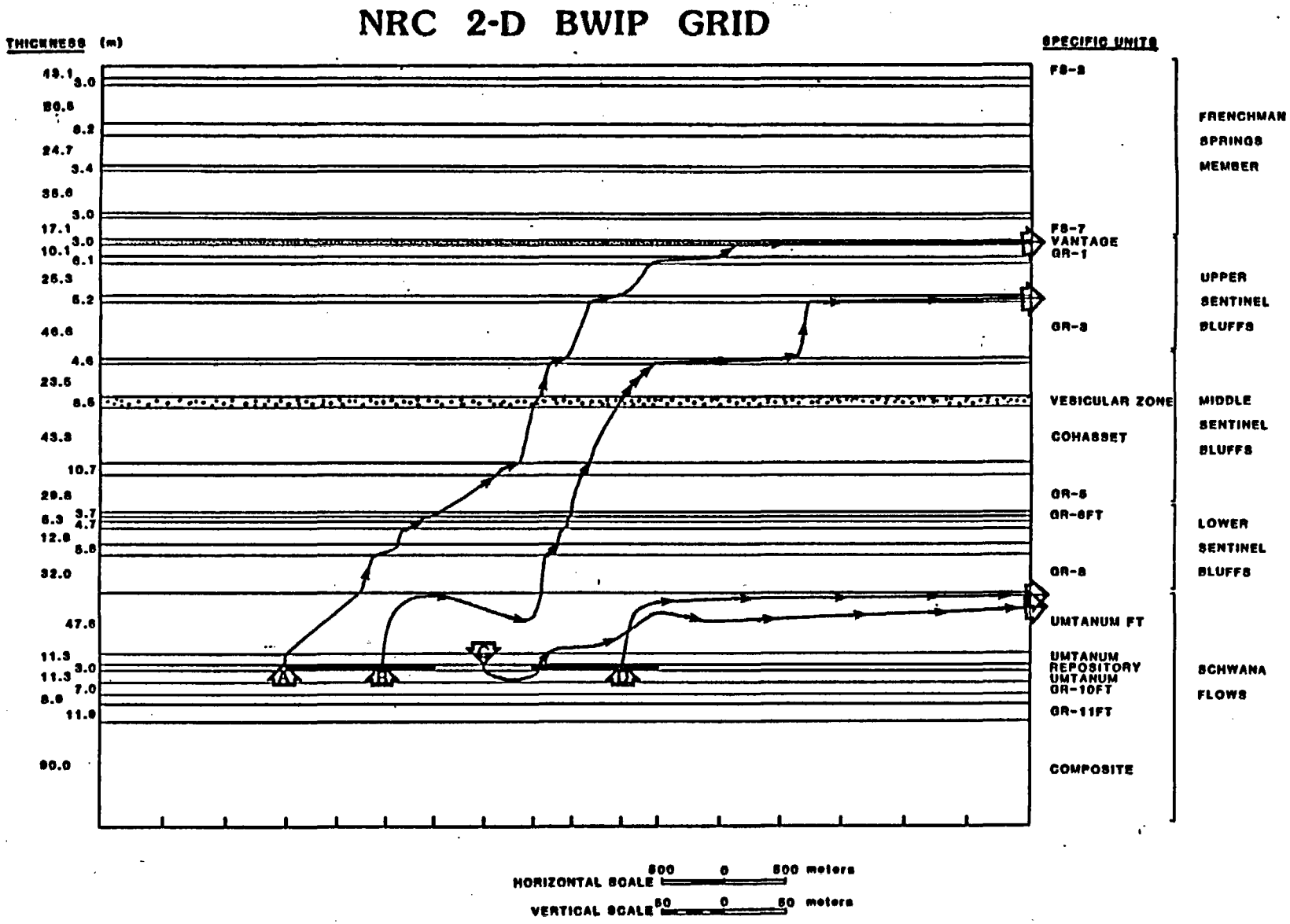

Figure 19. Post-emplacement pathlines for the transient 1-U-1 model. Particles are released from the repository at 1000 years after waste emplacement. Distance between two succeeding arrow tips is distance traveled in 1000 years. For example, particle D travels to the right boundary in approximately 5,000 years.

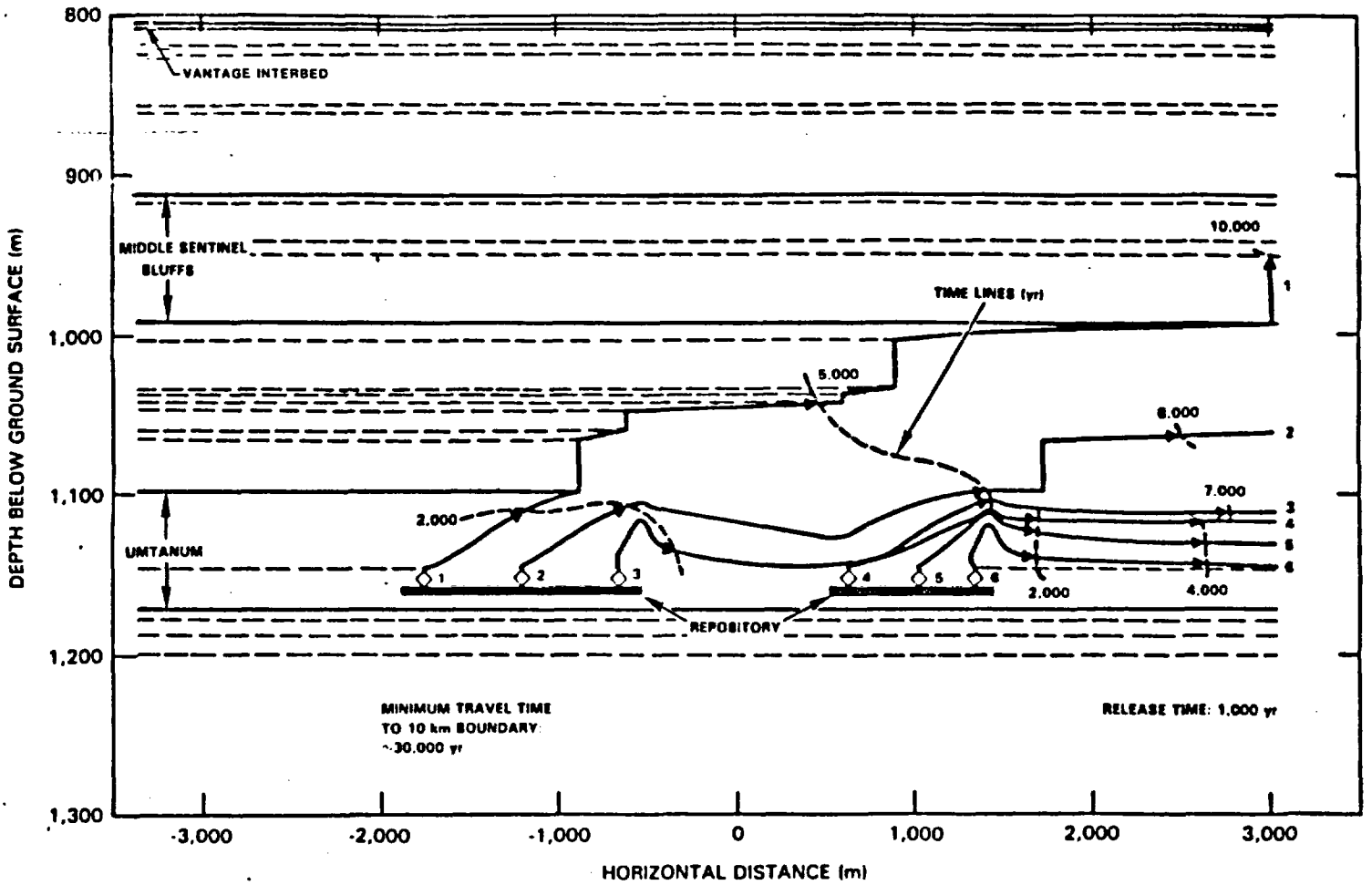

Figure 20. Groundwater pathlines and travel times for the PORFLO Base Case with the repository in the Umtanum Dense Flow Interior (BWIP, SCR, p. 12.4-39, 1982).

Particle A and Particle 1 are similar. However, in the NRC simulation Particle (A) travels roughly 200 meters higher than Particle 1. The travel times for Particle A and Particle 1 remain nearly identical until Particle A reaches the Vantage layer, which has triple the conductivity of the other flow tops. Once in this layer, Particle A travels three times faster, resulting in a relatively shorter travel time.

PORFLO Particle 2 and SWIFT Particle B, which would be nearly equivalent to Particle 2, exhibit the same upward flow, at first remaining in the Umtanum flow top and arcing slightly downward until they reach the area above the right repository half. At this point, both particles begin to rise again. The NRC simulation shows Particle B rising about 300 meters higher than the PORFLO Particle 2. They exhibit similar travel rates, the NRC Particle B taking roughly 1,000 years longer to reach the distance to DOE's grid boundary due to the increased path length.

The path and travel time for Particle D in Figure 19 and equivalent particles 5 and 6 in Figure 20 are nearly identical. Both particles begin with an upward, lateral path, arc slightly downwards away from the repository and exit the grids in the Umtanum flow top. SWIFT Particle D travels slightly faster than PORFLO Particle 6, traveling about 1.4 kilometers further in about the same 5000 year time. An equivalent to Particle C was not tracked in the figure provided in the SCR.

Discussion: 1-U-1 Model

Generally, it can be said that the SWIFT simulation produced results comparable to the PORFLO results. The path shapes and travel times are similar. Due to the uncertainties involved with creating an exact duplication of the PORFLO models, the duplication exercise is considered successful. It is known that the DOE utilized a smaller vertical

gradient boundary condition below the repository. The ambient temperatures used by the DOE were slightly (-8°C) different than those used by the NRC. Also, the conductivities in the DOE simulation were input for each layer using the layer temperature as the reference temperature; the NRC input all the conductivities at the reference temperature of 25°C. (Both models adjust the conductivities for subsequent changes in temperature.) The difference in reference temperatures is therefore in excess of 30°C at the repository horizon between the two models. This difference can cause a difference in the actual hydraulic conductivities applied in the model by a factor of up to approximately 1.7, due to the strong temperature dependence of viscosity.

The SWIFT 1-U-1 simulation was performed prior to receiving the information in the above paragraph. It is expected that adjusting these details to more accurately mimic DOE's PORFLO input would produce more similar simulation results. In spite of these disparities, the SWIFT code has shown itself to be an acceptable tool for performing two-dimensional heat transport and groundwater flow simulations.

2.4.2 Other Cases

The gradients, conductivities, porosities and hydrostratigraphy chosen in the 1-U-1 conceptual model described above are considered by the NRC to be non-conservative compared to data and information published elsewhere in the SCR, and described in Section 2.1. Three alternative conceptual models are examined, described and compared below.

2-U-1 Modeling Results

The initial, steady-state (pre-emplacement) 2-U-1 head distribution (Figure 21) is very similar to that of the 1-U-1 model, which demonstrates the control of the boundary conditions in the two models. The highest heads are located in the lower left corner within the composite unit below the repository horizon. The range of heads is from 122.4 m to 114.2 m. Since the head profile along the center line of the grid in the pre-emplacement 2-U-1 model more closely approximates the desired head profile as recorded in RRL-2, the conductivity distribution within the model may be a more accurate representation of the conductivities of the hydrostratigraphic units at BWIP than that of the 1-U-1 model. It must be stressed, however, that a given head distribution is not a unique function of a distribution of hydraulic conductivities, since boundary conditions also control the internal head profiles.

The sharp contrast in conductivities between the Umtanum flow top (3E-7 m/s) and the dense flow interior of the Umtanum (3E-9 m/s) is represented by the refraction of the head contours along the contact. The inversion of the upward gradient above the mid-section of the grid, as specified along the lateral boundaries, is maintained within the grid by the high horizontal conductivities of the flow tops of the upper Sentinel Bluffs (GR-2FT and GR-3FT) and the Vantage interbed. The downward gradient at the top of the grid is maintained by the boundary pressures along the upper boundary.

The head distribution at 10 years after emplacement of the waste, as seen in Figure 22 illustrates the significant effect that the evolved heat has on the pre-emplacement groundwater flow system. Although conduction is the dominant heat transfer process, groundwater flows in response to both density variations (bouyancy) and natural hydraulic gradients through the repository. The temperature distribution within 2-U-1 at ten years is shown in Figure 23. The maximum temperature is significantly above that

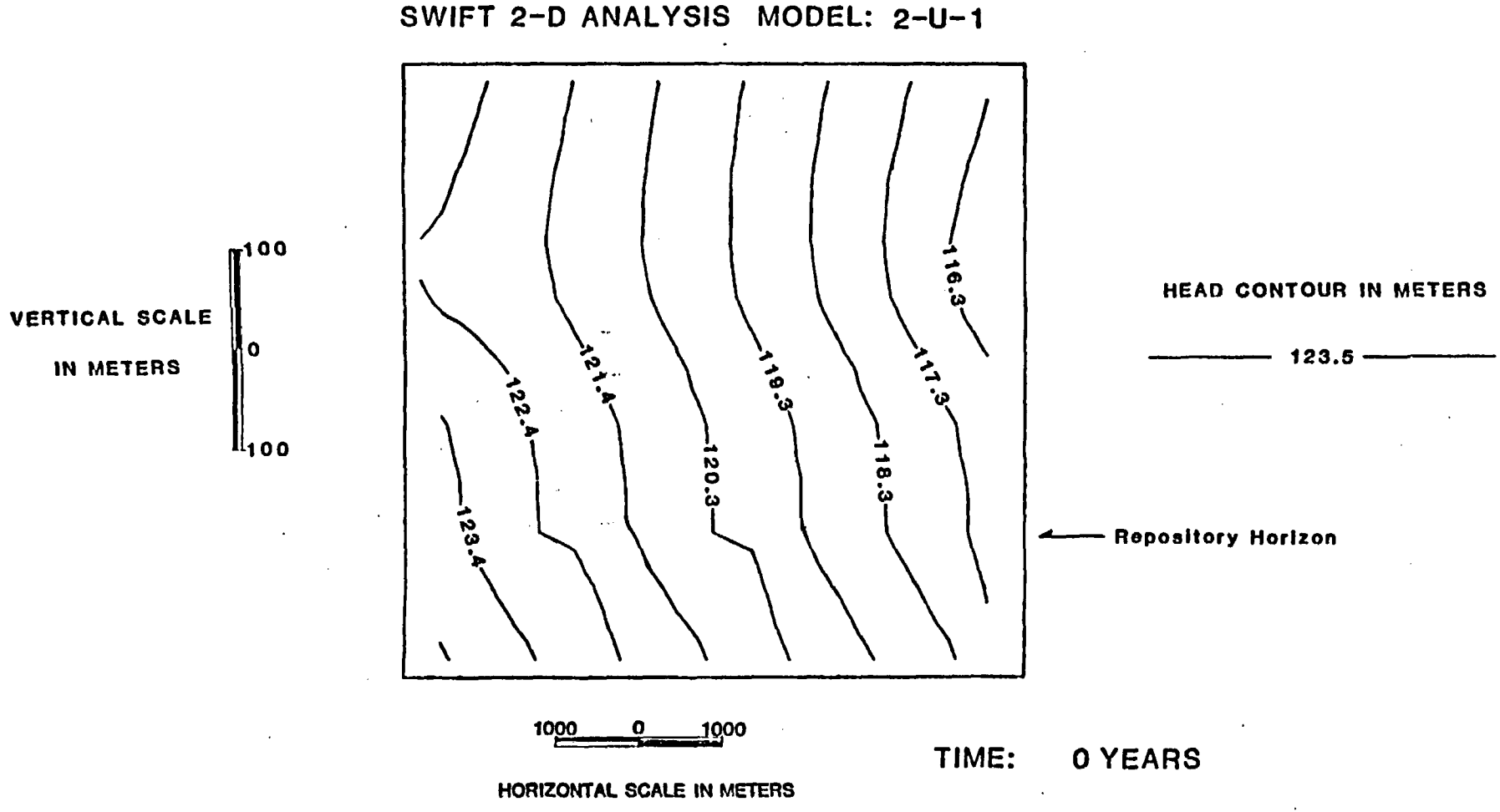

Figure 21. Initial, steady-state, pre-emplacement head distribution in the 2-U-1 model. Notice the similarity of the head profile along the grid centerline (vertical) with the vertical head profile measured in RRL-2. Also notice the refraction of the head contours along the contact of the Umtanum flow top and dense zone.

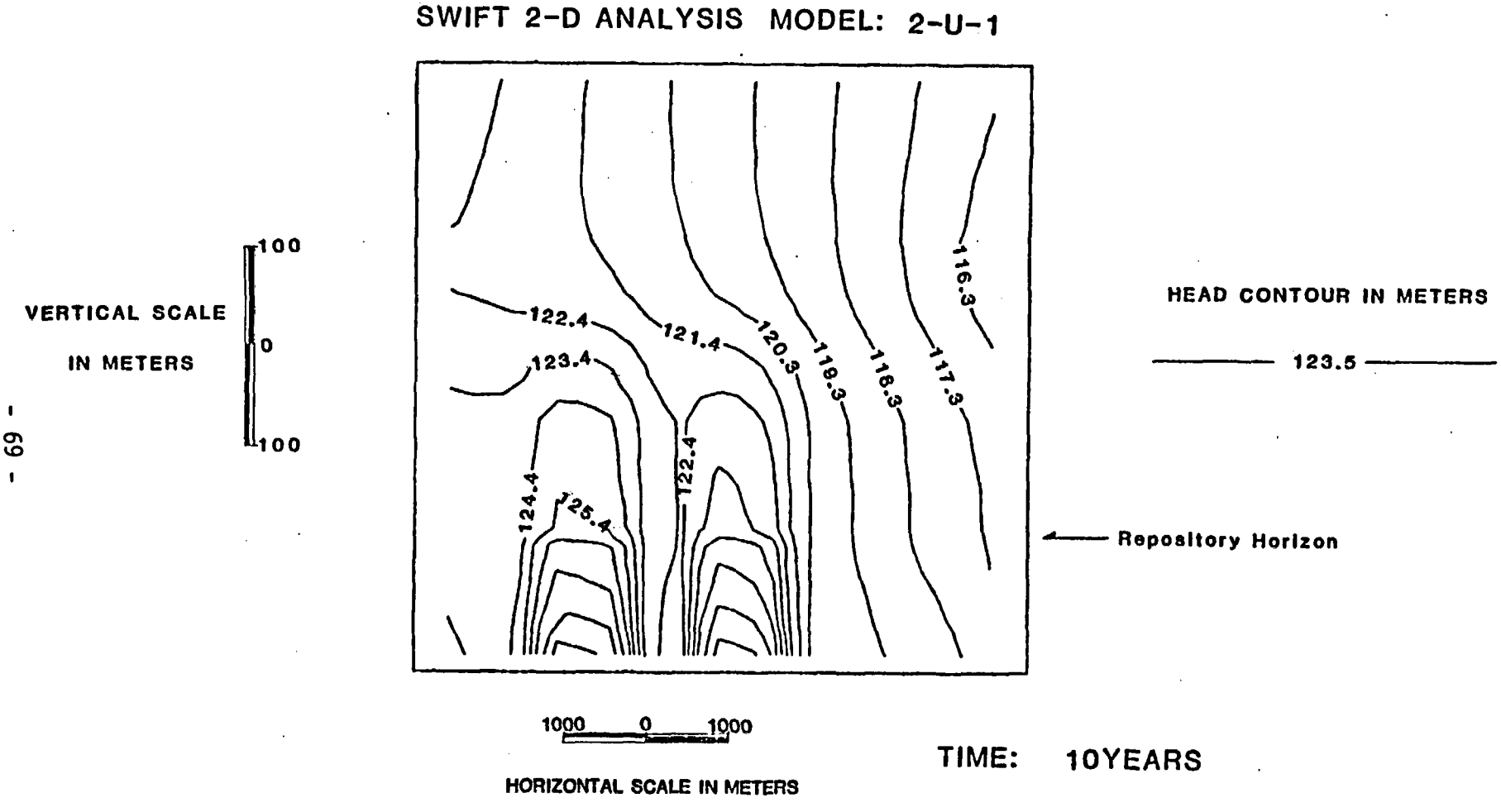

Figure 22. Head distribution in the 2-U-1 model at 10 years after waste emplacement.

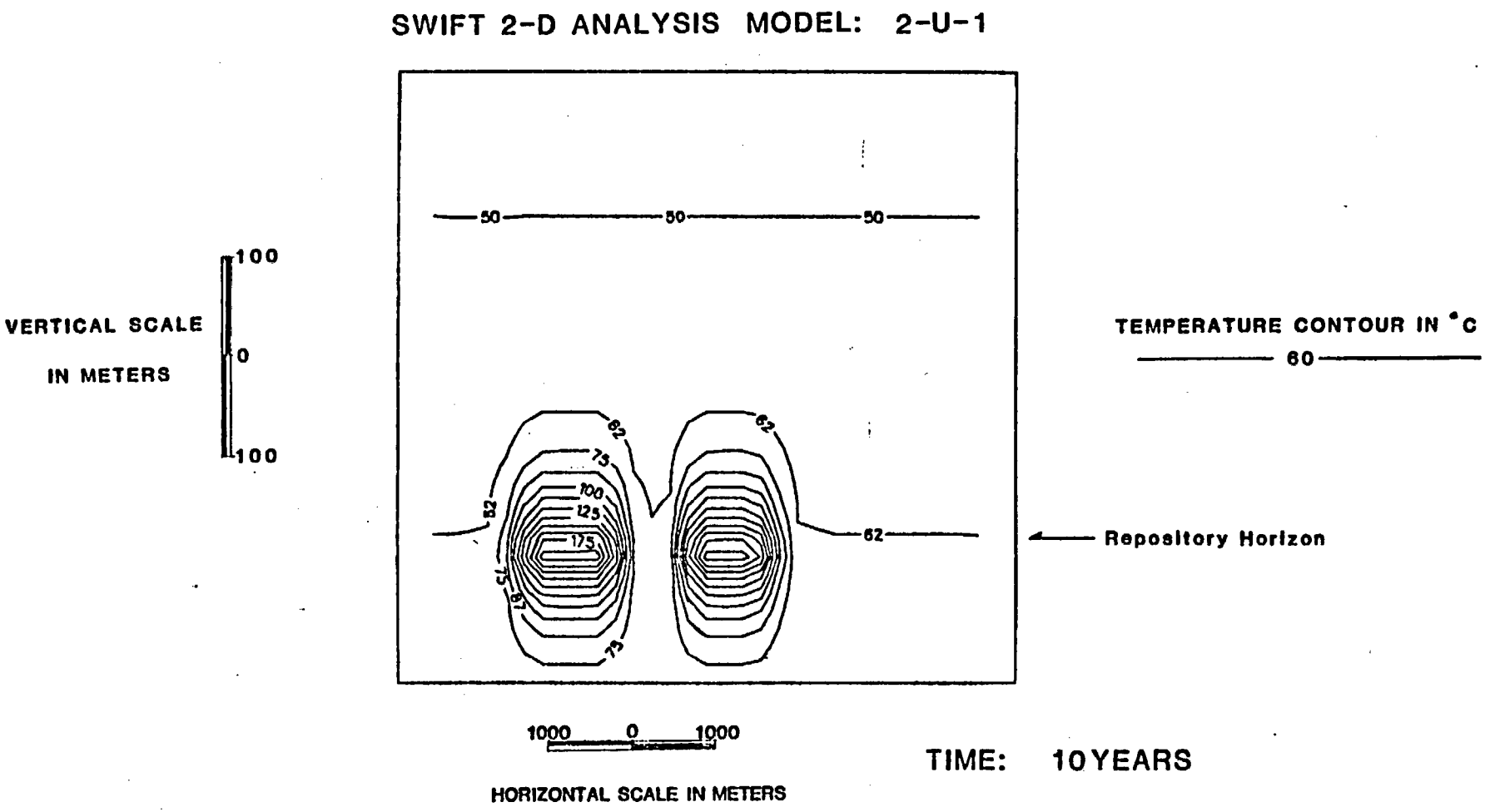

Figure 23. Temperature distribution around the repository in the 2-U-1 model at 10 years after waste emplacement. Maximum temperature at the repository is greater than 187, but less than 200 C.

of the 1-U-1 model due to the decreased porosity of the host rock. Since the porosities of the basalts in 2-U-1 are less than the porosities in the 1-U-1 model (for example, 3E-3 versus 1E-2 in the Umtanum flow top), the hydrostratigraphic units contain less water per unit volume, which increases the heat capacity of the saturated media.

Head gradients in the vertical and horizontal directions increase significantly. The horizontal gradient below the left half of the repository, for example, increases an order of magnitude from the initial gradient of 1E-3 m/m. The head profile, as in the 1-U-1 transient simulations, is altered substantially from that of the RRL-2 profile. The head distribution continues to change with time as more heat is evolved from the repository, and the hydrogeological system responds to the thermal and pressure perturbations. This change may be observed by comparing the head distribution at 10 years (Figure 22) with the head distribution at 100 years (Figure 24).

Within 100 years, the downward gradient originally present at the top of the model has been reversed, and flow from the repository is predominantly upwards toward the more conductive units such as the Vantage and GR-2FT.

The temperature distribution at 100 years is seen in Figure 25. By this time, the temperature in the host rock surrounding the repository has increased more than 160°C above ambient to a maximum temperature of greater than 220°C. (The reader should take note of the vertical exaggeration of ten times). Even within the highly conductive units several hundred meters above the repository, the temperature of the groundwater and rock is elevated by 10 °C above the pre-emplacement ambient temperature.

Travel times of non-sorbing particles that are released at 1000 years after waste emplacement are several orders of magnitude less than those calculated for the 1-U-1 transient model. The pathlines of these

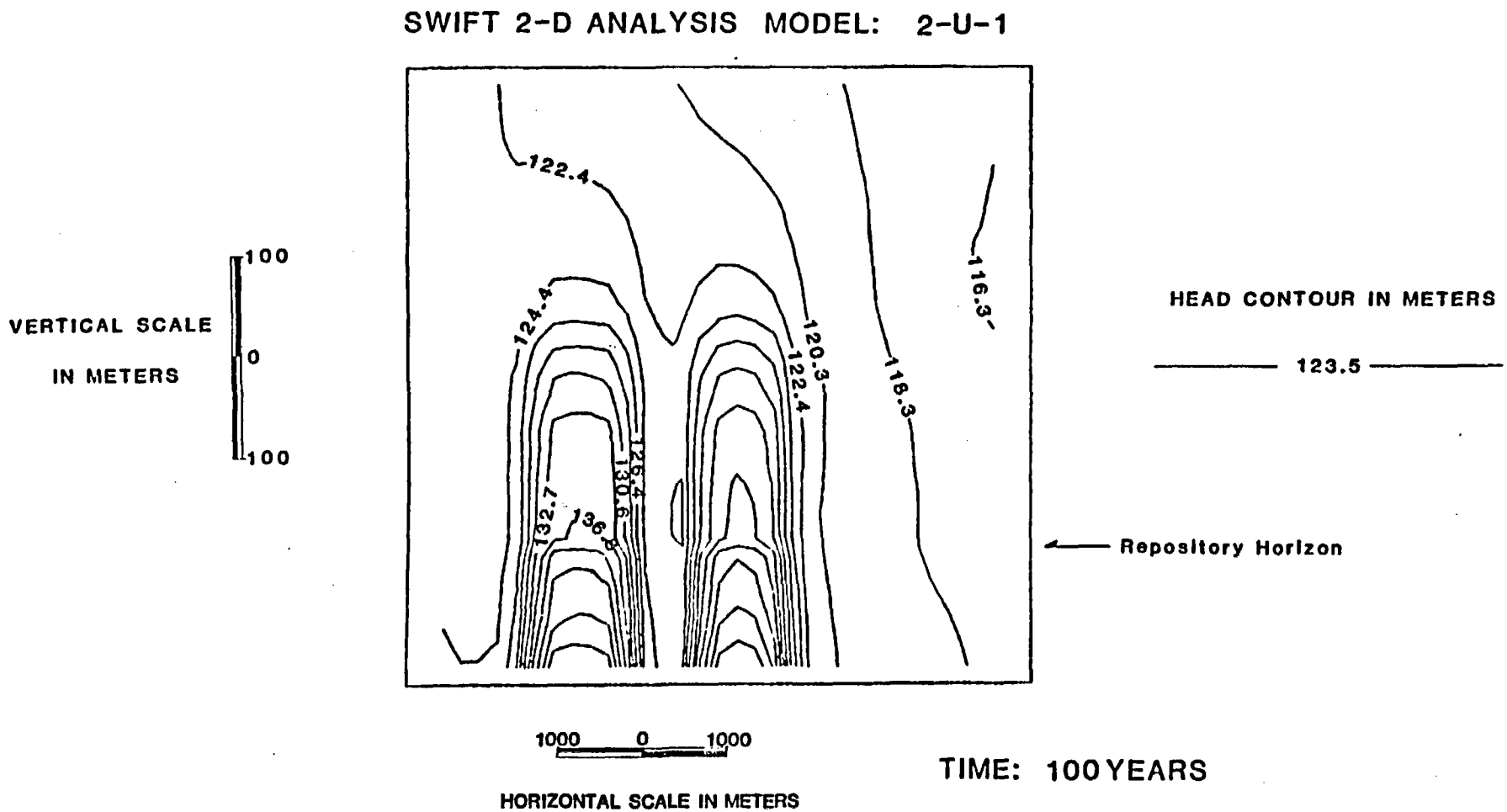

Figure 24. Head distribution in the 2-U-1 model at 100 years after waste emplacement. Compare with the head distribution at 10 years and 0 years.

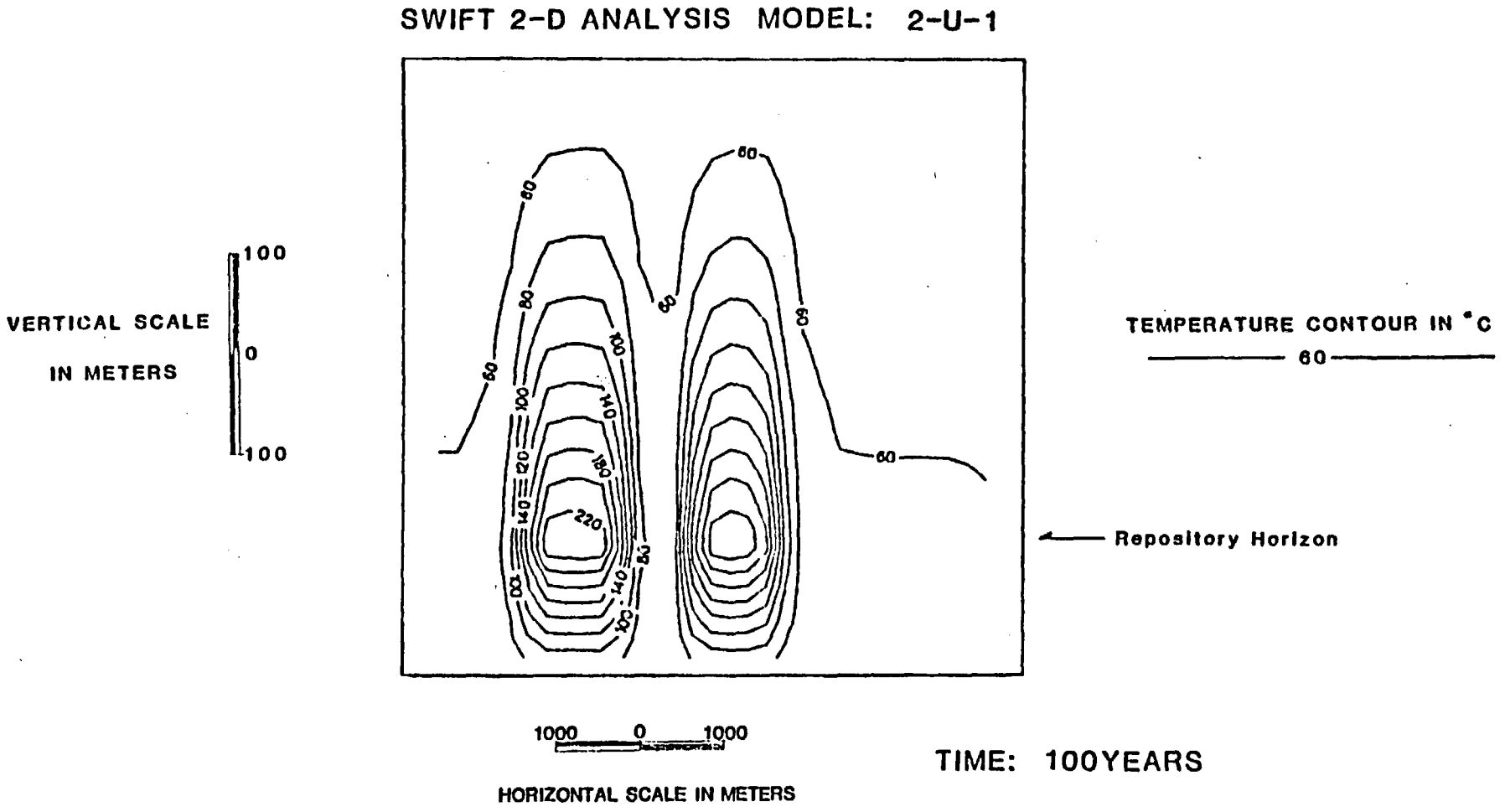

Figure 25. Temperature distribution around the repository in the 2-U-1 model 100 years after waste emplacement. Maximum temperature within the repository is greater than 220 , but less than 240° C.

particles are illustrated in Figure 26. The pathline and release time from the model were determined using calculated linear velocities (non-interpolated between adjacent grid blocks) as described in the results section of the 1-U-1 model. A particle released from near the center top of the left half of the repository travels vertically upwards until it reaches the second flow top unit of the Upper Sentinel Bluffs (GR-3FT). Once in GR-3FT, the particle tracks principally horizontally until it reaches the upper contact of the flow top. After traveling vertically through GR-2, the overlying dense flow interior, this particle resumes lateral migration within the flow top of GR-2 and reaches the laterally boundary of the model after an elapsed travel time of 70.4 years.

Another particle, which is released from the right half of the shorter (right) half of the repository follows a similar pathline configuration, but instead of exiting the model in GR-2FT, it exits within 66.8 years from GR-3FT. This particle travels 3.3 km, whereas the other particle travels 5.3 km in a similar time span. Projections of these linear velocities outside of the grid to the accessible environment is not valid, since an estimation of thermal effects and fluid velocities cannot be extrapolated beyond the grid. The travel times of fluid particles in this non-dispersive flow system are at least two orders of magnitude less than the travel times calculated for the 1-U-1 model. These travel times indicate the lack of conservatism in the 1-U-1 model and the significant effects of changes in hydraulic conductivity and porosity from the values used in the 1-U-1 model. Head distributions at 1000, 2000, and 3000 years are included as Figures 27, 28, and 29 to show the decreasing effect that the repository has on the groundwater flow system.

Results of 3-U-1

The steady-state initial 3-U-1 head distribution, shown in Figure 30, indicates the isotropic, non-layered character of the 3-U-1 BWIP system. The absence of sharp bends in the head contours reflects the absence of

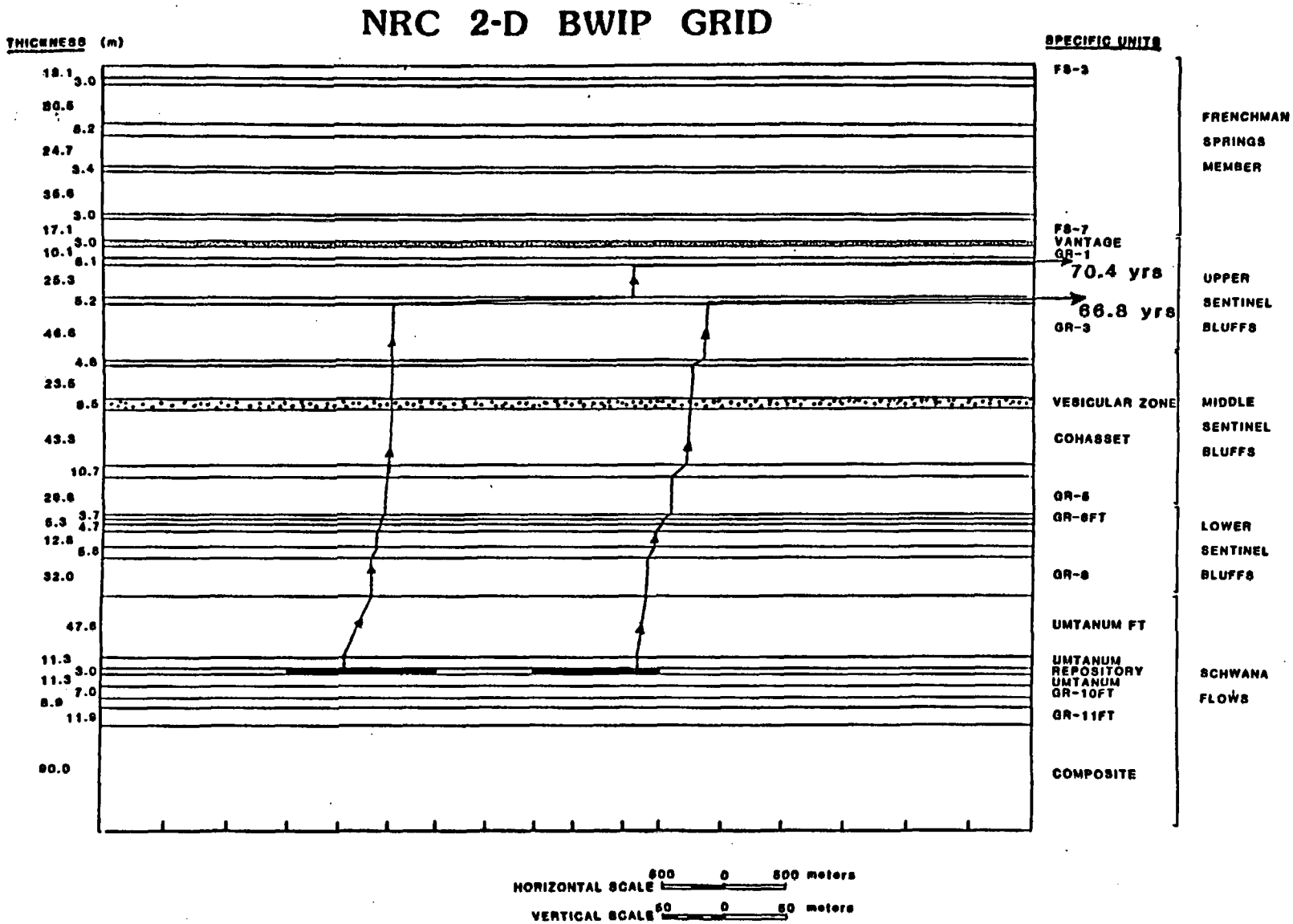

Figure 26. Pathlines of particles released at the top of the hypothetical repositories at 1000 years. The particle on the left exits the grid in GR-2FT 70.4 years after release. The particle on the right exits the grid in GR-3FT 66.8 years after release. Pathlines are calculated using linear velocities at 1000 years for the 2-U-1 model.

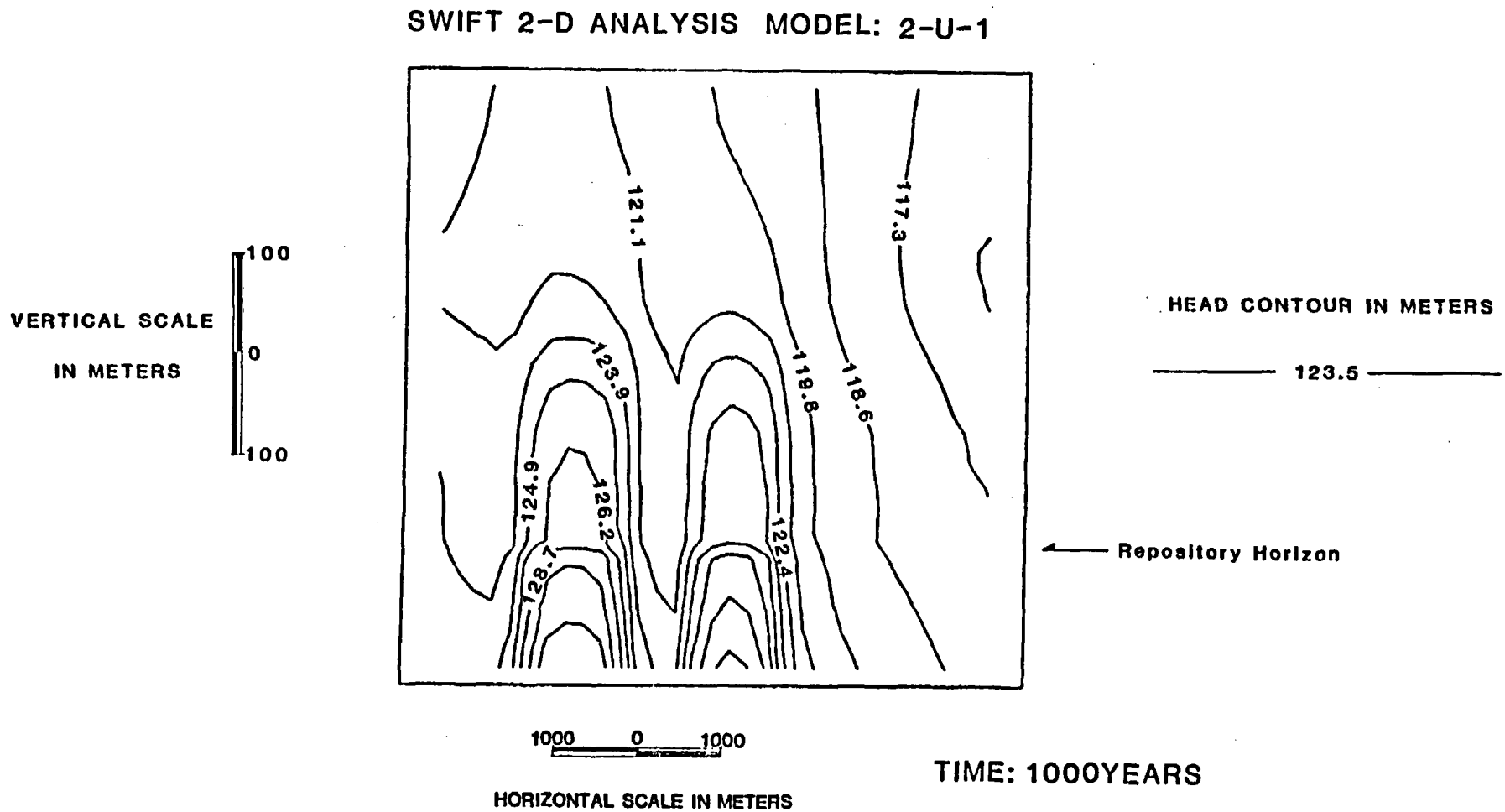

Figure 27. Head distribution in the 2-U-1 model at 1000 years after waste emplacement.

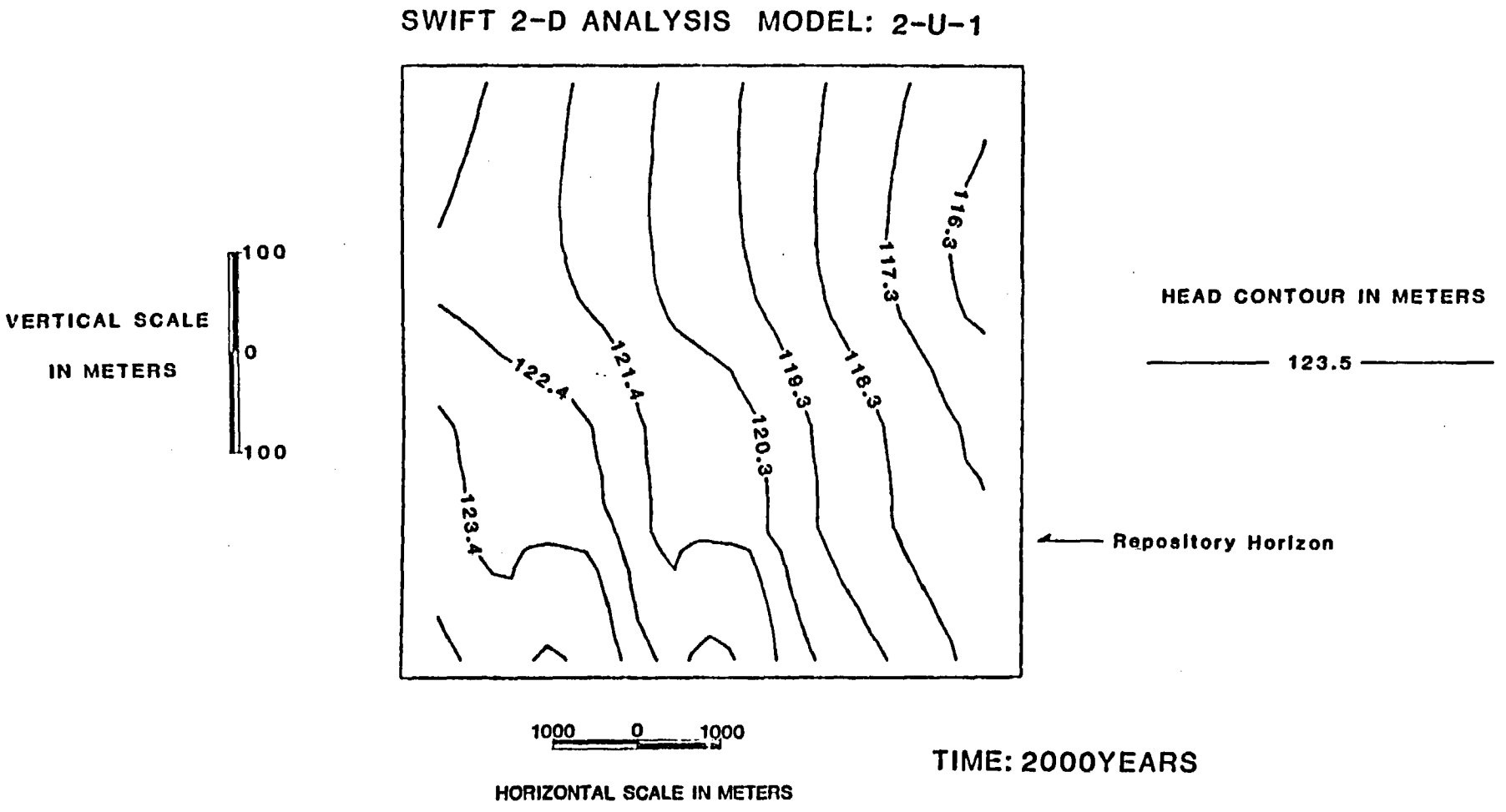

Figure 28. Head distribution in the 2-U-1 model at 2000 years after waste emplacement.

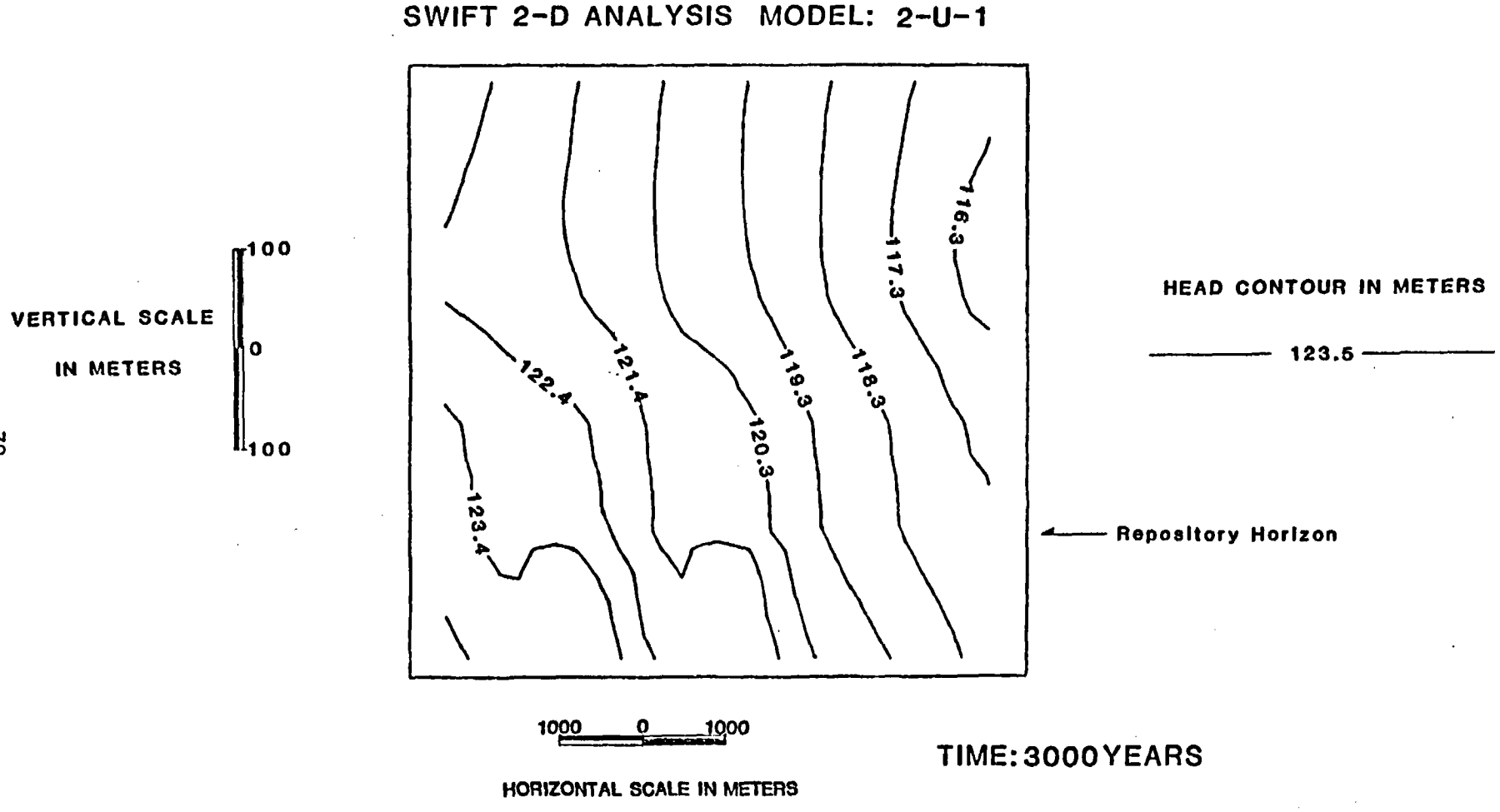

Figure 29, Head distribution in the 2-U-1 model at 3000 years after emplacement of waste.

conductivity contrasts between adjacent grid blocks. The vertical gradient throughout the model is uniform and equal to approximately 2E-3 m/m, while the horizontal gradient is also uniform but approximately equal to 1E-3 m/m.

The decreased resistance to vertical groundwater flow in this model after the repository begins to produce heat is obvious from a comparison of head distributions at 10 years for models 1-U-1 and 3-U-1. Vertical and horizontal hydraulic gradients increase to 1E-2 m/m around the repository by this early time, demonstrating the significance of thermal effects in controlling groundwater flow in the near- and meso-field around a HLW repository. Although the groundwater is driven away from the repository by mixed convection, bouyancy of the heated groundwater is dominating the flow system as the pre-emplacement (ambient) head distribution is masked by the post-emplacement head distribution (see Figure 31). The temperature distribution at 10 years for model 3-U-1 is portrayed in Figure 32. The temperature in the near-field is in excess of 187°C.

By 100 years, the heads around the repository have built up sufficiently to create hydraulic gradients 30 times greater than the pre-emplacement gradients (see Figure 33). Travel times for particles released from the right end of the two repository halves are about half the travel times of of the 2-U-1 models when the particles travel to the Vantage interbed. The particles, once released from the repository, travel to the Vantage in 33.7 and 32.6 years. The particle from the right half of the repository travels only 36 m to the left, whereas the particle from the left half of the repository travels 40 m to the right. All pathlines from the repository are virtually vertical upwards towards the upper boundary of the grid. The disturbed zone, or the zone of significant perturbation to the pre-emplacement flow system, extends from the repository outward to the model boundaries, so the boundaries are too close to the repository in this model.

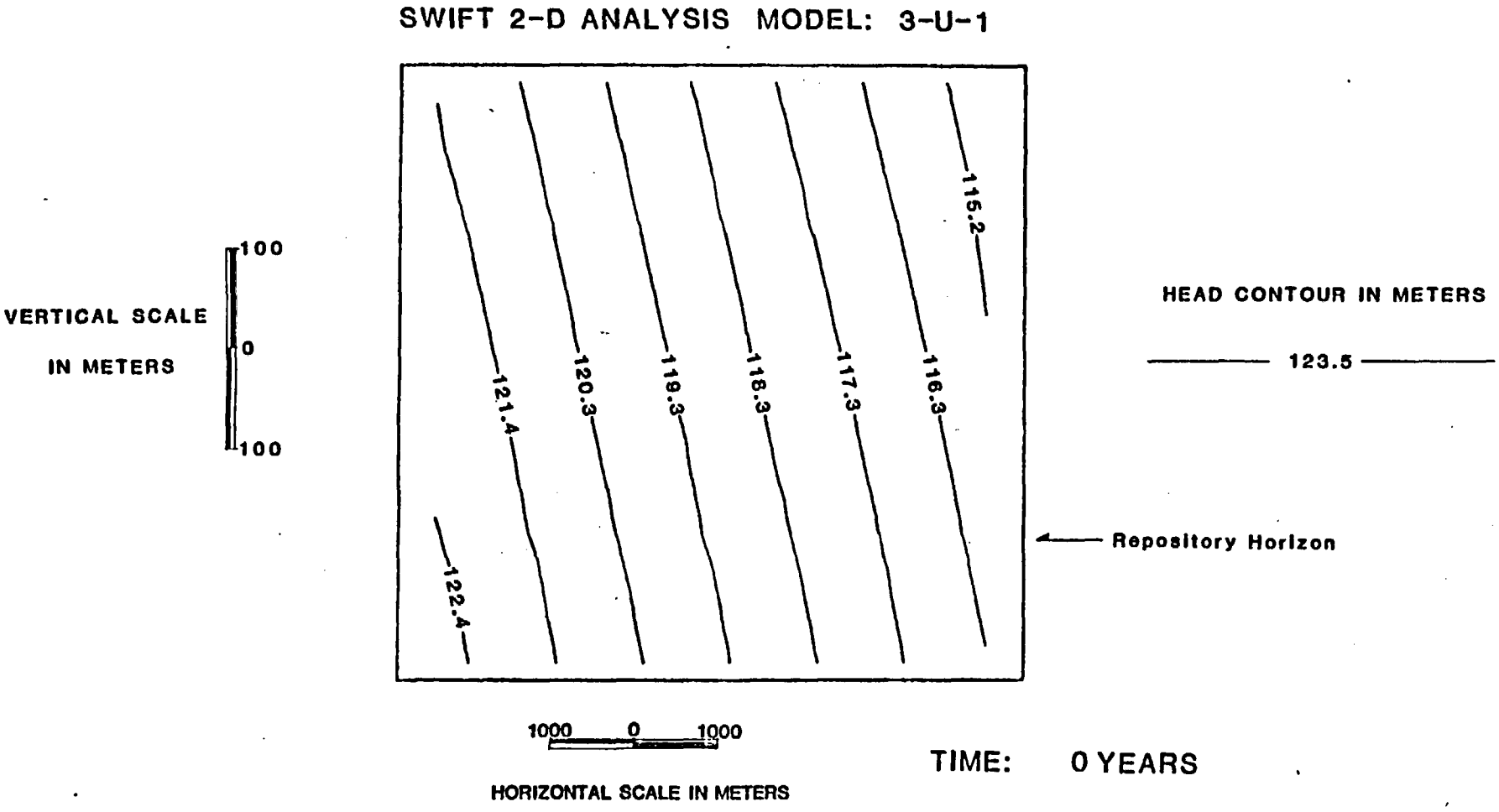

Figure 30. Head distribution in the 3-U-1 model at 0 years (initial, steady-state, pre-emplacement conditions). Notice uniform hydraulic gradients throughout the model.

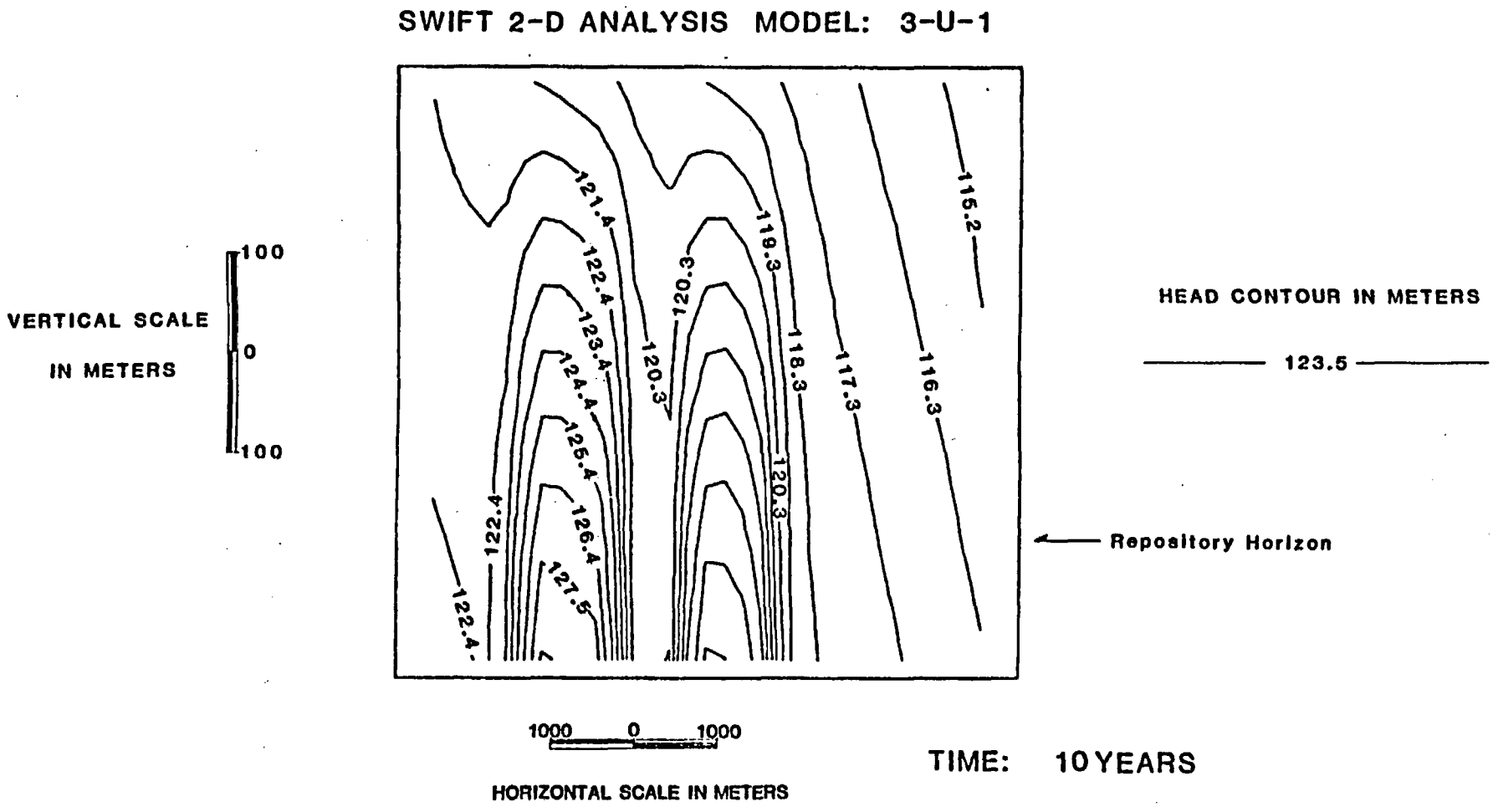

Figure 31. Head distribution in the 3-U-1 model at 10 years.

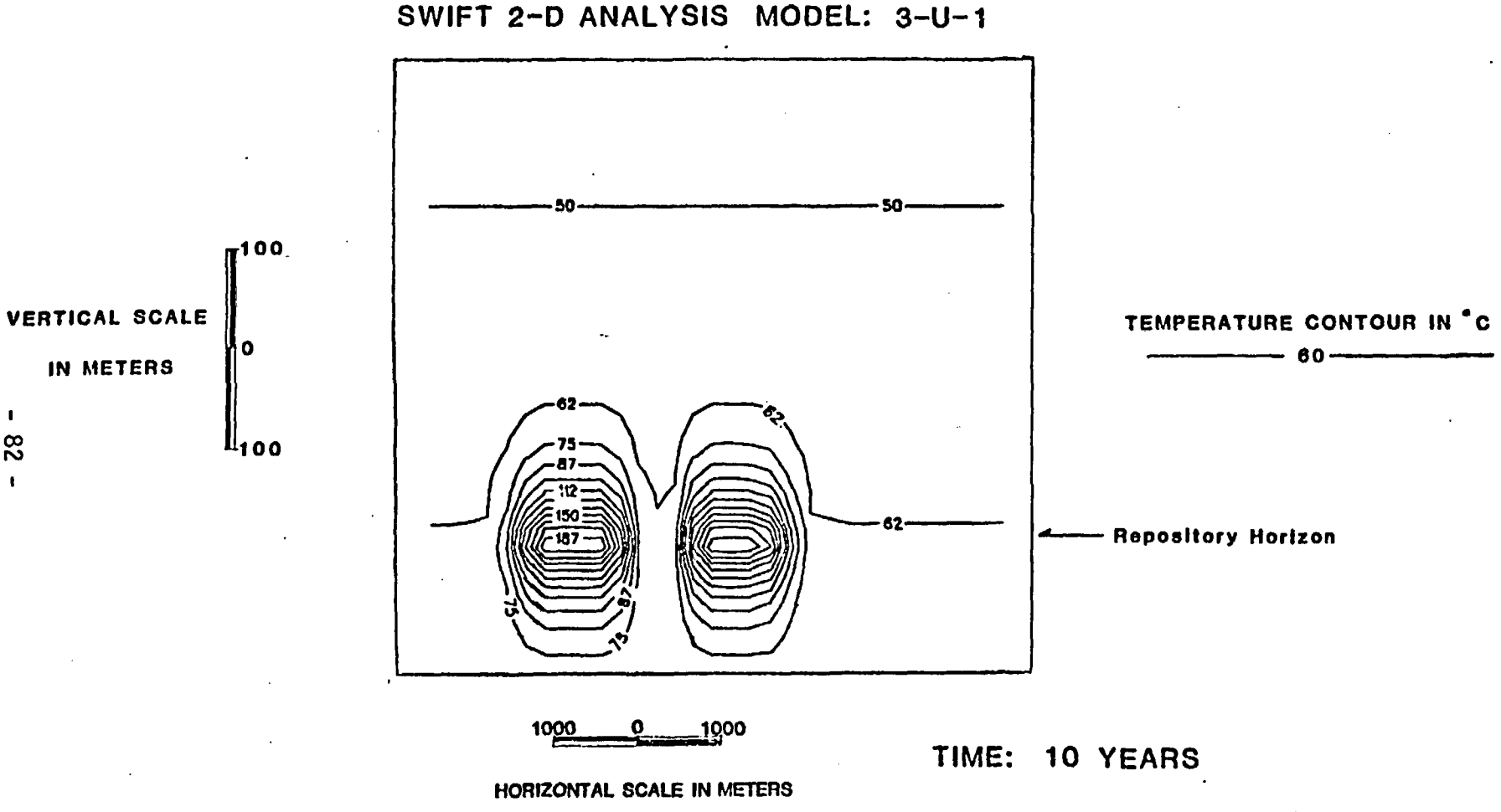

Figure 32. Temperature distribution around the repository in the 3-U-1 model at 10 years. Maximum temperature at the repository is above 187, but less than 200°C.

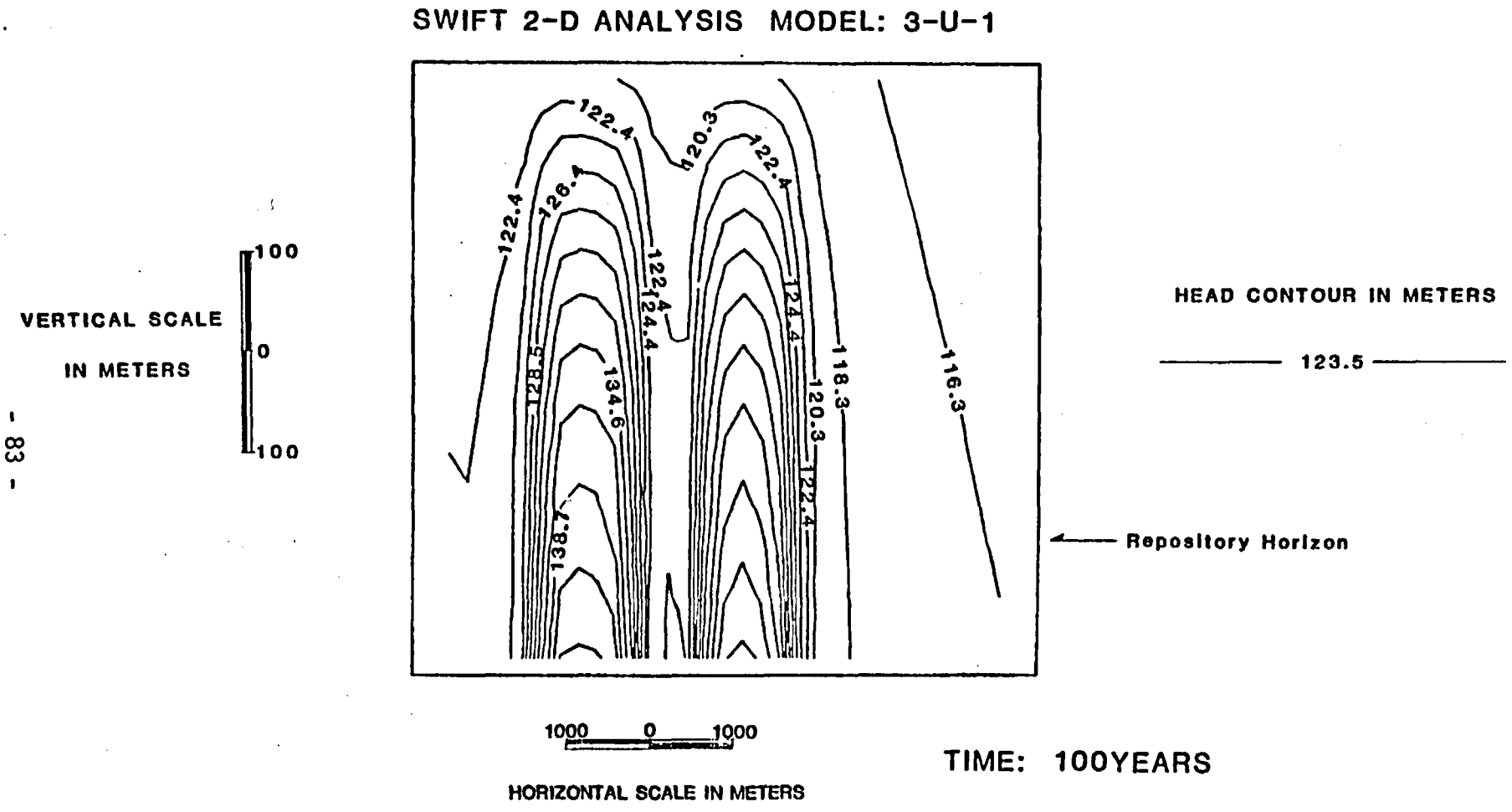

Figure 33. Head distribution in the 3-U-1 model at 100 years.

4-U-1 Modeling Results

The results of model 4-U-1, as in models 1-U-1, 2-U-1, and 3-U-1, demonstrate the dominance of the repository in determining the head distribution and gradients around the repository after waste emplacement. Figure 34 represents the head distribution around the repository at 10 years. The hydraulic gradient has increased from hydrostatic (~ 0 m/m) to approximately 1E-2 m/m immediately below the repository. The effect of heat on travel times from the repository to the accessible environment may be demonstrated by examining the travel time calculation.

$$\text{If } T = \frac{D\Phi}{KI}$$

where D = distance traveled,
Φ_E = effective porosity,
K = hydraulic conductivity,
I = hydraulic gradient, and
T = travel time,

then orders of magnitude of change in the hydraulic gradient term, will alone cause decreases of orders of magnitude in the travel time if all other parameters are held constant. Although elementary, this analysis stresses the significance of the thermal effects of the repository on the hydrogeologic system at BWIP as seen in Figures 34 and 35. The elevated heads continue to propagate away from the repository, as seen by comparing Figures 34 and 35 at 10 and 100 years, respectively.

The Darcy velocity distribution (Figure 36) at 100 years in the 3-U-1 model illustrates the formation of a bouyancy cell that is driven by the repository. Lower density groundwater moves upward above the two halves of the repository and diverges laterally in the more hydraulically conductive units near the top of the model. Cooler, more dense water completes the cell by flowing vertically downwards along the sides of the

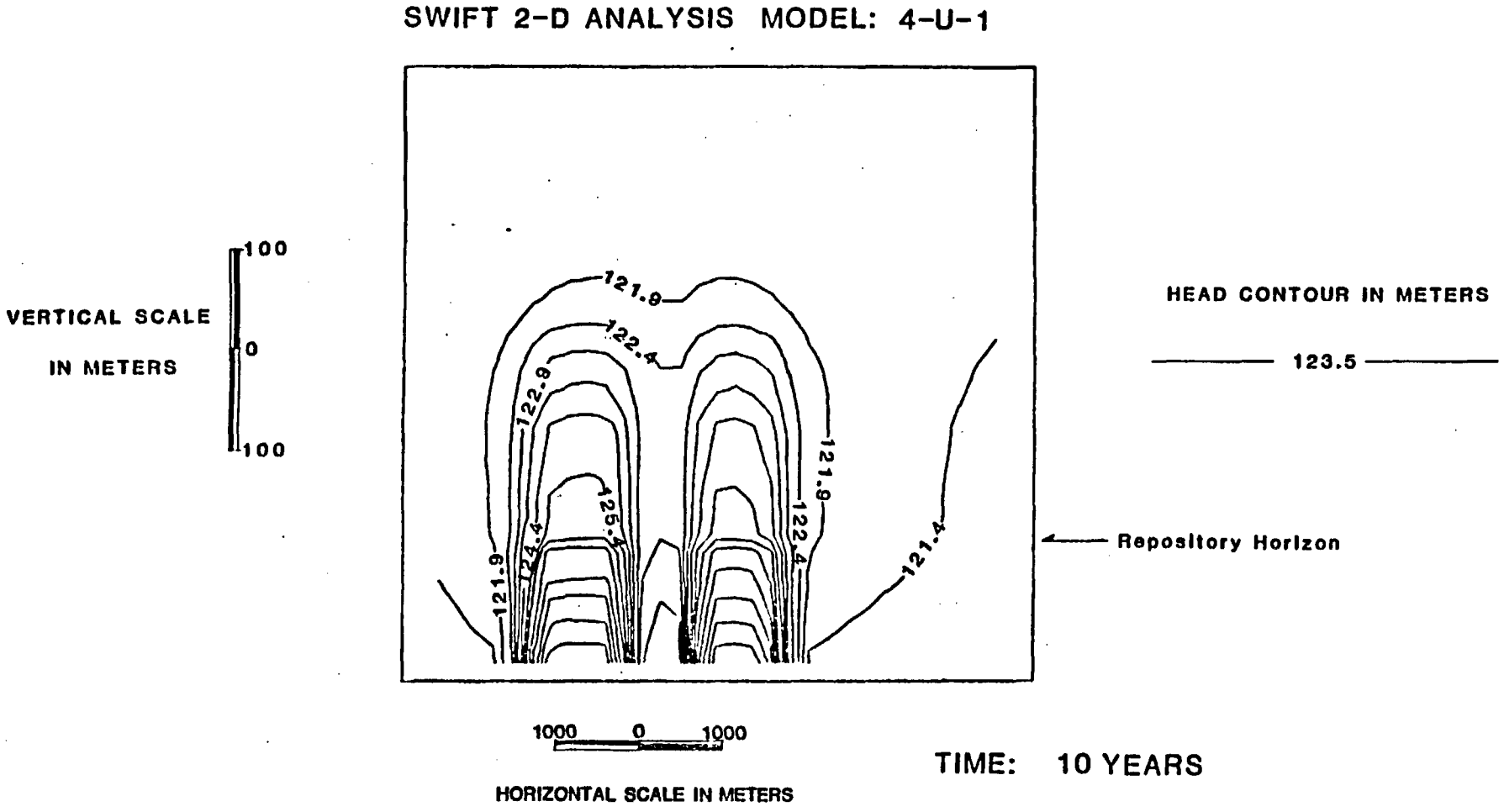

Figure 34. Head distribution in the 4-U-1 model at 10 years. Significant hydraulic gradients are building up around the repository after emplacement of waste.

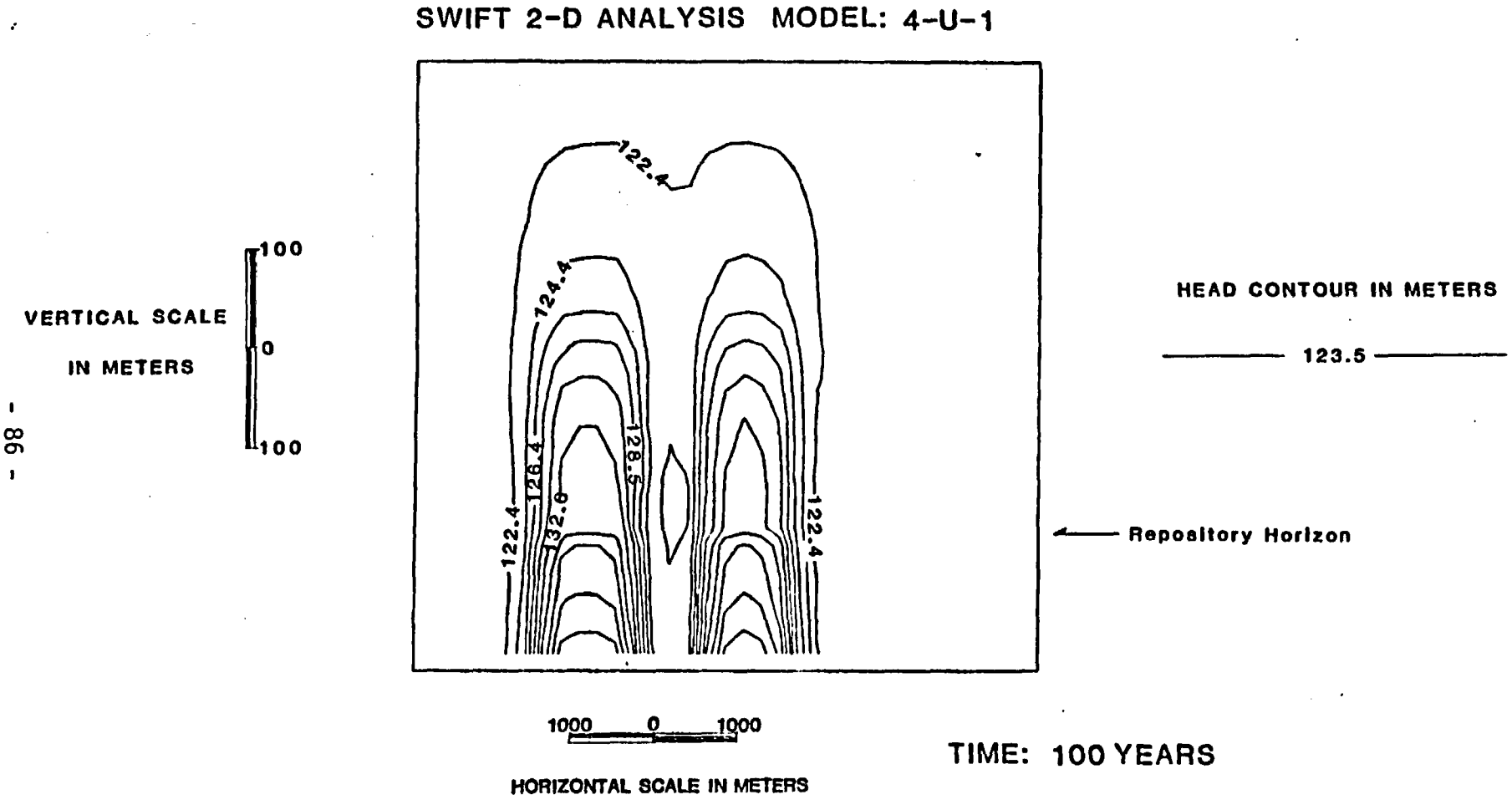

Figure 35. Head distribution in the 4-U-1 model at 100 years.

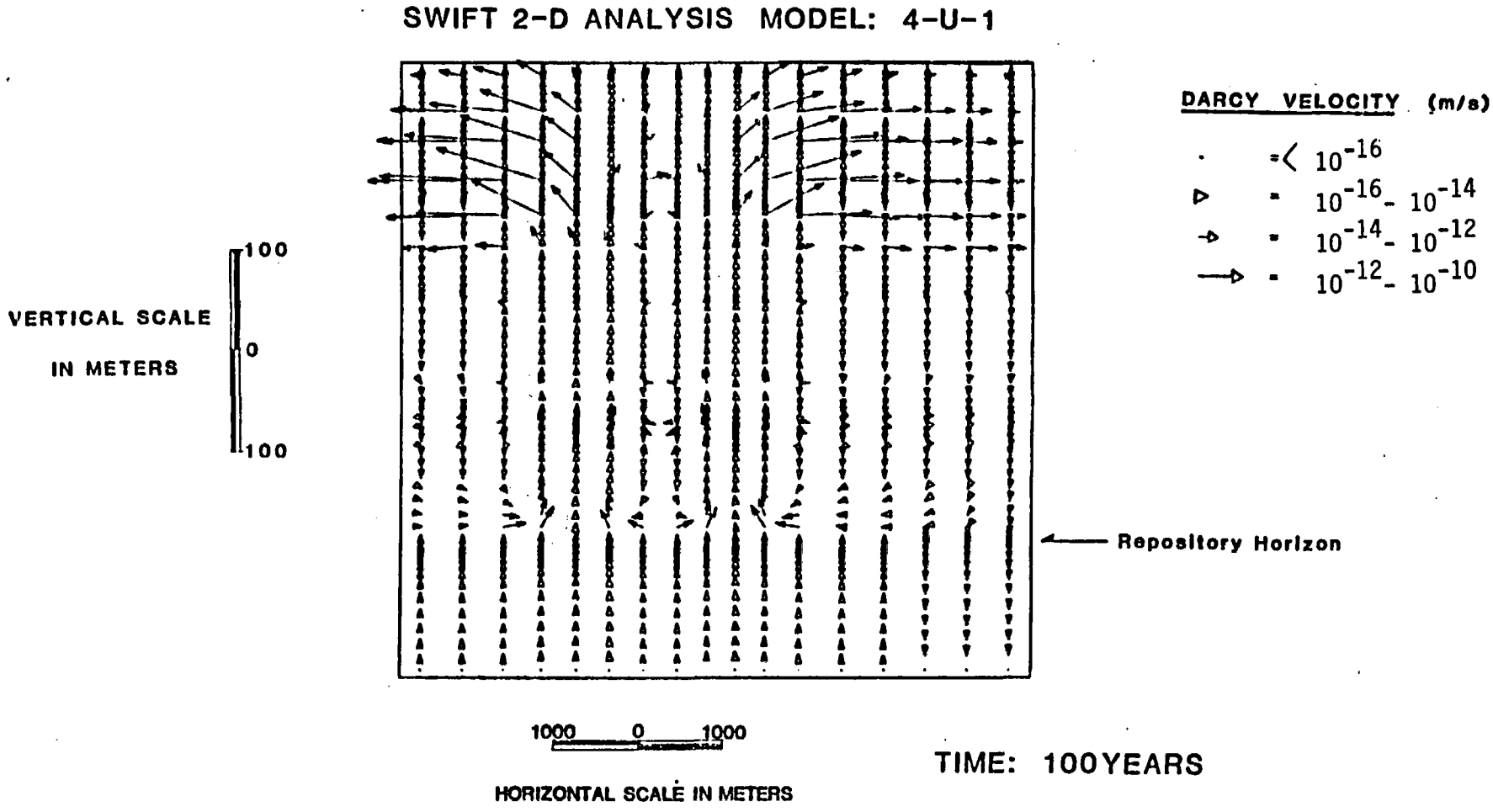

Figure 36 . Darcy veolcity distribution in the 4-U-1 model at 100 years. Notice the convective cells around the repositories. Groundwater moves downward between the two halves of the repository.

model. Upon reentering the Umtanum flow top, this water flows laterally until it heats up and begins to flow vertically upwards towards the top of the model. Figure 37 illustrates the temperature distribution at 100 years around the repository.

After thermal production from the decaying waste decreases, the head contours retreat back toward the repository to approach pre-emplacement initial conditions as seen in Figure 38 at 3000 years. As the repository temperature decreases, the elevated heads subside, and the hydraulic gradients away from the repository decrease, thereby reducing the extent of the thermally disturbed zone around the repository. By 3000 years the hydraulic gradients around the repository have been reduced to 2E-3 m/m. The time required for this retreat will be a function of the hydraulic properties of the components of the system. Although the 4-U-1 model (with the properties of the 2-U-1 model) has almost returned to pre-emplacement conditions in 3000 years, the thermal and hydraulic effects of the repository are still quite evident in the 1-U-1 model at 50,000 years.

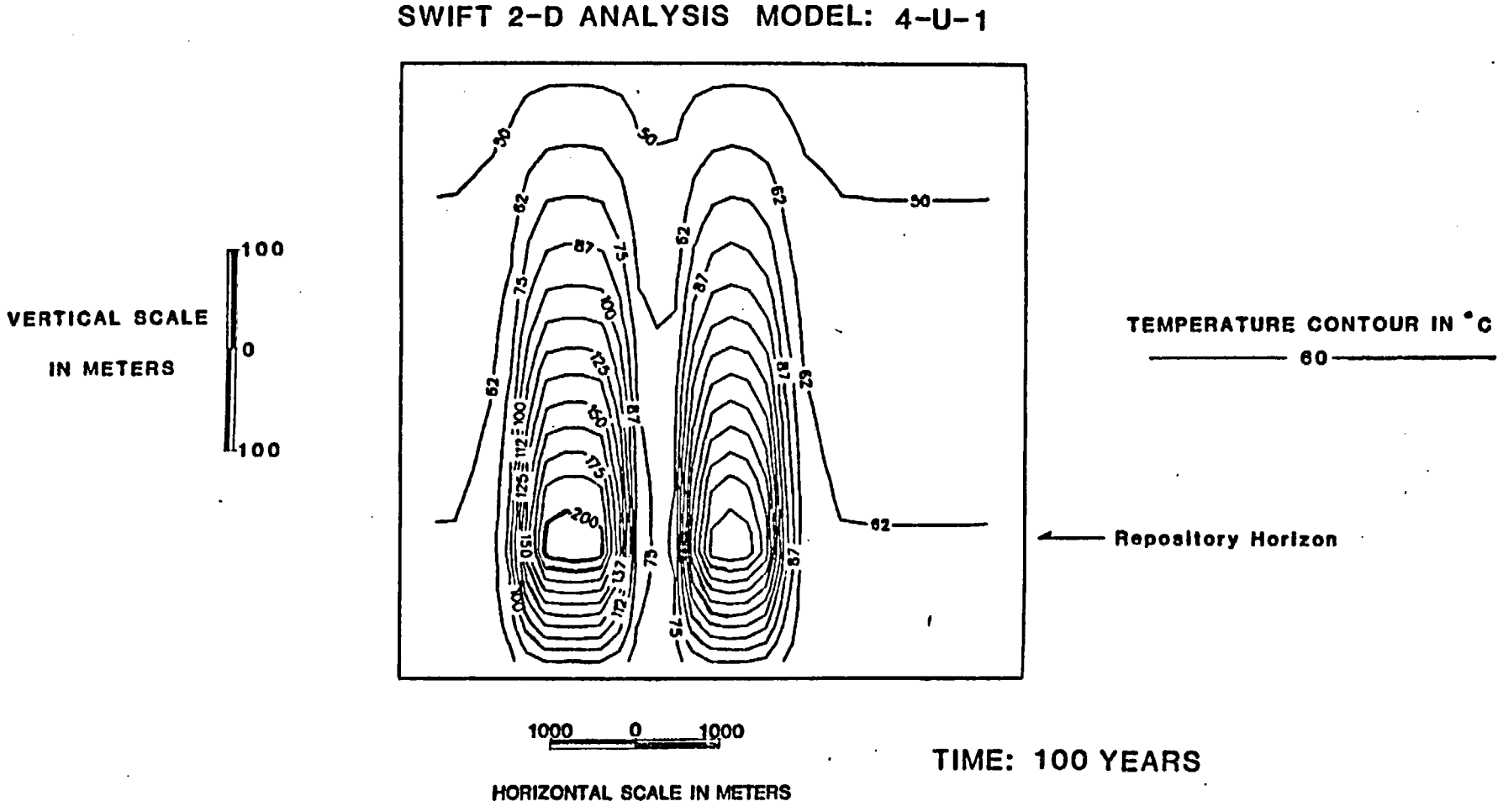

Figure 37 . Temperature distribution around the repository in the 4-U-1 model at 100 years. Maximum temperature at the repository is greater than 200, but less than 212.5 °C. Notice the thermal perturbation within the units near the top of the model, which are several hundred meters above the repository horizon.

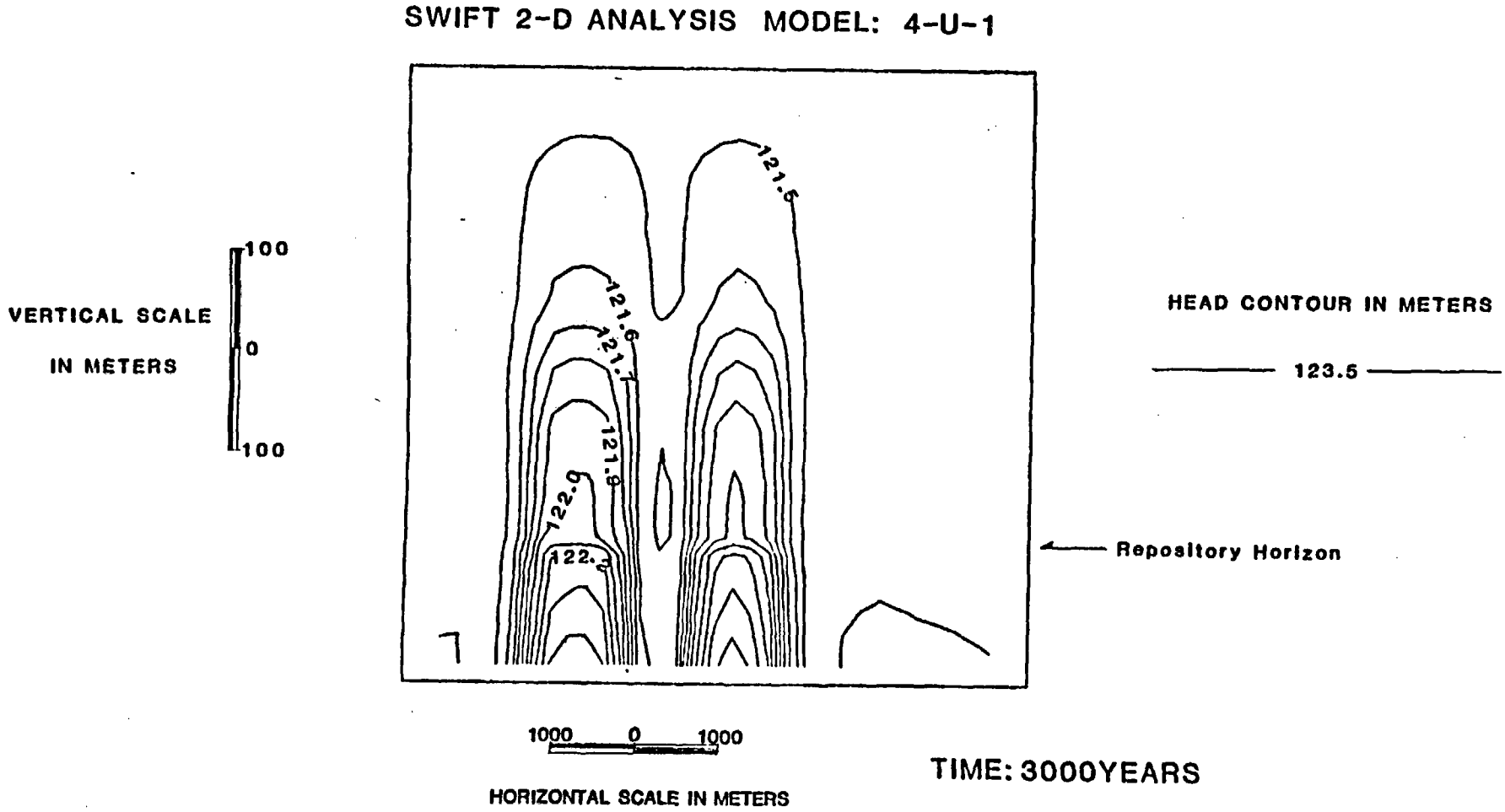

Figure 38. Head distribution in the 4-U-1 model at 3000 years.

III. Conclusions

3.1 Manipulation of SWIFT

These modeling results demonstrate the NRC's in-house capability to perform two-dimensional non-isothermal flow and heat transport modeling of BWIP on the scale described herein with SWIFT. The results obtained are consistent with scientific intuition and the results of the 1-U-1 simulation compare favorably with those published by DOE. There are, however, several concerns which have arisen in the course of our modeling efforts. The first is the expense, due to computer time requirements, of SWIFT. The large number of options in SWIFT and its memory-intensive matrix solution technique make it less efficient than other codes, while at the same time offering more generalized solutions to a wider variety of situations. Its use of fluid pressures rather than hydraulic heads makes small head gradients between adjacent nodes susceptible to round-off error.

It also became evident as we attempted to model with SWIFT that the present SWIFT documentation is incomplete for model use. For example, there is no explanation in any SWIFT manual which explains the exact method and location of specified boundary pressures,temperatures, and concentrations. Such an explanation is critical for effective use of the code. Several unlisted options of the code, which have proven to be useful, are also not listed in any manual. Although we were able to obtain necessary and helpful information directly from the writers of the code, more complete documentation of the code is required. However, the code has been extensively benchmarked and verified.

Because of core storage limitations on the CDC 7600 on which the SWIFT runs were made, there is a limitation to the resolution of the grid. In

practice, on the CDC 7600 it has been estimated that a SWIFT grid should encompass less than approximately 1500 blocks. Thus the grid used by NRC of 74 x 17 blocks was near the core space limitations of the computer as allocated within the program. The grid used by the DOE in their PORFLO model contained on the order of 10^4 grid blocks. For future modeling it may become necessary to either alter the matrix solution technique to make it more storage-economical, or to transfer the code to a larger computer, e.g., the CRAY or similarly sized computer.

Another way to cut cost and storage would be to solve a smaller set of equations. It is apparent from our results that heat transport is governed entirely by conduction. Since thermal conductivities are constant throughout the BWIP model, it may be possible to solve the heat transport equation separately, with a much coarser grid, and then use the solutions for nodal temperatures in a separate flow model. This would be much more economical in terms of computer time; however, it may require a great deal of staff time to perform the coupling between the two separate transient models. This option will be investigated prior to further non-isothermal modeling.

3.2 Validity of Two-Dimensional Modeling

The two-dimensional models employed in this sensitivity analysis have an advantage over three-dimensional models in representing schematic, site-specific situations with reduced data requirements. Two-dimensional simulations also permit simpler computer input and storage requirements.

However, it has not been adequately demonstrated whether, and on what scale, two-dimensional non-isothermal modeling of BWIP can be considered valid. In order to model the BWIP site two-dimensionally for a sensitivity analysis, it must be assumed that some two-dimensional slice,

in which all flow is within the plane, can be found. This two-dimensional "slice" can, of course, be following a line that is not straight from a plan view. However, it could not be used to simulate a fully three-dimensional flow situation. Layered, alternating sequences of confined aquifers with isolated flow systems are inherently three-dimensional. Also, the convective cells produced by a repository heat source are, in the most general case, fully three-dimensional in a Cartesian system, and cannot be modeled accurately by a two-dimensional system. It may be acceptable to model a heat-source in a cylindrical system, which is quasi-two-dimensional.

In the non-isothermal case examined in this report, the problems of modeling scale have been evident. It can be seen from the results in Figures 12 through 38 that the grid extent in both the horizontal and vertical directions may make the simulations susceptible to numerical boundary effects. Since the boundaries of the grid are forced to maintain certain pressure and temperature conditions, the disturbance caused by the thermal effects of the repository may be unrealistically damped near the boundaries. Even if the boundary effects are ignored, it is obvious from the temperature plots that the effects of the repository heat source are felt at the top and the bottom of the NRC grid. Therefore, the validity of a model grid of this size for post-emplacement simulations, as used by both the NRC and the DOE, is in question.

3.3 Comments on DOE's PORFLO Model

The PORFLO model presented in the SCR is insufficiently documented at the present time. The code has not yet been publicly benchmarked, verified, or validated. Therefore, it is not known whether the code can be expected to perform satisfactorily in this type of modeling effort. It

is, however, possible to make several comments on DOE's application of the code.

First, it has been noted in the previous section that two-dimensional modeling of BWIP can only be valid if a plane can be constructed through which all flow is within the plane. As noted in the DSCA, a unique flow path from the repository to the accessible environment has not been determined up to this time. In fact, there is evidence to support a number of different possible flow directions. No two-dimensional model can presently be chosen to represent any actual cross-sections of the site. Therefore, the results of the PORFLO model cannot be interpreted in such a manner as to yield site-specific minimum groundwater travel times from a repository to the accessible environment.

The choice of boundary conditions for the PORFLO model is not adequately justified by the data. In particular, the choice of the RRL-2 head profile to represent the vertical boundary head profiles is not supportable. The downward gradient in the Frenchman Springs and above, indicated by the RRL-2 profile, is not found in other wells on the site. This downward gradient may be the result of artificial recharge due to disposal ponds located in the vicinity of RRL-2, and would not represent equilibrium conditions in the basin. The downward gradient inhibits upward flow from the Frenchman Springs and above, keeping contaminants from reaching higher, more accessible flow systems. The use of a more conservative vertical profile has been discussed in Section 2.1.

The horizontal conductivities applied in the model were also non-conservative, representing DOE's "best estimate," rather than true conservative values. Data from various holes in the basin indicate that conductivities as much as 6 orders of magnitude higher for the flow tops have been encountered (SCR pp. 5.1-27 through 5.1-47). The choice of any

vertical to horizontal hydraulic conductivity ratio is arbitrary, since no vertical conductivity measurements have been reported. The choice of an anisotropy ratio of 10:1 for the dense zones is non-conservative, based on the jointing and fracturing of the basaltic rocks.

The porosities assigned to the PORFLO basalt model are also non-conservative. Only one measurement "in the range of 10^{-2} to 10^{-4}" (p. 5.1-46, SCR) is cited. The PORFLO model, however, assumes values on the higher end of this range (10^{-2} and 10^{-3}), which will result in smaller average liner velocities, and longer travel times, than if they had assumed more conservative porosities.

The effects of these non-conservative assumptions have been analyzed in Section 2.4.3, and have been shown to result in a non-conservative model of the site.

The PORFLO model also assumes a layered horizontally homogeneous hydrostratigraphic system. This assumption inhibits vertical communication between aquifers due to the presence of laterally continuous confining layers between each aquifer. The model therefore discounts the effects of faulting and folding, and ignores the possibility of subsurface geologic structures, such as are inferred on page 3.7-29 of the SCR. (Though a "fault scenario" is examined with PORFLO in the SCR, it is not considered valid by the NRC. This is because the presence of the 1-meter wide fault in the PORFLO fault scenario model has been masked by averaging its properties within a 16,000,000 square meter grid block.) The NRC may perform sensitivity analyses on these assumptions using the methodology demonstrated in this report.

For the above reasons, the NRC considers the use of the PORFLO modeling results (as described in Chapter 12 of the SCR) for estimation of

"minimum" groundwater travel times and radionuclide discharges to the accessible environment to be inappropriate.

IV. Recommendations

On the basis of the analysis contained in this report, the following recommendations are made:

- DOE should consider obtaining more data on vertical conductivities and porosity. DOE should also consider providing more justification for their assumption of a layered system with minimal vertical intercommunication between aquifers. DOE modeling efforts should consider using more conservative assumptions of boundary conditions and hydraulic and thermal parameters based on the entire set of available data.

- Until more detailed regional and basin-scale modeling is done, the boundary conditions to be applied to smaller scale models will be highly uncertain. Therefore it will be impossible to accurately model the site-specific near-field flow in a predictive sense. It is suggested that the DOE more strongly emphasize their regional and basin-scale modeling and data-collection efforts. Additional deep wells may be needed off-site, particularly to the north and southeast of the Hanford site.

- The NRC should monitor regional and basin-scale modeling developments by the DOE, USGS, Washington State, and other agencies. Also, the NRC should consider undertaking modeling efforts at the same scale. The support of the NRC Office of Nuclear Regulatory Research might be enlisted to aid NMSS in preparing and reviewing regional models.

- To facilitate future SWIFT modeling efforts, the NRC should continue to develop pre-processing programs for SWIFT. The particle tracking

post-processor, STLINE, should be updated to accomodate transient simulations.

- The DOE and the NRC should continue sensitivity analyses which consider the uncertainties in the conceptual model. Two-dimensional modeling is acceptable for this purpose, but should not be considered to represent accurate predictions of hydrologic behavior at the site. The grids presently used by the NRC and DOE in their two-dimensional modeling should be extended to avoid boundary effects.

- A comprehensive NRC strategy for sensitivity analyses on both flow and transport must be developed and agreed to by all interested NRC parties. This strategy must involve scenario (ie., conceptual model) selection, probabilistic analysis, and the coupling of flow models to transport and dose models. In considering which scenarios to examine, the expected impact on flow and transport should be roughly evaluated before proceeding with modeling, to avoid unnecessary expense.

- Since the stated purpose of the NRC's sensitivity analyses is generally to identify data which must be obtained by the DOE prior to NRC licensing, the following questions should be considered by the NRC prior to any such request for data:

  1) Is the data requested by the NRC reasonably obtainable by the DOE in the time available?

  2) If not, does the importance of this data warrant a delay in the licensing process (or a denial of a license) until such data is obtained?

- Up to this time, the DOE has considered the repository location as the origin for all travel time estimates. However, the NRC Rule 10 CFR 60 states that the 1000-year minimum groundwater travel time applies to the distance between the disturbed zone boundary and the accessible environment. Therefore, the DOE should identify the maximum extent of the disturbed zone, and calculate the travel times from various points on that boundary. Non-isothermal modeling of the type described in this report can provide meaningful information regarding the extent of the disturbed zone.

- Before the DOE can adequately address the question of the extent of the disturbed zone at BWIP, the NRC must provide a sound definition of "the disturbed zone". By comparing the post-emplacement head and temperature profiles to the pre-emplacement head and temperature profiles, it should be possible to identify a relationship between the extent of the disturbed flow zone and the temperature rise induced by the repository within that zone. Alternatively, it may be desirable to define the disturbed zone by a zone of significantly altered Darcy velocities. From the analysis contained in this report, it is evident that the thermal disturbance introduced by the repository may strongly affect the flow even at large distances. To develop a generic definition of the disturbed flow zone, a thorough generic sensitivity analysis must be performed.

References

Arnett, R. C., et al., Preliminary Hydrologic Release Scenarios for a Candidate Repository Site in the Columbia River Basalts, Rockwell Internationsl, RHO-BWI-ST-12, 1980.

Arnett, R. C., et al., Pasco Basin Hydrologic Modeling and Far-Field Radionuclide Migration Potential, Rockwell International, RHO-BWI-LD-44, 1981.

BWIP, Site Characterization Report for the Basalt Waste Isolation Project, Rockwell Hanford Operations, DOE/RL 82-3, 1982.

Dove, F. H., et al., AEGIS Technology Demonstration for a Nuclear Waste Repository in Basalt, Pacific Northwest Laboratory, PNL-3632, 1982.

Gephart, R. E., et al., Hydrologic Studies Within the Columbia Plateau, Washington, Rockwell International, RHO-BWI-ST-5, 1979.

Guzowski, R. U., et al., Repository Site Definition in Basalt: Pasco Basin, Washington, NUREG/CR-2352, 1982.

Lehman, L. and E. Quinn, Comparison of Model Studies: The Hanford Reservation, U. S. Nuclear Regulatory Commission, 1982.

Luzier, J. and R. Burt, Hydrology of Basalt Aquifers and Depletion of Ground Water in East-Central Washington, Water-Supply Bulletin No. 33, Washington State Department of Ecology, 1974.

Mercer, J. W. and C. Faust, Groundwater Modeling, GeoTrans, Inc., 1981.

Mercer, J. W., S. D. Thomas, and B. Ross, Parameters and Variables Appearing in Repository Siting Models, NUREG/CR-3066, 1982.

Myers, C. W., et al., Geologic Studies of the Columbia Plateau: A Status Report, Rockwell International, RHO-BWI-ST-4, 1979.

Quinn, E., Analysis of Boundary Conditions and Conductivity Ratios Used in Pasco Basin Modeling, U. S. Nuclear Regulatory Commission, 1982.

Reeves, M. and R. M. Cranwell, User's Manual for the Sandia Waste-Isolation Flow and Transport Model (SWIFT), NUREG/CR-2324, 1981.

Silar, J., Groundwater Structures and Ages in the Eastern Columbia Basin, Washington, Bulletin 315, Washington State University, College of Engineering, 1969.

U. S. Department of Energy, Final Environmental Impact Statement (GEIS), Management of Commercially Generated Radioactive Waste, DOE/EIS/0046F, 1980.

U. S. Nuclear Regulatory Commission, Draft Site Characterization Analysis (DSCA), NUREG/0960, 1983.

APPENDIX A

SAMPLE INPUT DECK FOR THE SWIFT 2-U-1 MODEL

MARCH, 1983

```
ROCK-FALL 2-D MODEL NO. 1 12/82
GUNDUP , , MEHEN                                                    M=1
     4     0     0     0     0     0     0     1                                                  M=2
    17     1    74     2     0     1     3     1     6  200     2     0     0     0     0
   4.0E+10   4.0E+15   5.7E+4   4.1HE3   2.77E4                                                  R1=1
       2.2       2.2       2.2       1.0      25.0      25.0    1.E-30                          R1=2
    2.77E3       0.0      25.0    1000.0    1000.0                                             R1=3
     0     0     0     2                                                                       R1=6
      25.0    1.0E+3      25.0    1.0E+3                                                       R1=7
     500.0      44.2                                                                          R1=11
    1450.0      74.2                                                                          R1=11
     0     0                                                                                  R1=12
      25.0       1.0       0.0       0.0                                                     R1=16
3*500.,5*0.,3*500.,4*0.,3*0.,6*500.,
1.0
8.0,5.1,3.6,5.0,10.0,3.0,7.5,8.2,5.0,7.5,7.5,4.7,3.4,4.6,7.0,10.0,8.6,5.0,
3.0,5.0,7.1,5.0,3.0,5.0,5.0,5.1,6.1,7.3,10.0,8.0,5.2,10.0,10.0,10.0,10.0,6.6,
4.6,6.5,15.0,8.5,10.0,10.0,10.0,10.0,13.3,10.7,15.0,8.8,6.0,3.7,5.3,4.7,6.0,8.8,
5.8,10.0,12.0,10.0,10.0,1.10.0,13.5,10.0,6.3,5.0,3.0,5.0,6.3,7.0,8.9,11.9,
15.,15.,15.,15.,15.,15.
   1.0E+10   1.0E+10   1.0E+4   1.0E+3      0.0       0.0     500.0     R1=20
    1   17    1    1    3    3                                          R1=21
   3.0E+5    3.0E+5    3.0E+5   1.0E+1
    1   17    1    1    8    8
   3.0E+5    3.0E+5    3.0E+5   1.0E+1
    1   17    1    1   13   13
   3.0E+5    3.0E+5    3.0E+5   1.0E+1
    1   17    1    1   18   18
   3.0E+5    3.0E+5    3.0E+5   1.0E+1
    1   17    1    1   23   23
   1.0E+7    1.0E+7    1.0E+7      1.0
    1   17    1    1   28   28
   3.0E+5    3.0E+5    3.0E+5   1.0E+1
    1   17    1    1   33   33
   3.0E+5    3.0E+5    3.0E+5   1.0E+1
    1   17    1    1   38   38
   3.0E+7    3.0E+7    3.0E+7   3.0E+2
    1   17    1    1   39   39
  1.0E+11   1.0E+11   3.0E+9   1.0E+2
    1   17    1    1   44   44
   3.0E+7    3.0E+7    3.0E+7   3.0E+2
    1   17    1    1   48   48
   4.0E+7    3.0E+7    3.0E+7   3.0E+2
    1   17    1    1   50   50
   3.0E+7    3.0E+7    3.0E+7   3.0E+2
    1   17    1    1   53   53
   3.0E+7    3.0E+7    3.0E+7   3.0E+2
    1   17    1    1   57   60
   3.0E+7    3.0E+7    3.0E+7   3.0E+2
    1   17    1    1   27   29
  1.0E+10   1.0E+10   1.0E+4   1.0E+1
    1   17    1    1   31   35
  1.0E+10   1.0E+10   1.0E+8   1.0E+3
    1   17    1    1   37   38
  1.0E+11   1.0E+11   3.0E+9   1.0E+3
    1   17    1    1   40   43
  1.0E+11   1.0E+11   3.0E+9   1.0E+3
    1   17    1    1   46   48
   3.0E+7    3.0E+7    3.0E+7   3.0E+2
```

```
 1   17    1    1    45   47
1.0E-11   1.0E-11    3.0E-9    1.0E-3
 1   17    1    1    49   49
1.0E-10   1.0E-10    1.0E-8    1.0E-3
 1   17    1    1    51   52
1.0E-10   1.0E-10    1.0E-8    1.0E-3
 1   17    1    1    54   56
1.0E-10   1.0E-10    1.0E-8    1.0E-3
 1   17    1    1    AR   6A
 3.0E-7    3.0E-7    3.0E-7    3.0E-2
 1   17    1    1    A1   74
1.0E-11   1.0E-11    3.0E-9    1.0E-3
 1   17    1    1    20   25
1.0E-10   1.0E-10    1.0E-8    1.0E-3
 0    0    1    1    A3   63
 1.E-10    1.E-10    1.E-10    1.E-1     0.0       0.0      2.5E6
 9   11    1    1    A3   63
 1.E-10    1.E-10    1.E-10    1.E-1     0.0       0.0      2.5E6
                                                                    R1=21
 1   17    1    1    1   74
    1.0       1.0       1.0       0.1     0.0       0.0

 4    1
 1    1    1    1    2    2    0                                    R1=27
    1.00.191691EA      45.32       0.0
 1    1    1    1    3    3    0
    1.00.201153EA      45.52       0.0
 1    1    1    1    4    4    0
    1.00.270011E6      45.64       0.0
 1    1    1    1    5    5    0
    1.00.31A0 3EA      45.44       0.0
 1    1    1    1    6    6    0
    1.00.415571E6      16.24       0.0
 1    1    1    1    7    7    0
    1.00.49259AE6      46.56       0.0
 1    1    1    1    A    A    0
    1.00.5A4956E6      46.A6       1.0
 1    1    1    1    9    9    0
    1.00.613696E6      47.19       0.0
 1    1    1    1   10   10    0
    1.00.692A53E6      47.39       0.0
 1    1    1    1   11   11    0
    1.00.7A4958E6      47.69       0.0
 1    1    1    1   12   12    0
    1.00.83759AE6      47.99       0.0
 1    1    1    1   13   13    0
    1.00.8A3124E6      48.19       0.0
 1    1    1    1   14   14    0
    1.00.915A32E6      48.32       0.0
 1    1    1    1   15   15    0
    1.00.9A3180E6      48.50       0.0
 1    1    1    1   16   16    0
    1.01.020119E6      48.78       0.0
 1    1    1    1   17   17    0
    1.01.128729E6      49.20       0.0
 1    1    1    1   18   18    0
    1.01.211A65E6      49.54       0.0
 1    1    1    1   19   19    0
    1.01.259473E6      49.74       0.0
 1    1    1    1   20   20    0
```

	1.07.2AA774E6			49.8A		0.0
1	1	1	1	21	21	0	
	1.07.3371A9E6			50.06		0.0
1	1	1	1	22	22	0	
	1.07.4154238E6			50.34		0.0
1	1	1	1	23	23	0	
	1.07.4542A8E6			50.58		0.0
1	1	1	1	24	24	0	
	1.07.4A3197E6			50.6A		0.0
1	1	1	1	25	25	0	
	1.07.5314758E6			50.8A		0.0
1	1	1	1	26	26	0	
	1.07.5A071AE6			51.07		0.0
1	1	1	1	27	27	0	
	1.07.63A658AE6			51.31		0.0
1	1	1	1	28	28	0	
	1.07.7AA722E6			51.60		0.0
1	1	1	1	29	29	0	
	1.07.8A3A52E6			52.00		0.0
1	1	1	1	30	30	0	
	1.07.A791AAE6			52.32		0.0
1	1	1	1	31	31	0	
	1.07.9295A3E6			52.53		0.0
1	1	1	1	32	32	0	
	1.08.0264A0E6			52.93		0.0
1	1	1	1	33	33	0	
	1.08.1232A7E6			53.33		0.0
1	1	1	1	34	34	0	
	1.08.2251A2E6			53.74		0.0
1	1	1	1	35	35	0	
	1.08.3164A0E6			54.13		0.0
1	1	1	1	36	36	0	
	1.08.3A17A2E6			54.43		0.0
1	1	1	1	37	37	0	
	1.08.4256A1E6			54.5A		0.0
1	1	1	1	38	38	0	
	1.08.5074A4E6			54.92		0.0
1	1	1	1	39	39	0	
	1.08.6540A0E6			55.52		0.0
1	1	1	1	40	40	0	
	1.08.7373A4E6			55.86		0.0
1	1	1	1	41	41	0	
	1.08.8354A7E6			56.24		0.0
1	1	1	1	42	42	0	
	1.08.9330A3E6			56.64		0.0
1	1	1	1	43	43	0	
	1.09.0414A0E6			57.04		0.0
1	1	1	1	44	44	0	
	1.09.1A14A6E6			57.52		0.0
1	1	1	1	45	45	0	
	1.09.2A0520E6			58.02		0.0
1	1	1	1	46	46	0	
	1.09.3134A2E6			58.62		0.0
1	1	1	1	47	47	0	
	1.09.4496A0E6			58.97		0.0
1	1	1	1	48	48	0	
	1.09.5583A8E6			59.21		0.0
1	1	1	1	49	49	0	
	1.09.5944A1E6			59.3A		0.0
1	1	1	1	50	50	0	

	1.09.8465	59.57		0.0		
1	1 1 1	51 51	0			
	1.09.8925	59.76		0.0		
1	1 1 1	52 52	0			
	1.09.7512	60.00		0.0		
1	1 1 1	53 53	0			
	1.09.8177	60.27		0.0		
1	1 1 1	54 54	0			
	1.09.8745	60.50		0.0		
1	1 1 1	55 55	0			
	1.09.9714	60.90		0.0		
1	1 1 1	56 56	0			
	1.01.0389	61.34		0.0		
1	1 1 1	57 57	0			
	1.01.0187	61.74		0.0		
1	1 1 1	58 58	0			
	1.01.0284	62.19		0.0		
1	1 1 1	59 59	0			
	1.01.0423	62.79		0.0		
1	1 1 1	60 60	0			
	1.01.0557	63.27		0.0		
1	1 1 1	61 61	0			
	1.01.0651	63.69		0.0		
1	1 1 1	62 62	0			
	1.01.0712	63.94		0.0		
1	1 1 1	63 63	0			
	1.01.0761	64.14		0.0		
1	1 1 1	64 64	0			
	1.01.0793	64.26		0.0		
1	1 1 1	65 65	0			
	1.01.0838	64.46		0.0		
1	1 1 1	66 66	0			
	1.01.0892	64.71		0.0		
1	1 1 1	67 67	0			
	1.01.0977	64.99		0.0		
1	1 1 1	68 68	0			
	1.01.1054	65.35		0.0		
1	1 1 1	69 69	0			
	1.01.1104	65.82		0.0		
1	1 1 1	70 70	0			
	1.01.1132	66.42		0.0		
1	1 1 1	71 71	0			
	1.01.1457	67.02		0.0		
1	1 1 1	72 72	0			
	1.01.1501	67.62		0.0		
1	1 1 1	73 73	0			
	1.01.1746	68.22		0.0		
17	17 1 1	1 1	0			
	2.00.0307	85.00		0.0		
17	17 1 1	2 2	0			
	2.00.1183	85.32		0.0		
17	17 1 1	3 3	0			
	2.00.1577	85.52		0.0		
17	17 1 1	4 4	0			
	2.00.1985	85.64		0.0		
17	17 1 1	5 5	0			
	2.00.2458	85.84		0.0		
17	17 1 1	6 6	0			
	2.00.3120	86.23		0.0		
17	17 1 1	7 7	0			

	2.00.4192	86.58		0.0		
17	17 1 1	8 8	0			
	2.00.4916	86.86		0.0		
17	17 1 1	9 9	0			
	2.00.5711	87.19		0.0		
17	17 1 1	10 10	0			
	2.00.6194	87.39		0.0		
17	17 1 1	11 11	0			
	2.00.6914	87.69		0.0		
17	17 1 1	12 12	0			
	2.00.7484	87.99		0.0		
17	17 1 1	13 13	0			
	2.00.8197	88.19		0.0		
17	17 1 1	14 14	0			
	2.00.8823	88.32		0.0		
17	17 1 1	15 15	0			
	2.00.8862	88.50		0.0		
17	17 1 1	16 16	0			
	2.00.9547	88.79		0.0		
17	17 1 1	17 17	0			
	2.01.0554	89.21		0.0		
17	17 1 1	18 18	0			
	2.01.1406	89.54		0.0		
17	17 1 1	19 19	0			
	2.01.1800	89.74		0.0		
17	17 1 1	20 20	0			
	2.01.2155	89.84		0.0		
17	17 1 1	21 21	0			
	2.01.2450	90.05		0.0		
17	17 1 1	22 22	0			
	2.01.3326	90.34		0.0		
17	17 1 1	23 23	0			
	2.01.3800	90.54		0.0		
17	17 1 1	24 24	0			
	2.01.4000	90.64		0.0		
17	17 1 1	25 25	0			
	2.01.4502	90.86		0.0		
17	17 1 1	26 26	0			
	2.01.5078	91.07		0.0		
17	17 1 1	27 27	0			
	2.01.5557	91.31		0.0		
17	17 1 1	28 28	0			
	2.01.6455	91.60		0.0		
17	17 1 1	29 29	0			
	2.01.7504	92.00		0.0		
17	17 1 1	30 30	0			
	2.01.8059	92.32		0.0		
17	17 1 1	31 31	0			
	2.01.8563	92.53		0.0		
17	17 1 1	32 32	0			
	2.01.9532	92.94		0.0		
17	17 1 1	33 33	0			
	2.02.0501	93.33		0.0		
17	17 1 1	34 34	0			
	2.02.1100	94.73		0.0		
17	17 1 1	35 35	0			
	2.02.2137	94.13		0.0		
17	17 1 1	36 36	0			
	2.02.2470	94.41		0.0		
17	17 1 1	37 37	0			

	2.00+.352131E+			54.58		0.0	
17	17	1	1	38	38	0	
	2.00+.434491E+			54.92		0.0	
17	17	1	1	39	39	0	
	2.00+.5+0+1E+			55.52		0.0	
17	17	1	1	40	40	0	
	2.00+.6+4216E+			55.86		0.0	
17	17	1	1	41	41	0	
	2.00+.7+2315E+			56.26		0.0	
17	17	1	1	42	42	0	
	2.00+.8+029+E+			56.66		0.0	
17	17	1	1	43	43	0	
	2.00+.9583+1E+			57.06		0.0	
17	17	1	1	44	44	0	
	2.00+.+++++4E+			57.59		0.0	
17	17	1	1	45	45	0	
	2.00+.1951+2E+			58.02		0.0	
17	17	1	1	46	46	0	
	2.00+.3+0377E+			58.62		0.0	
17	17	1	1	47	47	0	
	2.00+.+265+7E+			58.97		0.0	
17	17	1	1	48	48	0	
	2.00+.+55+-5E+			59.21		0.0	
17	17	1	1	49	49	0	
	2.00+.52153+E+			59.34		0.0	
17	17	1	1	50	51	0	
	2.00+.573+03E+			59.57		0.0	
17	17	1	1	51	51	0	
	2.00+.6194+2E+			59.74		0.0	
17	17	1	1	52	52	0	
	2.00+.6741+9E+			60.01		0.0	
17	17	1	1	53	53	0	
	2.00+.74+72+E+			60.27		0.0	
17	17	1	1	54	54	0	
	2.00+.8+1+93E+			60.56		0.0	
17	17	1	1	55	55	0	
	2.00+.8++207E+			60.93		0.0	
17	17	1	1	56	56	0	
	2.01+.+1+75E7			61.38		0.0	
17	17	1	1	57	57	0	
	2.01+.+1+5+E7			61.78		0.0	
17	17	1	1	58	58	0	
	2.01+.02+56E7			62.19		0.0	
17	17	1	1	59	59	0	
	2.01+.03+-6E7			62.75		0.0	
17	17	1	1	60	60	0	
	2.01+.0++17E7			63.29		0.0	
17	17	1	1	61	61	0	
	2.01+.057+77E7			63.69		0.0	
17	17	1	1	62	62	0	
	2.01+.+6397+E7			63.94		0.0	
17	17	1	1	63	63	0	
	2.01+.+++2+E7			64.14		0.0	
17	17	1	1	64	64	0	
	2.01+.1717+6E7			64.24		0.0	
17	17	1	1	65	65	0	
	2.01+.1765+3E7			64.46		0.0	
17	17	1	1	66	66	0	
	2.01+.1+2+91E7			64.71		0.0	
17	17	1	1	67	67	0	

	2.01+.1+4+75E7			64.99		0.0	
17	17	1	1	68	68	0	
	2.01+.1+8+7+E7			65.35		0.0	
17	17	1	1	69	69	0	
	2.01+.1+9542E7			65.82		0.0	
17	17	1	1	70	70	0	
	2.01+.1+3991E7			66.42		0.0	
17	17	1	1	71	71	0	
	2.01+.1++4+6E7			67.02		0.0	
17	17	1	1	72	72	0	
	2.01+.152++7E7			67.62		0.0	
17	17	1	1	73	73	0	
	2.01+.167+34E7			68.22		0.0	
17	17	1	1	74	74	0	
	2.01+.1+176+E7			68.82		0.0	
1	1	1	1	1	1	0	
	5.00+.111+7+E+			85.00		0.0	
1	1	1	1	74	74	0	
	6.01+.1++++17E7			68.82		0.0	
2	2	1	1	1	1	0	
	5.00+.1+++1+E+			85.00		0.0	
2	2	1	1	74	74	0	
	6.01+.1++431E7			68.82		0.0	
3	3	1	1	1	1	0	
	5.00+.1+1++2E+			85.00		0.0	
3	3	1	1	74	74	0	
	6.01+.1++++5E7			68.82		0.0	
4	4	1	1	1	1	0	
	5.00+.+++++2E+			85.00		0.0	
4	4	1	1	74	74	0	
	6.01+.1++++7E7			68.82		0.0	
5	5	1	1	1	1	0	
	5.00+.1+5++1E+			85.00		0.0	
5	5	1	1	74	74	0	
	6.01+.1++7+1E7			68.82		0.0	
6	6	1	1	1	1	0	
	5.00+.+++++E+			85.00		0.0	
6	6	1	1	74	74	0	
	6.01+.1++++2E7			68.82		0.0	
7	7	1	1	1	1	0	
	5.00+.+++++E+			85.00		0.0	
7	7	1	1	74	74	0	
	6.01+.1++++4E7			68.82		0.0	
8	8	1	1	1	1	0	
	5.00+.+++++E+			85.00		0.0	
8	8	1	1	74	74	0	
	6.01+.1++++1E7			68.82		0.0	
9	9	1	1	1	1	0	
	5.00+.+++++E+			85.00		0.0	
9	9	1	1	74	74	0	
	6.01+.1++++1E7			68.82		0.0	
10	10	1	1	1	1	0	
	5.00+.+++++E+			85.00		0.0	
10	10	1	1	74	74	0	
	6.01+.1++++7E7			68.82		0.0	
11	11	1	1	1	1	0	
	5.00+.+++++E+			85.00		0.0	
11	11	1	1	74	74	0	
	6.01+.1++++3E7			68.82		0.0	
12	12	1	1	1	1	0